CONCERT-Japan
Research and Innovation Joint Call

Efficient Energy Storage and Distribution
Resilience against Disasters

RAPSODI Project

Risk Assessment and design of Prevention Structures
fOr enhanced tsunami DIsaster resilience

Deliverable D1- Existing tools, data, and literature on tsunami impact, loads on structures, failure modes and vulnerability assessment
1st year of funding

20120768-01-R
17 March 2014
Revision:1 / February 2015

NGI PARI Middle East Technical University Civil Engineering Department Technische Universität Braunschweig

CONCERT JAPAN
Connecting and Coordinating
European Research and Technology Development with Japan
www.concertjapan.eu

This work was supported by funding received from the CONCERT–Japan Joint Call on Efficient Energy Storage and Distribution/Resilience against Disasters

Project information

Name of the project:	RAPSODI
Start of the project:	01 July 2013
Duration (no. of months):	24
End of the project	01 July 2015
Name and country/region of each partner	NGI, Norway; PARI, Japan; TU-BS, Germany; METU, Turkey
Overall budget	383 k€

Client

Client:	CONCERT-Japan Joint Call Secretariat
Client's contact persons:	CONCERT-Japan Coordinator The Scientific and Technological Research Council of Turkey (TUBITAK) Ms. Filiz Hayirli (filiz.hayirli@tubitak.gov.tr) concertjapan@tubitak.gov.tr Phone: + 90 312 468 5300 (ext.1910) CONCERT-Japan Joint Call Secretariat Centre national de la recherche scientifique (CNRS) Ms. Lucie Durocher (lucie.durocher@cnrs-dir.fr) Phone: + 33 (0)1 44 96 47 14 Fax: + 33 (0)1 44 96 48 56 http://www.concertjapan.eu
Contract reference:	NGI 229578/H20; METU 113M556; TUBS 01DR13016;
Settlement numbers	PARI 2013 H25国際第1-33号 2014 H26国際第1-17号

For NGI

Project manager:	C.B. Harbitz
Prepared by:	Dr. Gulizar Ozyurt Tarakcioglu, Dr.Ahmet Cevdet Yalciner, Gozde Guney Dogan
Reviewed by:	G. Kaiser, C.B. Harbitz

CONCERT JAPAN
Connecting and Coordinating European Research and Technology Development with Japan

Publishable summary

The consortium of Risk Assessment and design of Prevention Structures fOr enhanced tsunami DIsaster resilience (RAPSODI) project aims to develop a method for quantitative tsunami risk assessment and to design tsunami mitigation structures to improve resilience against tsunami impacts. The project focuses on the quantitative assessment of vulnerability and on the analysis of tsunami impact on structures. The initial step of the project requires a thorough investigation of the numerical modelling tools, vulnerability assessment methods as well as failure mechanisms of buildings and coastal protection structures exposed to tsunamis. Deliverable 1 - *Report on existing tools, data, and literature on tsunami impact, loads on structures, failure modes and vulnerability assessment* provides a summary of the existing literature on numerical modelling tools, proposed formulas to calculate tsunami loads on structures including a catalogue of failure modes based on observations of the 2011 Tohoku tsunami and existing knowledge. It also provides a summary of vulnerability assessment models used in tsunami research with examples of the application to different regions around the world. Finally, different types of coastal structures and buildings are listed against potential failure modes with examples from the 2011 Tohoku Tsunami event in two separate matrices.

An analysis of the current tsunami numerical modelling tools has determined that, some of the models focus on the tsunami generation, propagation and inundation (eg. TUNAMI, NAMIDANCE, MOST) whereas some others are developed for a wider range of applications such as near shore wave processes, advection-dispersion or sediment transport that can be used for tsunami modelling (eg. BOSZ, MIKE21, etc). Almost all of the numerical models have the capability of modelling earthquake generated tsunamis. In terms of the source mechanism, some of the tools can model landslide generated tsunamis but only a few of them consider other tsunami generation mechanisms. The numerical tools have been applied to several different tsunami events around the world. Especially, after the 2004 and 2011 events, more attention has been paid to the accuracy of inundation modelling including the velocity and fluxes considering different roughness patterns, which turn out to be very important.

Direct effects of tsunamis on coastal and marine structures can be extensive and often disastrous. Tsunami waves can (1) move entire structures off their foundations and carry them inland; (2) damage buildings through impact with vessels carried from offshore and other debris accumulated as the wave advances inland; (3) undercut foundations and pilings with erosion caused by receding waves; (4) overturn structures by suction of receding or thrust of advancing waves; and (5) cause the impact of large ships with docks during oil or cargo transfer operations, often causing fires. Principal forces associated with tsunami consist of: (1) hydrostatic force, (2) hydrodynamic (drag) force, (3) buoyant force, (4) surge force and (5) impact of debris. Three parameters are essential for defining the magnitude and application of these forces: (1) inundation depth, (2) flow velocity, and (3) flow direction. The parameters mainly depend on: (a) tsunami wave height and wave period; (b) coastal

topography; and (c) roughness of the coastal inland. When it comes to the tsunami impact on coastal structures, the important parameters are current velocity, maximum dynamic wave pressure, sustained wave pressure, impact standing wave pressure and overflowing wave pressure. There also exist several experimental studies investigating the tsunami forces on sea walls and tsunami-induced loading on both coastal structures and land structures.

Furthermore, many researchers investigated the failure mechanisms of coastal structures under tsunami attack by conducting experiments or gathering information from post-event surveys especially after the 2004 Indian Ocean Tsunami and 2011 Great East Japan Earthquake and Tsunami events. According to the reports from different authors, an overview of different failure modes is given with short examples, the source of information, and further details. Most of the structures surveyed in the field were overtopped and therefore functional failure occurred. Scour is the most common failure mechanism among almost all types of coastal protection structures. Overturning, slope instability, soil instability and sliding are the other common failures. The mechanisms are categorized according to the two tsunami induced loading conditions as the water level difference across the structure and wave forcing. Most of the information regarding failure modes of coastal structures cover the type of structures located in Japan. Thus, there exists an important gap of knowledge on the performance of rubble mound structure which is very common in Europe under tsunami attack. Additionally, many of the failure modes related to wave impact is not investigated thoroughly. This could be an important source of diminished resilience after a tsunami event, even if no overflow occurs, thus it should be considered for further research work.

In addition to coastal structures, it is verified especially after the 2004 Indian Ocean Tsunami and the 2011 Great East Japan Earthquake that it is necessary to design structures and important infrastructure to survive tsunami effects. Observation and analysis of the tsunami impact on land structures as well as the related loading condition are essential to develop proper design approaches. Failure mechanisms of land structures such as buildings, walls, columns or bridges are affected significantly by the wave run-up heights and flow velocity as well as the debris carried by water. In this regard, a failure modes matrix of land structures is presented after a review of both experimental and field observation studies in literature. The failure mechanisms are classified according to the impulsive tsunami loading and the standing tsunami pressure condition. Many kinds of structures such as reinforced concrete, steel and wooden ones are considered and examples are also provided within a discussion part.

Finally, the tsunami vulnerability assessment approaches throughout the literature are reviewed and grouped under the topics of general tsunami vulnerability assessment approaches, tsunami fragility and social and ecological tsunami vulnerability. Under the topic of general tsunami vulnerability, the authors demonstrate the importance of the vulnerability component in tsunami risk assessment as a very dynamic factor dependent on a number of parameters relating to the built environment, sociological, economic, environmental and physical data.

The vulnerability assessment generally starts with exposure estimation (i. e. determination of “who” and “what” is exposed to tsunami), but it should be noted that exposure does not equal to vulnerability - the susceptibility to harm or damage during tsunami inundation. This requires an assessment of the people, homes, commerce, industry, natural resources, etc., that are in the tsunami inundation zones for a given event and that process is mostly carried out by in-situ assessment, remote sensing and using GIS tools. Then comes the numerous methods that have emerged to evaluate vulnerability, and these range from highly technical, statistical, quantitative assessments to simple, qualitative assessments. The best assessments would combine these methods, treating each hazard separately, as well as incorporating considerations for multiple and cumulative hazards occurrences into the overall assessment framework and methodology. It should also be noted that, vulnerability is treated as a component of the risk calculations in many approaches. Tsunami fragility curves has been widely used to develop relationships between damage and tsunami characteristics such as inundation depth, velocity or flux. However, there exists gaps of knowledge especially in terms of classification of damage levels for different types of structures as well as the significance of velocity on the fragility curves. Further clarification on the damage discussion as well new relationships between other characteristics of tsunami should be part of further research agenda in order to improve the risk assessment and non-structural mitigation strategies.

Contents

1 Introduction

Tsunamis are water waves generated by large-scale short duration energy transfer to the entire water column by earthquakes, coastal and submarine landslides, volcanic eruptions, caldera collapse, or meteor impact. Tsunamis and landslide waves may attain large amplitudes in closed basins or shallow regions (Yalciner et al. 2001; 2002; 2004; and 2005). They are generally classified as long period waves and now all are referred to as tsunamis. Landslide generated waves generally have only nearfield impact. They are of a shorter wavelength than tectonic tsunamis, and their initial amplitude depends on the depth, thickness, and initial acceleration of the triggering slide. The amplitude of tectonic tsunamis depends on the length of fault rupture and the slip. Generally tectonic tsunamis radiate energy in a direction perpendicular to the length of the triggering fault (Ben-Menahem and Rosenman 1972), whereas landslide tsunamis radiate energy in a radial fashion. The runup distribution on adjacent shorelines is so different between landslide waves and tsunamis that it allows discrimination of the source (Okal and Synolakis 2004).

The interest in tsunami research has increased in recent years after the terrible consequences of the 2004 Indian Ocean tsunami and of the 11th March 2011 tsunami in Japan. The Tohoku tsunami 2011 event clearly showed the potential for massive destruction of buildings, infrastructure and coastal protection by tsunami waves. Moreover a huge amount of data has been collected during and after the event, allowing a retrospective analysis. The 2011 Tohoku tsunami impact caused failures of foundations and prevention structures, which are not yet fully understood. Moreover, today's tsunami vulnerability and risk models are descriptive and limited; some are based on simple empirical relationships between tsunami flow depth and structural damage or fatalities. Thus, better understanding of the overall vulnerability to tsunamis, the specific mechanisms that lead to or contribute to the collapse of buildings and infrastructure as well as the performance of selected coastal structures is required to be analysed in detail for developing efficient mitigation measures against future tsunami events. In light of the new observations and ongoing research, the consortium of **R**isk Assessment and design of **P**revention **S**tructures f**O**r enhanced tsunami **DI**saster resilience (RAPSODI) project aims to develop a method for quantitative tsunami risk assessment and to design tsunami mitigation structures to improve resilience against tsunami impacts.

The project focuses on the quantitative assessment of vulnerability and on the analysis of loads on structures. The initial step of the project requires a thorough investigation of the numerical modelling tools, vulnerability assessment methods as well as failure mechanisms of buildings and coastal protection structures exposed to tsunamis. Deliverable 1 - *Report on existing tools, data, and literature on tsunami impact, loads on structures, failure modes and vulnerability assessment* is prepared to provide a summary of the existing literature on numerical modelling tools (Chapter 2), proposed formulas to calculate tsunami loads on structures including a catalogue of failure modes based on observations of the 2011 Tohoku tsunami and existing knowledge (Chapter 3). In Chapter 4 a matrix is presented where different types of

coastal structures are listed against potential failure modes with examples from the 2011 Tohoku Tsunami event. Additionally, a preliminary matrix of failure modes for buildings is provided that summarizes some of the available information and observations from 2011 Great East Japan Earthquake (GEJE) tsunami. A summary of vulnerability assessment models used in tsunami research are also provided with examples of the application to different regions around the world (Chapter 5). Finally, Chapter 6 provides a summary and some conclusions from this study.

2 Tsunami Numerical Modeling

There are many reasons to study tsunamis computationally, and ample motivation for developing faster and more accurate numerical methods. Applications include the development of more accurate real-time warning systems, the assessment of potential future hazards to assist in emergency planning, and the investigation of past tsunamis and their sources. Real-time warning systems rely on numerical models to predict whether an earthquake has produced a dangerous tsunami, and to identify which communities may need to be warned or evacuated. Mistakes in either direction are costly: failing to evacuate can lead to loss of life, but evacuating unnecessarily is not only very expensive but also leads to poor response to future warnings. Another use of tsunami modelling is to better understand past tsunamis, and to identify the earthquakes that generated them.

The primary objective in this field involves establishing and developing Tsunami Warning Systems (TWS) and inundation maps. The mathematical modelling and computation of propagating tsunami waves play an important role in TWS. Precision and robustness of the algorithm will affect the performance and reliability of the whole system. Therefore, over the past few decades, a variety of tsunami propagation models have been developed, based on a variety of governing equations, numerical methods, spatial and temporal discretization techniques, and wetting-drying algorithms used to predict tsunami run-up.

2.1 Existing Tools

A comprehensive overview of numerical models together with their general aspects is provided in table 2.1. Detailed information on validation studies of the models, usage platforms and information about developers is provided in section 2.2.

Table 2.1 – Numerical models used in tsunami studies

MODEL FEATURES	Equation Type	Numerical Schemes	Mesh/Grid Type	Tsunami Source	Wetting& Drying	Operating System	Programming Languages
TUNAMI-N2	Shallow water wave equations	Finite Difference, Leap-frog scheme	Rectangular constant grid domain	Co-seismic	Yes	Windows	Fortran
TUNAMI-N2-NUS							
TUNAMI-N3	Shallow water wave equations	Finite Difference, Leap-frog scheme	Nested grids	Co-seismic	Yes	Dos, Windows, Unix	Fortran
VOLNA Code	Nonlinear Shallow Water equations	Finite Volumes method	Unstructured Triangular Meshes	Co-seismic+ Landslides	Yes		C++
UBO-TSUFD & UBO-TSUFD-VB	Shallow water wave equations	Finite Difference, Leap-frog scheme	Rectangular constant grid domain, Version with nested grid	Co-seismic	Yes	Any implementing a Fortran 90/95 compiler	Fortran 90/95
UBO-TSUFE	Shallow water wave equations	Finite Element, Two step integration	Triangular Elements	Co-seismic	No	Any implementing a Fortran 77 compiler	Fortran 77
AQUILON	Navier-Stokes + VOF or Shallow water wave equations	Finite Volumes method	Curvilinear or cartesian	Landslides	Yes	Windows, Linux	Fortran 90
MOST	Nonlinear Shallow Water equations	Finite Difference Method with splitting ADI and characteristics technique	Non-uniform Nested grids	Co-seismic	Moving mesh technique, (Titov-Synolakis1995)	Linux	Fortran 77
TWO_LAYER	Shallow water wave equations	Finite Difference, Leap-frog scheme	Rectangular Constant Grids	Co-seismic+ Landslides	Yes	Windows	Fortran
ComMIT	Nonlinear Shallow Water equations	Finite Difference Method	Non-uniform Nested grids	Co-seismic		Windows, Mac OS, Unix	Java
ALASKA TSUNAMI MODEL	Shallow water wave equations	Finite Difference Method	Arakawa C-grid(Arakawa and Lamb, 1977)	Co-seismic+ Landslides			Fortran

MODEL FEATURES	Equation Type	Numerical Schemes	Mesh/Grid Type	Tsunami Source	Wetting& Drying	Operating System	Programming Languages
ATFM (AlaskaTsunami ForecastModel)	Shallow water wave equations	Finite Difference Method	Structured, nested meshes	Co-seismic	Yes	Any implementing a Fortran 90 compiler	Fortran 90
TsunAWI	Nonlinear Shallow Water equations	Finite Element Method	Unstructured Mesh Finite Element Grid	Co-seismic	Yes		
GEOWAVE	Boussinesq-type equations			Landslides (Coupled to FUNWAVE)		Unix, Linux	
COMCOT	Shallow water wave equations	Finite Difference, Leap-frog scheme	Arakawa C grid, Staggered, nested grids	Co-seismic+ Landslides	Yes	Windows (32- bits)	Fortran 90
TSUNAMICLAW	Nonlinear Shallow Water equations	Finite Volume Riemann Solvers	2D+1 rectangular mesh with adaptive refinement	Co-Seismic	Yes	Unix, Linux	Fortran 77
NAMI DANCE	Shallow water wave equations	Finite Difference, Leap-frog scheme	Rectangular constant grid	Co-Seismic	Yes	Windows XP (capable using multiprocessors if available in the computer by open MP capability)	C++
NEOWAVE	Depth-integrated, Non-hydrostatic Equation	Finite Difference Method	Two-way nested computational grids	Co-seismic+ Landslide (Initiate TSUNAMI3D)	Yes		
ANUGA	Shallow water wave equations	Finite Volume Method	Triangular Cells	Co-seismic	Yes		Python
SELFE	Hydro./ Nonhydro.	Finite element/ Finite volume	Unstructured Triangular Grids	Co-seismic+ Landslides			
THETIS	Multi-fluid Navier-Stoke Equations	Finite Volume Method	Fixed Mesh (Cartesian, cylindrical or curvilinear)	Co-seismic+ Landslides			
TSUNAMI3D	Navier-Stokes Equations	Finite Difference Method	Eulerian mesh of rectangular cells (var.size)	Co-seismic+ Landslides			Fortran

MODEL FEATURES	Equation Type	Numerical Schemes	Mesh/Grid Type	Tsunami Source	Wetting& Drying	Operating System	Programming Languages
BOSZ	Boussinesq-type equations	Finite Volume Method		Co-seismic			Matlab
MIKE 21	2D shallow water equations, Reynolds - Averaged Navier-Stokes Equations	Finite Volume Method	Flexible mesh	Co-seismic	Yes	Windows	
TSUNAMI-SKREDP	Shallow water wave equations	Finite Difference, Second Order Explicit	Arakawa C Grid	Co-seismic+ Landslides	No	Linux, Unix	Fortran 77
POL/BGS	Shallow water wave equations	Finite Difference Method	Arakawa C Grid	Co-seismic	Yes	Linux, Unix	Fortran 77
1HD	Boussinesq formulation & full potential theory	Finite Difference and Element Method, Boundary Integral Method	Adaptive Mesh	Co-seismic+ Landslides	Yes	Linux, Unix	Fortran 77, C++, Python
GLOBOUSS	Boussinesq equations	Finite Differences, implicit method. ADI iteration for implicit equations	Arakawa C Grid	Co-seismic	No	Linux, Unix	Fortran 77, Scripting Tools(perl)
DPWAVES	Mild Slope Boussinesq, potential formulation	Finite Elements, Second Order, implicit	Regular or irregular Finite Elements Adaptive Mesh	Co-seismic+ Landslides	No	Linux, Unix	Diffpack(C++ Library)
HySEA Numerical Model	Nonlinear Shallow Water equations	PVM-IFCP finite volume schemes	Structured and non-structured grids	Co-seismic	Yes		
HySEA-Landslide Model	Savage-Hutter Shallow-Water	PVM-IFCP finite volume schemes (Castro and Nieto, 2012)	Structured and non-structured grids	Landslides			
STOC-CADMAS	3D Reynolds -Averaged Navier-Stokes Equations	Finite difference and volume of fluid	Rectangular Nested Grids	Co-seismic	Yes	Linux, Unix	Fortran 90

2.2 Detailed Information on the Numerical Models

TUNAMI MODEL, Tsunami Numerical Simulation of Dr. Fumihiko Imamura, Prof. of Tsunami Engineering School of Civil Engineering, Asian Inst. Tech. and Disaster Control Research Center, Tohoku University is prepared in June, 1995 for TIME project. The TIME (Tsunami Inundation Modeling Exchange) started in 1991 as a joint effort Of IUGG and IOC/UNESCO during IDNDR. The Disaster Control Research Center (DCRC), Tohoku University, Japan has been acting as the center of TIME, to transfer numerical technique of tsunami simulation to the countries which suffered or will suffer tsunami hazards. (http://tunamin2.ce.metu.edu.tr/)

The TUNAMI code consists of;
TUNAMI-N1 (Tohoku University's Numerical Analysis Model for Investigation of Near-field tsunamis, No.1),
TUNAMI-N2,
TUNAMI-N3,
TUNAMI-F1 (linear theory for propagation in the ocean in the spherical co-ordinates) and
TUNAMI-F2 (linear theory for propagation in the ocean and coastal waters)

The TUNAMI-N2 model is tested, validated, discussed and verified in the NSF Workshop on Benchmark Problems on Tsunami Modeling in Catalina Island. It is developed by Disaster Control Research Center, Tohoku University, Japan and Ocean Engineering Research Center, Middle East Technical University, Turkey for operational and research purposes. Model is generated for fault dislocation based on Okada 1985 for co-seismic tsunamis. Arbitrary shape of initial wave, dynamic input of wave at arbitrary location and shape can be controlled by user. The model creates the initial wave from different sources and generates the sea state at specific time intervals of tsunami during simulation. There are more than 25 institutions using this code. The model is applied to Indian Ocean, Tanzania, Andaman sea, South China Sea, Malacca Strait, Malaysia, Java- Indonesia, Singapur, Sumatra- Indonesia, Mediterranean Sea, Maldives, Aegean Sea, India, Marmara Sea, Macran Case, Black Sea, Madagascar, Scenarios for Istanbul, Caribbean Sea.

Dao and Tkalich (2007) describe further development of original TUNAMI-N2 model to take into account additional phenomena: astronomic tide, sea bottom friction, dispersion, Coriolis force, and spherical curvature in their study. The code is modified to be suitable for operational forecasting, and the resulting version (TUNAMI-N2-NUS) is verified using test cases, results of other models, and real case scenarios. Using the 2004 Tsunami event as one of the scenarios, they examined sensitivity of numerical solutions to variation of different phenomena and parameters, and the results are analyzed and ranked accordingly. Furthermore, Dao and Tkalich (2013) reviewed and hindcasted recent significant earthquake and tsunami events in South East Asia using TUNAMI-N2-NUS model, with the purpose of the model validation and the source estimation. All these three powerful tsunamigenic earthquakes occurred on the boundary of the Indo-Australian Plate and Eurasia Plate, or the Sunda trench (Dao and Tkalich, 2013).

TUNAMI-N3 is an open source, fully tested model and verified for most of tsunami past events. The model is applied to 1833 Sumatera (Bengkulu) Tsunami, 1996 Toli-toli (Sulawesi) Tsunami, 1883 Krakatau Tsunami, 1996 Biak Tsunami, 1935 North Sumatera Tsunami, 2000 Banggai Tsunami, 1992 Flores Tsunami, 2004 Aceh Tsunami, 1994 East Java Tsunami, 2006 South Java Tsunami, Scenarios for Fethiye and Pylos and Caribbean Sea.

The numerical code VOLNA is a novel tool for tsunami wave modeling which is able to handle the complete life cycle of a tsunami (generation, propagation and run-up

along the coast). The code was developed in close collaboration with R. Poncet and F. Dias when the first author was at CMLA, ENS de Cachan. The VOLNA code is operational and is able to run in complex and rapidly varying conditions. Owing to the implementation of various types of boundary conditions, the code VOLNA can be coupled to other solvers and treat exclusively the zones where the NSWE are physically relevant. The code is validated for accuracy, run-up algorithm and treatment of steep depth fields and time varying bathymetry in a conservative shallow water framework by using different analytical benchmarks. (Dutykh et al., 2011). Moreover, the capability of the code to model realistic events is also shown using an experimental benchmark.

UBO-TSUFE is another model to simulate tsunami generation and propagation developed by Università di Bologna, Dip. di Fisica, Settore Geofisica, Italy for research purposes. In the model, multi- fault vertical co- seismic displacements are computed through Okada´s formulas and corrected for bathymetric effects in the case of an earthquake source; impulses are computed through UBO- TSUIMP in case of moving body. Loss of energy due to the interaction with the boundaries and with sea bottom is observed. Coriolis force can be included in the model and it has command line interface. Tsunami Research Team of the University of Bologna has applied this model to the scenarios in the Mediterranean Sea (simulation of historical events in the Adriatic Sea, Ionian Sea, Tyrrhenian Sea, 1999 Izmit bay earthquake-induced tsunami, and scenarios in the Gulf of Corinth and of Mediterranean-wide tsunamis), and in the Indian Ocean (2004 Sumatra, 2006 Java, and several scenarios).

The models UBO- BLOCK1 & UBO-BLOCK2 are also developed for research purposes by Università di Bologna, Dip. di Fisica, Settore Geofisica, Italy. They are used for the simulation of the landslides (the motion of the sliding masses). The equations used in this model are equations of motion for a set of contiguous blocks interacting each other and interacting with the bottom topography. Numerical model for the calculation of the dynamical evolution of a body sliding down topography is observed. The model has also command line interface. Tsunami Research Team of the University of Bologna has applied this model to several areas such as Stromboli island shallow landslide and sector collapse (Italy), Ischia island flank collapse (Italy), Izmit Bay small slump (Turkey), Corinth Gulf shallow landslide scenarios (Greece), The Vajont landslide evolution (Italy) and Oshima-Oshima sector collapse (Japan).

The models UBO-TSUFD & UBO-TSUFD-VB are developed for research purposes by Università di Bologna, Dip. di Fisica, Settore Geofisica, Italy. Multi- fault vertical co- seismic displacements computed through Okada´s formulas and corrected for bathymetric effects. The model has command line interface. Tsunami Research Team of the University of Bologna has applied this model to the scenarios in the Mediterranean Sea, 2004 Sumatra tsunami, 2006 Java tsunami, and scenario tsunamis in the Indian Ocean.

AQUILON is developed in France by UMR TREFLE CNRS and University of PAU (UPPA). The landslide generated tsunami model is fully tested for research purposes. Landslides are simulated as fluids either Newtonian or non-newtonian. Rigidity is achieved by setting the viscosity value to infinity. The user interface is through text files and keywords. The reference user of the model is fluid mechanics community in France and they applied the model to academic problems such as wave breaking, wave run-up, waves generated by landslides, dam breaking.

The model, TWO_LAYER, which is created in Tohoku University Disaster Control Research Centre in Japan, is developed by Japan and Turkey for research and operational purposes. The code is tested, validated, discussed and verified in the NSF Workshop on Benchmark Problems on Tsunami Modeling in Catalina Island. The model uses landslide characteristics, Okada 1985 for Co-seismic Tsunamis and arbitrary shape of initial wave (determined by user). More than five institutions (Reference users: Middle East Technical University Ocean Engineering Research Center, Ankara., Department of Applied Mathematics Russian Academy of Sciences, Nizhny Novgorod, Russia., Department of Nonlinear Geophysical Institute of Applied Physics, Russian Academy of Science, Russia) have applied the model to Indian Ocean, South China Sea, Sumatra- Indonesia, Mediterranean Sea, Aegean Sea, Caribbean Sea, Marmara Sea, and Black Sea.

The MOST (Method of Splitting Tsunami) model, developed by Prof. Titov of PMEL (Pacific Marine Environmental Laboratory) and Prof. Synolakis of University of Southern California, is a suite of numerical simulation codes capable of simulating three processes of tsunami evolution: earthquake, transoceanic propagation, and inundation of dry land. The code is tested, validated, discussed and verified with experimental data and in the 3rd International Workshop on Long wave runup models in Catalina Island. The model is based on elastic deformation theory of Gusiakov (1978) and Okada (1985). MOST is applied to Indian Ocean, Pacific Ocean, Mediterranean Sea, and Aegean Sea by NOAA and FORTH. MOST is the standard model used at the NCTR (Noaa Center for Tsunami Research) in the development of tsunami inundation forecast models. Some examples of the use of the MOST model are Trans-Pacific Propagation: The June 10 and 1996 Andreanov tsunami as a test of the MOST propagation model. Inundation of the Aonae peninsula during the July 12, 1993 Hokkaido-Nansei-Oki tsunami is also computed with the MOST model. (http://nctr.pmel.noaa.gov/Titov/show/)

To develop a web-based community tsunami model, the United States Agency for International Development (USAID) funded NOAA/PMEL/NCTR to develop a tool that would assist in achieving this goal. The NCTR subsequently developed ComMIT, which is a rich graphical interface to a precomputed tsunami scenario database and to the MOST model. ComMIT is designed analogously to MOST's command-line operation. It addresses concerns regarding proprietary bathymetry data, while allowing dissemination of results to the tsunami research community. ComMIT uses initial conditions from a precomputed propagation database, has an easy graphical interface to output modeling results, and requires minimal hardware.

ComMIT also allows incorporation of other tsunami models such as TsunAWI (Harig et al., 2008) or TUNAMI (Imamura, 1995). The interface also allows for Internet sharing of the model results, either as a Google Earth animation, or through the use of shared databases via the OPeNDAP protocol (http://opendap.org). Since this community modeling tool was developed by the NCTR, more than 60 researchers from Indian Ocean countries have been trained in inundation modeling with ComMIT. (Titov, V. V., et al., 2011). Including all the courses, almost 150 scientists have been trained not only in ComMIT, but also in the basics of tsunami science. It is important to emphasize that the MOST model and the interface ComMIT are only accessible to professionals who undergo training through these specialized training courses.

ALASKA TSUNAMI MODEL is developed at the Geophysical Institute, University of Alaska Fairbanks as a numerical model of the wave dynamics in Passage Canal, Alaska during the Mw 9.2 mega thrust earthquake. The suit of numerical models employed by the State of Alaska for the tsunami inundation mapping project comprises tectonic tsunami model, landslide-generated tsunami model and seiche tsunami model. The model computes inundation by each type of wave during the 1964 event. Tectonic tsunami model is a numerical model that has been described and tested through a set of analytical, laboratory, and field benchmark problems (Nicolsky et al., 2011). To simulate tsunamis produced by underwater slope failures, a numerical model of a viscous underwater slide with full interactions between the deforming slide and the water waves that it generates is used. Nicolsky and others, (2010) considered a fixed coordinate system to model run-up of the seiche tsunami by considering motion of the reservoir.

The Alaska Tsunami Forecast Model (ATFM) was developed at the West Coast/Alaska Tsunami Warning Center in coordination with the University of Alaska, Fairbanks Institute of Marine Sciences. The system first went into operations in 1997 and an upgrade to a newer version was in progress in 2010.

The ATFM is a completely pre-computed forecast model that is scaled by observations during an event. Other than simple scaling, no computations are performed during the event. Model output includes energy propagation maps and wave height forecasts for over 500 DART and coastal locations throughout the Pacific. Over 600 pre-computed runs provide energy maps and amplitude forecasts for over 500 locations throughout the North American continent and Hawaii. The ATFM is very simple to use during an event, requiring only a few keystrokes and seconds of time. It instantly displays coastal forecasts at many locations, providing the Watchstander a quick look at an event's danger level. ATFM output is also used before events to help set warning zones for specific events. (http://www.meted.ucar.edu/tsunami/warningsystem/print.htm#page_3.4.3)

The tsunami model TsunAWI simulates all stages of a tsunami from the origin and the propagation in the ocean to the arrival at the coast and the inundation on land. In the framework of the German-Indonesian Tsunami Early Warning System

(GITEWS), the tsunami modeling group at AWI (Alfred Wegener Institute) has developed the operational model code TsunAWI and provided the warning centre at the Indonesian Agency for Meteorology, Climatology, and Geophysics (BMKG), Jakarta, Indonesia, with a repository of 3470 prototypic tsunami scenarios (Rakowsky, 2013). The development of TsunAWI started as a spin-off of the ocean model FESOM (Finite Element Sea-Ice Ocean Model) (Wang et al., 2012b, and references therein). The model includes Coriolis, bottom friction and viscosity forcing terms. It proves to be accurate and useful for inundation studies, sensitivity analysis, and hazard assessment (Behrens, 2008).

GEOWAVE is a comprehensive tsunami simulation model formed in part by combining the Tsunami Open and Progressive Initial Conditions System (TOPICS) with the fully non-linear Boussinesq water wave model FUNWAVE. Funwave is a phase-resolving, time-stepping Boussinesq model for ocean surface wave propagation in the nearshore. Boussinesq wave models have become a useful tool for modeling surface wave transformation from deep water to the swash zone, as well as wave-induced circulation inside the surfzone. TOPICS uses curve fits of numerical results from a fully nonlinear potential flow model to provide approximate landslide tsunami sources for tsunami propagation models, based on marine geology data and interpretations. GEOWAVE is validated with successful case studies of the 1946 Unimak, Alaska, the 1994 Skagway, Alaska, and the 1998 Papua New Guinea events. (Watts et al., 1999). GEOWAVE simulates accurate runup and inundation at the same time, with no additional user interference or effort, using a slot technique. Wave breaking, if it occurs during shoaling or runup, is also accounted for with dissipative breaking model acting on the wave front.

COMCOT (Cornell Multi-grid Coupled Tsunami Model) is a model developed in Cornell University, USA for research purposes. It is tested (compared with both experiments and field data) and beta version is released. COMCOT is a tsunami modeling package, capable of simulating the entire lifespan of a tsunami, from its generation, propagation and runup/rundown in coastal regions. Waves can be generated via incident wave maker, fault model, landslide, or even customized profile. To implement the fault model in COMCOT, totally NINE parameters need to know: latitude and longitude of epicenter, focal depth, length and width of fault plane, dislocation, strike angle, slip angle and dip angle. The users for this code is research groups in Japan, Taiwan, US, Sri Lanka and Spain. The model is applied to tsunami propagation, run-up and inundation, tsunami mitigation fields. It has been used to investigate several historical tsunami events, such as the 1960 Chilean tsunami, the 1992 Flores Islands (Indonesia) tsunami (Liu, 1994; Liu et al., 1995), the 2003 Algeria Tsunami (Wang and Liu, 2005) and more recently the 2004 Indian Ocean tsunami (Wang and Liu, 2006).

GeoClaw is a variant of the Clawpack open source software (LeVeque et al., n.d.) that LeVeque and collaborators have been developing since 1994. It allows one to model various flooding problems, particularly global-scale tsunamis and inundation on a latitude-longitude grid (or smaller local flooding on a Cartesian grid) with a

diverse range of spatial and temporal scales. This is accomplished by using a single coarse level 1 grid for the entire domain, and evolving rectangular Cartesian sub-grids of higher refinement, level 2, , level n, that track moving waves and inundation at the shoreline. Up to six levels may be used (though typically four or less is recommended). At any given time in the calculation, a particular level of refinement may have numerous disjoint grids associated with it. User specified integers determine the refinement ratios between particular levels, which can lead to a large degree of refinement even for a small number of levels. GeoClaw was initiated in the PhD work of David George (George, 2006; LeVeque and George, 2004; George and LeVeque, 2006; George, 2008) and was originally called TsunamiClaw which was applied to Sumatra for tsunami propagation, run-up and inundation. GeoClaw supersedes the TsunamiClaw package and provides the original plus additional functionality. Validation studies of the more recent GeoClaw software have been presented in several peer-reviewed papers: the Chile 2010 tsunami used as a test problem in Berger et al. (2011), further tests in LeVeque et al. (2011), Grid refinement studies and comparison with field data for the widely studied Malpasset dam failure in George (2010), tests performed for a tsunami-like wave propagating on the full sphere, using a novel mapped grid that covers the sphere with a logically rectangular finite volume grid in Berger et al. (2009). GeoClaw Tsunami Modeling Group, University of Washington, has modeled the Great Tohoku Tsunami of 11 March 2011. Some results were posted online as computed in the days after the event and can be viewed at http://www.clawpack.org/links/honshu2011/.

NAMI DANCE is a computational tool developed by Profs Andrey Zaytsev, Ahmet Yalciner, Anton Chernov, Efim Pelinovsky and Andrey Kurkin as a collaboration by Ocean Engineering Research Center, Middle East Technical University, Turkey and Department of Nonlinear Geophysical Institute of Applied Physics, Russian Academy of Science, Russia especially for tsunami modeling. It provides direct simulation and efficient visualization of tsunamis to the user and for assessment, understanding and investigation of tsunami generation and propagation mechanisms. The model is tested and verified for research and operational purposes.

NAMI DANCE has been developed by using the identical computational procedures of TUNAMI N2. Both codes are cross tested also verified in international workshops specifically organized for testing and verifications of tsunami models (Synolakis, Liu, Yeh, 2004, Yalciner et. al., 2007b). These models have been applied several tsunami application all over the world (some of references are Yalciner et. al. 1995, 2002 a,b,c 2007 a,b, Zahibo et. al. 2003 a,b).

As well as tsunami parameters, NAMI DANCE computes:
- tsunami source from either rupture characteristics or pre-determined wave form,
- propagation,
- arrival time,
- coastal amplification,
- inundation (according to the accuracy of grid size),
- distribution of current velocities and their directions at selected time intervals,

- distribution of discharge fluxes at selected time intervals,
- distribution of water surface elevations (sea state) at selected time intervals,
- relative damage levels (Froude Number and its square) according to drag force and impact force,
- time histories of water surface fluctuations at selected gauge locations,
-3D plot of sea state at selected time intervals from different camera and light positions,
-Animation of tsunami propagation between source and target regions (Yalciner et. al., 2006, 2007b).

The previous application areas include Indian Ocean, Tanzania, Andaman sea, South China Sea, Malacca Strait, Malaysia, Java- Indonesia, Singapore, Sumatra-Indonesia, Mediterranean Sea, Maldives, Aegean Sea, India, Marmara Sea, Macran Case, Black Sea, Madagascar, Scenarios for Fethiye and Pylos, Kenya, and Caribbean Sea. (http://namidance.ce.metu.edu.tr/)

NEOWAVE (Non-hydrostatic Evolution of Ocean WAVEs) is a shock-capturing, dispersive model for tsunami generation, basin-wide evolution and coastal inundation and run up (Yamazaki et al., 2011). It is developed as an advanced tsunami model by Yoshiki Yamazaki and Kwok Fai Cheung, Department of Ocean and Resources Engineering, University of Hawaii at Manoa. The depth-integrated model describes dispersive waves through the non-hydrostatic pressure and vertical velocity, which also account for tsunami generation from kinematic seafloor deformation. Previous studies have verified and validated the hydrostatic model for wave propagation, transformation, and run-up with analytical solution and laboratory data (Kowalik&Murty, 1993, Kowalik et al., 2005, 2006, Yamazaki et al., 2009). The resulting tsunami of 2009 Samoa Earthquake occurred near Tonga Trench is reconstructed using Neowave to examine the disparities such as variation of the run-up and impact between adjacent beachfront villages (Koshimura et al., 2009, Okal et al., 2010) in the recorded data(Yamazaki et al.,2010). Some of the application areas of NEOWAVE are the tsunami inundation mapping of Hawaii, Northwest Hawaiian Islands, American Samoa, Western Samoa, the US Gulf coasts, Puerto Rico and Chile, the storm surge and wave modeling of Pacific Islands, and the US East coasts and the tsunami modeling workshop of Chile. Recent and future tsunami researches are also the resonance analysis due to insular shelf of the 2009 Samoa Tsunami (Roeber, V., Yamazaki, Y., and Cheung, K.F., 2010), the resonance analysis over continental shelf of the 2010 Chile Tsunami (Yamazaki, Y., and Cheung, K.F., 2011), the earthquake and tsunami source study of the 2010 Mentawai Tsunami (Lay, T., Ammon, C.J., Kanamori, H., Yamazaki, Y., and Cheung, K.F., 2011) and the impact study of the 1700 Cascadia Tsunami on coastal infrastructure (Cheung et al., 2011).

The 3-D model, dubbed TSUNAMI3D (for Tsunami Solution Using Navier-Stokes Algorithm with Multiple Interfaces) has been developed by the University of Alaska Fairbanks (UAF) and by Texas A&M University at Galveston (TAMUG). The basic mode of operation is for single fluid calculation having multiple free surfaces. However, TSUNAMI3D can also be used for calculations involving two fluids

separated by either a sharp or indefinite (diffusive) interface, for instance, water and mud. In either case, the fluids may be treated as incompressible. Internal obstacles or topography are defined by blocking out fully or partly any desired combination of cells in the mesh. The TSUNAMI3D code was exclusively developed for tsunami calculations. The current TSUNAMI3D code has undergone dramatic changes from its original conception. In particular, the VOF algorithm for tracking the movement of a free surface interface between two fluids or between a fluid and a void has been simplified especially for the 3-D mode of operation. The simplification accounts for the horizontal distortion of the computational cells with respect to the vertical scale that is proper in the construction of efficient 3-D grids for tsunami calculations. In addition, the pressure term has been split into two components, hydrostatic and non-hydrostatic. The splitting of the pressure term allows users of the model to obtain a hydrostatic solution by merely switching off the non-hydrostatic pressure term. Therefore, TSUNAMI3D can be used to separate out non-hydrostatic effects from the full solution while keeping the three dimensional structure. TSUNAMI3D is suitable for complex tsunami generation because it is capable of modeling: (1) moving or deformable objects, (2) subaerial/subsea landslide sources, (3) soil rheology, and (4) complex vertical or lateral bottom deformation.

The tsunami propagation and inundation model SELFE (Zhang and Baptista 2008a) is envisioned at its inception to be an open-source community-supported 3-D hydrodynamic/hydraulic model. This philosophy remains the corner stone of the model to this day. Originally developed to address the challenging 3-D baroclinic circulation in the Columba River estuary, it has since been adopted by 65+ groups around the world and evolved into a comprehensive modeling system encompassing such physical/biology processes as general circulation (Burla et al. 2010), tsunami and hurricane storm surge inundation (as in the on-going IOOS sponsored SURA project), ecology and water quality (Rodrigues et al. 2009ab), sediment transport (Pinto et al. 2011), wave–current interaction (Roland et al. 2011) and oil spill (Azvedo et al. 2009). The time stepping in SELFE is done semi-implicitly for the momentum and continuity equations, and together with the Eulerian-Lagrangian method (ELM) for the treatment of the advection, the stringent CFL stability condition is bypassed. The remaining stability conditions are related to the horizontal viscosity and baroclinic gradient terms, which are very mild (in the case of tsunami applications, these conditions are absent). For seismic tsunamis, it is also explicitly modeled the earthquake stage (i.e., with moving bed) in order to obtain accurate initial acceleration (Zhang and Baptista 2008b). Since 2007, all components of the SELFE modeling system have been fully parallelized using domain decomposition and Message Passing Protocol (MPI). This has further enhanced efficiency. For example, in the recent simulation of the impact of the 1964 Alaska event on the US west coast, a large grid is used (with 2.9 million nodes and 6 million elements) to resolve 12 major estuaries and rivers in the PNW (Zhang et al. 2011). With 256 CPUs on NASA's Pleiades cluster, the 6-hour simulation took only 2.25 hours wall-clock time. The largest grid implemented on Pleiades for SELFE so far has over 10 million nodes in the horizontal and 26 levels in the vertical.

HySEA numerical model for the simulation of earthquake generated tsunamis is presented in Macias et al. (2013) study. In their study, the initial sea surface deformation is computed using Okada model. Generation, propagation and inundation phases are all integrated in a single code and computed coupled and synchronously when they occur at the same time. Inundation is modeled by allowing cells to dynamically change from dry to wet and reciprocally when water retreats from wetted areas. They state that the GPU model implementation allows faster than real time (FTRT) simulation for real large-scale problems. The model is verified by hindcasting the wave behavior in several benchmark problems in their study. In addition, numerical results for an earthquake-generated tsunami in the Mediterranean Sea are presented and computing time analysed. González-Vida et al. (2012) presented a work in collaboration with the NOAA Center for Tsunami Research to apply the GPU version of the HySEA-Landslide model to the 1958 landslide generated mega-tsunami of Lituya Bay. The HySEA-Landslide is a Savage-Hutter Shallow-Water coupled model based on the PVM-IFCP finite volume schemes (Castro and Nieto, 2012). In this model, a layer composed of fluidized granular material is assumed to flow within an upper layer composed of an inviscid fluid (e.g. water) and it is discretized using a two dimensional finite volume scheme implemented on GPU cards for increasing the speed-up. This model has been validated by using the two-dimensional physical laboratory experiments data from H. Fritz (2009). In order to simulate the 1958 Lituya Bay mega-tsunami, González-Vida et al. (2012) have reconstructed the previous topo bathymetry based on USGS geological surveys. A sensivity analysis of some parameters has been performed in order to determine the best parameters of the model able to reproduce the real event.

STOC-CADMAS System is a numerical tool used for simulating tsunami and storm surge events developed by Japanese researchers. These simulations include information on generation, propagation, amplification and inundation characteristics in addition capabilities to estimate damage on the coastal structures. STOC-CADMAS System consists of three different numerical models (STOC-ML, STOC-IC and CADMAS-SURF) that are applied as a nested (layered) grid system. STOC-ML is the multi-level model to compute the tsunamis in a wide sea area in comparatively small computation time. STOC-IC is the non-hydrostatic pressure model used to estimate tsunamis in an area near a coastal city. CADMAS-SURF is also a non-hydrostatic pressure model applied in the smallest layer to estimate tsunami impact on coastal structures. The difference between STOC-IC and CADMAS-SURF is the method to determine free surface. STOC-IC uses the integrated continuity equation and CADMAS-SURF uses volume of fluid (VOF) method to analyse the position of free surface (Tomita et al., 2006, Takahashi et al., 2007)). This model is tested in various benchmark tests. The model is applied not only in Japanese coasts, but also in different places around the world including the Sea of Marmara, Turkey. (Yalciner et al., 2014)

The model TSUNAMI-SKREDP is developed for operational and research purposes by the Department of Mathematics, University of Oslo/Norwegian Geotechnical Institute/ICG, Norway. The model is certified (as critical software at NGI) and fully

tested (grid refinement, comparison with analytic solutions, comparison with results from independent codes, careful assessment of features). Any initial sea surface deformations, prescribed source functions for landslides and earthquakes, or input from files are the generation input for this model. The model is considered simple, fast and robust. The model has Norwegian command driven interface. The user community for TSUNAMI-SKREDP is NGI and University of Oslo. The model has been applied to North East Atlantic, Arctic Ocean, Norwegian Fjords, Mediterranean, Indian Ocean, South China Sea, hydropower reservoirs in Norway and The Philippines for research and consulting purposes.

POL/BGS is a model developed by POL, UK for research and pre- operational purposes. The generation model is Okada elastic dislocation or any surface deformation. The user interface is through several parameter files. The model is used by POL/BGS/UK Met Office researchers and is applied to Northwest European continental shelf, simulation of the Lisbon 1755 tsunami, and other scenarios that could affect the UK and Ireland.

THETIS is developed by the TREFLE CNRS laboratory at the University of Bordeaux I. It is a multi-purpose CFD code, freely available to researchers (http://thetis.enscbp.fr) and fully parallelized. THETIS solves the incompressible NS equations for water, air, and the slide. Basically, at any time, the computational domain is considered as being filled by one “equivalent” fluid, whose physical properties (namely density and viscosity) vary with space. Subgrid turbulent dissipation is modeled based on a Large Eddy Simulation approach, using a mixed scale sub grid model (Lubin et al., 2006). THETIS has been extensively validated for many theoretical and experimental flow cases. Hence, each new version of THETIS has to successfully solve more than 50 validation cases within a certain expected accuracy, before being released. Abadie et al. (2006, 2008, and 2010) simulated classical landslide tsunami benchmarks involving rigid bodies using THETIS. In these papers, rigid slides are simulated as a Newtonian fluid, for which deformation is prevented by specifying an infinite viscosity. With the use of this so-called penalty method, the slide displacement is computed implicitly and thus no longer prescribed as in most other similar studies. Abadie et al. (2010) performed convergence studies and showed that result accuracy on the free surface is satisfactory as long as enough grid cells are used to ensure that the slide motion is correctly reproduced. This penalty method is an improvement that may help NS models to become more suitable for more realistic applications or case studies, in which, of course, slide motion is always unknown. However, real slides are far more complex than solid bodies. Next step is thus to validate the model for waves generated by deformable slides. For that purpose, the generalized non Newtonian fluid model (i.e., a Herschel–Bulkley fluid) has been implemented in THETIS and are currently performing tests using this constitutive law.

ANUGA is a free and open source software tool for hydrodynamic modelling, suitable for predicting the consequences of hydrological disasters such as riverine flooding, storm surges and tsunamis. In order to simulate the behaviour of water flow

from such hazards within the built environment, Geoscience Australia and the Australian National University are developing this software modelling tool, ANUGA, for hydrodynamic simulations. ANUGA is currently being applied in a number of projects where impacts from tsunami events on coastal communities are simulated. ANUGA calculates the maximum water depth for the study area which is then provided as a map for use by emergency managers. Projects include Tsunami Impact Modelling for Western Australia (with Fire and Emergency Services Authority) and support to the Australian Tsunami Warning System.(http://www.ga.gov.au/hazards/our-techniques/modelling/our-models/what-is-anuga.html). ANUGA has been extensively validated against wave tank experiments and field studies where available. Examples include validation against the wave tank experiment for the Okushiri 1995 tsunami (Nielsen et al., 2005), wave tank runup experiments at University of Queensland (Barnes and Baldock, 2007), the 2004 Indian ocean tsunami impact at Patong Beach (Jakeman et al., 2010), comparison to other models (Drie et al., 2010).

BOSZ (Boussinesq model for Ocean & Surf Zones) is a numerical model for propagation, transformation, breaking, and runup of water waves (Roeber et al. (2010) and Roeber and Cheung (2012)). BOSZ was specifically designed for nearshore wave processes in the presence of fringing reefs in tropical and sub-tropical regions around the world. Typical nearshore processes that numerical models have to deal with are abrupt transitions from dispersion-dominated to flux-dominated flow through a wide range of wave breaking conditions. The formation, propagation, and runup of breaking waves or bores involve shock-related hydraulic processes in which additional treatments are necessary to enforce conservation laws across flow discontinuities. A numerical model designed for such extreme conditions provides a robust platform for a wide range of nearshore wave conditions elsewhere around the world. BOSZ was developed with the goal of obtaining reliable and robust results in addressing the complementary but somewhat opposing physical processes of flux and dispersion throughout a single numerical model. BOSZ is primarily used for modeling nearshore and surf-zone processes of swell and wind waves. The model can be applied to near-field tsunami scenarios. BOSZ combines the dispersive properties of a Boussinesq-type model with the shock capturing capabilities of the conservative form of the nonlinear shallow-water equations. BOSZ allows the simulation of dispersive waves up to medium order as well as supercritical flows with discontinuities. BOSZ is a NOAA approved model for inundation mapping and hazard mitigation.

MIKE 21 is a comprehensive modelling system for the simulation of hydraulics and hydraulic-related phenomena in estuaries, coastal waters and seas. It can be applied to any two-dimensional free-surface flows where stratification can be neglected. The various modules of the system simulate hydrodynamics, advection-dispersion, short waves, sediment transport, water quality, eutrophication and heavy metals. An extensive pre- and post-processing module allows analysis and graphical presentation of both data and model results. The model was developed by the Danish Hydraulic Institute (DHI) and the model simulates the growth, decay and

transformation of wind generated waves and swells in offshore and coastal areas. MIKE 21 has successfully been used for coastal flooding studies in hundreds of studies for more than 35 years. The model is also used in tsunami modelling studies. Gayer et al. (2010) studied the tsunami inundation modelling based on detailed roughness maps of densely populated areas performing with the MIKE 21 Flow Model. Kaiser et al. (2011) also used the numerical model MIKE 21 FM to hindcast the observed tsunami inundation and to draw conclusions on the influence of land cover on inundation patterns in their case study. They carried out detailed inundation simulations to support damage analysis and risk assessment related to the 2004 tsunami in Phang Nga and Phuket, Thailand. Another example is Gopinath et al. (2014) in which the inundation of the 2004 Indian Ocean tsunami is simulated for the coastlines of Chennai and Nagapattinam based on high-resolution topography. The authors employed the model Mike 21 HD to simulate the 2004 Indian Ocean tsunami.

The model 1HD is developed by the Department of Mathematics, University of Oslo/ICG, Norway for research and verification of other models. It is fully tested (grid refinement, careful assessment of features, inter-comparison of models, check against analytical solutions, benchmarks). The generation is by pre-described source functions for landslides and earthquakes and input from files. Assessment of grid resolution is required. It includes the dispersive effects and nonlinear effects in tsunami generation and propagation. The user interface is based on scripts, command driven and coded in mixed language. The model is used by University of Oslo, NGI, and ICG. The model is applied to North East Atlantic, Arctic Ocean, Norwegian Fjords, Indian Ocean, and Mediterranean.

The model GloBouss is also being developed by the Department of Mathematics, University of Oslo/Norwegian Geotechnical Institute/ICG, Norway for operational and research purposes since spring 2007 and is still in progress. The equations are presented in Pedersen and Lovholt (2008) with emphasis on the inclusion of spherical coordinates and the Coriolis force. They chose to start with the standard Boussinesq formulation, but have modified it to achieve improved dispersion properties for moderately short waves. The performance of the model is also compared to state of the art models (FUNWAVE/COULWAVE) in Pedersen and Lovholt's (2008) study. It is thoroughly tested (analysis of properties, grid refinement, inter-comparison of models, analytical solutions). The generation is by input from files. The model is suitably coded for dispersive transoceanic propagation. The user interface is command driven, front end scripts in English. The model is used by University of Oslo, NGI, and ICG and applied in most oceanic regions with major fault zones worldwide. The model is also used in tsunami modelling studies. Lovholt et al. (2008) used GloBouss for the wave propagation modeling in their study of Oceanic propagation of a potential tsunami from the La Palma Island. Lovholt et al. (2010) also carried out a research on Coupling of dispersive tsunami propagation and shallow water coastal response and combined the model GloBouss with ComMIT/MOST that is an operational shallow water tsunami model suitable for computation of coastal impact and runup. They illustrated the performance and

flexibility of the joint model approach by two case studies including inundation computations at selected cites (La Palma Island used as an example of slide generated tsunamis and Lesser Antilles example is a tsunami from a potential inverse thrust fault).

The model DPWAVES is developed by the Department of Mathematics, University of Oslo, Norway for operational and research purposes and is validated through basin oscillations, and solitary waves (Langtangen and Pedersen, 1998). The generation is by prescribed source functions for landslides and earthquakes or input from files. The model is flexible with respect to type of elements and different types of adaptive mesh can be generated. The user interface is command driven. NGI applied the model to the Indian Ocean, Paleo Barents Sea for research and to Norwegian fjords for consulting risk analyses (NGI, 2008).

2.3 Summary

Over the past decades, especially after 2004 Indian Ocean Tsunami event, a variety of tsunami propagation models have been developed, based on a variety of governing equations, numerical methods, spatial and temporal discretization techniques, and wetting-drying algorithms used to predict tsunami run-up. Available information on many of the models have been provided in the previous section. Several important points could be summarized as follows:

- Although most of the numerical models use seismic source information as the generation mechanism of tsunami, some models include landslide mechanisms as well. Models which work on the landslide generated tsunami event generally have limitations on the accurate representation of the landslide due to rigid body assumptions.
- Different equations such as shallow water, Navier-Stokes and Bousinessq equations are solved with a variety of numerical schemes. Each of these solutions require set of assumptions that could affect the performance of the models.
- Structured, unstructured and nested meshes are the most common types as mesh/grid in the models. The type of grid used by the model can determine the accuracy of representing the bathymetry/topography, accuracy of the inundation as well as the computation duration. Nested meshes have become widely used in the recent years, as different resolutions could be used in the model that can decrease the computation time.
- Some of the models presented above focus only on tsunami modelling while there are other models that could be applied to various types of hydraulic related phenomena. A number of models that are developed specifically for a location are also available.
- Most of the models cover the whole life cycle of the tsunami; from generation to propagation to inundation. However, there are a lot differences in terms of capabilities of reflecting the effects of dispersion, bottom roughness, bathymetry and land based structures. Many of the mentioned processes are still being integrated into the available modelling tools.

- Although providing universal benchmarking data is a continuous work of research, the numerical models mostly use information on historical events for validation and verification.

As real-time forecasting becomes more important, faster and more accurate numerical methods is very much sought after. Real-time warning systems rely on numerical models to predict whether an earthquake has produced a dangerous tsunami, and to identify which communities may need to be warned or evacuated. The first step of assessment of potential future hazards to assist in emergency planning and mitigation measures is also to work with reliable numerical models. Partners in RAPSODI project will continue to enhance their respective models such as NAMI-DANCE focusing on the modelling of tsunami parameters in high resolution geometries (eg. urban areas) as well as accurate computation of flow patterns.

3 Tsunami Impacts and Loads on Structures

As tsunamis approach coastlines or enter bays, they initially evolve in the classic manner predicted by linear long wave theory (Synolakis and Skjelbreia 1993). Close to the shore, nonlinear effects often become important, as the height increases and the wavelength decreases. If breaking occurs, bores often result as first documented in the 1960 Chilean Tsunami impact in Hilo, Hawaii, or as seen in the tens of amateur video clips from the beaches of Thailand, following the December 26, 2004 mega tsunami. Because the offshore wave length of tsunamis can be tens of kilometers, the resulting bores can penetrate a few kilometers inland.

Direct effects of tsunamis on coastal and marine structures can be extensive and often disastrous. Tsunami waves can (1) move entire structures off their foundations and carry them inland; (2) damage buildings through impact with vessels carried from offshore and other debris accumulated as the wave advances inland; (3) undercut foundations and pilings with erosion caused by receding waves; (4) overturn structures by suction of receding or thrust of advancing waves; and (5) cause the impact of large ships with docks during oil or cargo transfer operations, often causing fires. The damage can be quite unexpected. During the 1998 Hokkaido-Nansei-Oki Tsunami, Aonae in Okushiri was consumed by fires triggered after the waves subsided (Sumer et al., 2007).

3.1 Principal Tsunami Forces on Structures

The effects and estimation of tsunami-induced loading on near-shoreline structures have recently gained significant interest from researchers, engineers, and government agencies. Building codes do not explicitly consider tsunami loading, as it is understood that inland structures can be protected by proper site planning. However, recent catastrophic events (Indian Ocean, 2004; Solomon Islands, 2007, Japan Tsunami, 2011) indicate that tsunami loading should be considered in structural

design. A broken tsunami wave generates forces which affect structures located in its path. A comprehensive review of tsunami forces is presented by Nistor et al. (2008). Three parameters are essential for defining the magnitude and application of these forces: (1) inundation depth, (2) flow velocity, and (3) flow direction. The parameters mainly depend on: (a) tsunami wave height and wave period; (b) coastal topography; and (c) roughness of the coastal inland. The extent of tsunami-induced inundation depth at a specific location can be estimated using various tsunami scenarios (magnitude and direction) and numerical tools described in previous section. However, the flow velocity and direction is generally more difficult to estimate. Flow velocities change in magnitude, while flow direction varies due to onshore topography, soil cover, buildings and obstacles. Forces associated with tsunami consist of: (1) hydrostatic force, (2) hydrodynamic (drag) force, (3) buoyant force, (4) surge force and (5) impact of debris.

3.1.1 Hydrostatic Force

The hydrostatic force is the force of still or slow-moving water acting perpendicular onto planar surfaces. The formula to calculate the hydrostatic force per unit width, FHS, is proposed as the equation given below by the City and County of Honolulu Building Code (CCH)

$$F_{HS} = \frac{1}{2}\rho g\,(ds + \frac{up^2}{2g})^2 \quad \text{..... (3.1)}$$

where ρ is the seawater density, g is the gravitational acceleration, ds is the inundation depth and u_p is the normal component of flow velocity. Equation (3.1) accounts for the velocity head. The point of application of the resultant hydrostatic force is located at one third from the base of the triangular hydrostatic pressure distribution. Since it is assumed to be a negligible component of the hydrostatic force, FEMA 55 does not include the velocity head in its formulation. In the case of a broken tsunami wave, the hydrostatic force is significantly smaller than the drag and surge forces. However, the hydrostatic force can be important when the effect of tsunami is similar to a rapidly-rising tide (Dames and Moore 1980). Hydrostatic force is not of interest and thus, it is not considered in this deliverable other than the definitions provided above.

3.1.2 Buoyant Force

The buoyant force is the net uplift force acting through the center of mass of a submerged body vertically. Its magnitude is equal to the weight of the volume of water displaced by the submerged body.

$$F_B = \rho g V \quad \text{……. (3.2)}$$

where, *V* is the volume of water displaced by submerged structure. The effect of buoyant forces generated by tsunami flooding was clearly evident during the 2004 Indian Ocean Tsunami field observations where reinforced concrete slabs were lifted up and displaced due to buoyant forces. Buoyant forces can generate significant damage to structural elements,

3.1.3 Drag Force

As the tsunami bore moves inland with moderate to high velocity, structures are subjected to hydrodynamic forces caused by drag. Although there exists different proposed formulas to estimate the drag force, the general expression used by existing codes is given below.

$$F_D = \frac{\rho C_D A u^2}{2} \quad \ldots\ldots\ldots \text{(3.3)}$$

where, F_D is *the drag force* acting in the direction of flow and C_D is the drag coefficient that depends on the shape of the surface on which drag forces are applied, u is the tsunami bore velocity and A is the projected area of the body normal to the direction of flow. The flow is assumed to be uniform, and therefore, the resultant force will act at the centroid of the projected area A. Drag coefficient values of 1.0 and 1.2 are recommended for circular piles by CCH and FEMA 55, respectively. For the case of rectangular piles, the drag coefficient recommended by the same two codes is 2.0.

Estimation of the bore velocity remains to be one of the critical elements since the hydrodynamic force is directly proportional to the square of the tsunami bore velocity. However there is not a consensus on the selection of velocity in the literature which can vary significantly during a major tsunami inundation. One method is to assume a conservatively high flow velocity impacting the structure at a normal angle to estimate a conservative value for the drag force. Additionally, the effects of run-up, backwash and direction of velocity are not addressed in current design codes. The general form of the bore velocity is shown below.

$$u = C\sqrt{g d_s} \quad \ldots\ldots\ldots \text{(3.4)}$$

where C is a constant and d_s is the inundation depth. Various values of C were proposed by FEMA 55 (2003) based on Dames and Moore (1980), Iizuka and Matsutomi (2000), CCH (2000), Kirkoz (1983), Murty (1997), Bryant (2001), and Camfield (1980) for estimating the velocity of a tsunami bore in terms of inundation depth (*Fig. 3.1).* It can be seen that bore velocities calculated using CCH (2000) and FEMA 55 (2003) represent lower and upper bound values, respectively.

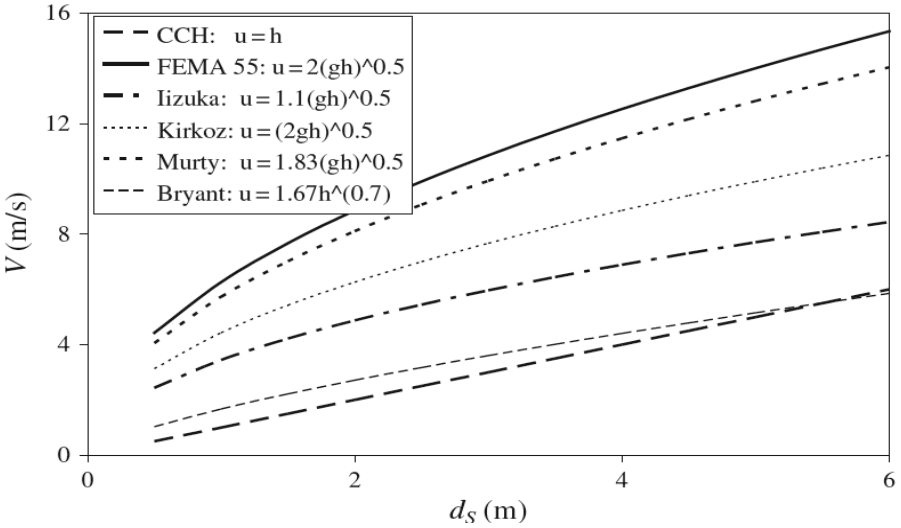

Fig. 3.1. Comparison of various tsunami-bore velocities as a function of inundation depth (Nouri et al., 2007)

3.1.4 Surge Force

The surge force is generated by the impingement of the advancing water front of a tsunami bore on a structure. There is significant uncertainty of the calculation of surge force exerted on structure due to available limited number of research. Based on research conducted by Dames and Moore (1980), CCH (2000) recommends the following expression for the computation of surge force FS on walls with heightsequal to or greater than three times the surge height (3h).

$F_S = 4.5\rho g h^2$ ……. (3.5)

where, F_S is the surge force per unit width of wall, and h is the surge height. The point of application of the resultant surge force is located at a distance h above the base of the wall. Structural walls with heights less than 3h require surge forces to be calculated using an appropriate combination of hydrostatic and drag forces for each specific situation. SMBTR (Structural Design Method of Buildings for Tsunami Resistance, proposed by the Building Center of Japan, Okada et al., 2005) recommends Eq. (3.6) for tsunami wave pressure derived by Asakura et al. (2000).

$qx = \rho g(3h - z)$ …… (3.6)

where qx is the tsunami wave pressure for structural design, z is the height of the relevant portion from ground level ($0 \leq z \leq 3$ h), ρ is the mass per unit volume of water and g is the gravitational acceleration. Integration of the wave pressure formula for walls with heights equal to or greater than 3h results in the same equation as the surge force formula recommended by CCH (Eq. (3.5)). The equivalent static pressure resulting from the tsunami impact is associated with a triangular distribution where water depth equals three times the tsunami inundation depth. The magnitude of the surge force calculated using Eqs. (3.5) and (3.6) generate a value equal to nine times the magnitude of the hydrostatic force for the same flow depth. However,

experimental research conducted by Ramsden (1996), Arnason (2005) did not indicate such differences in magnitude. Yeh et al. (2005) indicated that Eqn. (3.5) gives "excessively overestimated values". On the other hand, Nakano and Paku (2005) examined the validity of the proposed tsunami wave pressure formula given in Eq. (3.6) by extensive field surveys. The factor 3.0 in Eq. (3.6) was taken as a variable, α, and was calculated such that it could represent the boundary between damage and no damage in the surveyed data. The values of α was found to be equal to 3.0 and 2.0 for walls and columns, respectively. The former is in agreement with the proposed formulae by both CCH and SMBTR (Eqs. (3.5) and (3.6)). However it should be point out that in the use of Eq. (3.6) by SMBTR, the formula is assumed to account for all the components of tsunami wave force such as drag, etc..

3.1.5 Impacts by Floating Debris

A high-speed tsunami bore traveling inland carries debris such as floating automobiles, pieces of buildings, drift wood, boats and ships. The impact of floating debris can induce significant forces on a building, leading to structural damage or collapse (Saatcioglu et al. 2006b, c). Both FEMA 55 (2003) and CCH (2000) codes account for debris impact forces, using the same approach as given below.

$$Fi = m_b \frac{du_b}{dt} = m \frac{u_i}{\Delta t} \quad \text{..... (3.7)}$$

where Fi is the impact force, m_b is the mass of the body impacting the structure, u_b is the velocity of the impacting body (assumed equal to the flow velocity), u_i is approach velocity of the impacting body (assumed equal to the flow velocity) and Δt is the impact duration taken equal to the time between the initial contact of the floating body with the building and the instant of maximum impact force. According to FEMA 55 (2003), the impact force (a single concentrated load) acts horizontally at the flow surface or at any point below it. The impact force is to be applied to the structural element at its most critical location, as determined by the structural designer. The impact duration is calculated differently by CCH and FEMA 55. This difference has a significant effect on the magnitude of the force. For example, CCH recommends the use of impact duration of 0.1 s for concrete structures, while FEMA 55 provides different values for walls and piles for various construction types as shown in *Table 3.1*.

Table 3.1 Impact Duration of Floating Debris (FEMA55)

	Impact duration (seconds)	
Type of construction	Wall	Pile
Wood	0.7–1.1	0.5–1.0
Steel	N.A.	0.2–0.4
Reinforced concrete	0.2–0.4	0.3–0.6
Concrete masonry	0.3–0.6	0.3–0.6

Consideration must also be given to the current velocities of the runup. It is assumed that the velocity of the floating body goes from u_b to zero over some small finite time

interval Δt. Finding the most critical location of impact is a trial and error procedure that depends, to a large extent, on the experience and intuition of the engineer. The estimated current velocities of the 1933 tsunami at Kamaisi, Japan was found with a maximum value of one meter per second which was sufficient to destroy some buildings when the water depth reached a height of two meters Ishimoto and Hagiwara (1934). Shorter period tsunami waves which surge onto the shoreline, rather than rising as a uniform rise in water level, are associated with higher velocities. Keulegan (1950) and Fukui (1963) gives

$$u = Cgh \quad \ldots\ldots\ldots\ldots (3.8)$$

for the surge velocity, where h is the height of the surge and g is gravitational acceleration and C is a constant taken √2 by Keulegan and √1.83 by Fukui. In either case, the velocity would be about eight to nine meters per second for a two meter surge height.

In Yeh (2006), tsunami forces in the runup zone are evaluated by using the algorithm recently developed by Carrier et al. (2003) that is the tsunami runup onto a uniformly sloping beach with an arbitrary initial condition based on the one-dimensional, fully nonlinear shallow-water theory. This exact solution algorithm assumes no wave breaking but tsunamis sometimes break offshore. In such a case, a tsunami forms a bore prior to climbing up onto the beach. The runup of a bore was investigated analytically by many researchers (Ho and Meyer (1962) and Shen and Meyer (1963), by Hibberd and Peregrine (1979)). Yeh (2006) used the existing analytic and numeric solutions to develop the envelope curve of the maximum tsunami force distribution in the runup zone. However, the assumptions in the algorithm make the force evaluation valid only for the ideal and simplified situations; for instance, one-dimensional (1D) spatial variation on a uniformly sloping beach. In addition, the theory assumes inviscid-fluid motions in spite of the runup/rundown forming a thin layer. Although the simplified conditions do not accurately represent a real coastal environment, the proposed results could provide a convenient estimate of tsunami-force attenuation from the initial shoreline to the maximum runup location.

3.2 Tsunami Loads on Coastal Structures

3.2.1 Seawalls, Breakwaters and Bulkheads

Breakwaters and seawalls may provide protection from tsunamis. Breakwaters may decrease the volume of water flowing into a harbour and onto the coastline, and a high seawall or dike may prevent flooding of backshore areas. Proper placement of breakwaters may also decrease wave heights by changing the natural period of an inlet. Numerous instances of tsunamis damaging or destroying protective structures have been recorded therefore, care must be exercised in the design of the structures. Types of damage include movement of stones from rubble structures; erosion of dunes, embankments, and earthen dikes; scouring of backfill behind bulkheads; scouring of the sea ward base of a revetment or seawall; and overturning and sliding of structures such as caissons. The 1946 tsunami overtopped and breached the break

water at Hilo, Hawaii, removing 7.25 metric ton stones to a depth of about one meter below the water surface along nine sections of the breakwater crest with a total length of over 1,800 meters (U.S. Army Engineer District, Honolulu, 1960). Nasu (1948) developed some empirical criteria for the stability of breakwaters based on the geometric shape of the breakwater. For a breakwater with a seaward slope of 1:2.5 and a landward slope of 1:2, he gives:

$$u^2 < \frac{h_v + 0.89b}{0.0358} \quad \ldots\ldots \quad (3.10)$$

for the condition of geometric stability, where u is the current velocity in meters per second, h_v the height in meters of the vertical segment of the face of the breakwater against which the currents act, and b the top width of the breakwater in meters.

Mizutani and Imamura (2001), studied on measuring the wave force of tsunamis acting on prevention structures along the coast such as seawalls and breakwaters, carrying out hydraulic experiments, to analyze the hydrodynamic force of the tsunamis. In order to revise the existing wave force formula used for the design in the past, they introduced four types of wave pressure: kinetic, sustained (quasi-static), impact standing, and overflowing. According to Mizutani and Imamura (2001), impact standing wave pressure is observed in the collision of reflected and incident waves. Overflowing wave pressure occurs when waves running over a structure collide on the back. The values of these wave forces are found to be more significant than the kinetic and quasi-static pressures in their study. According to Mizutani and Imamura (2001), the design method should include any kinetic pressure that is significant and not negligible in the case of a tsunami attack.

In Mizutani and Imamura's study, by using the highly accurate sensor system with the appropriate intervals of time and points, the existence of impact standing and overflowing wave pressure and with a very large value in a short time and at local point are observed. The value of the impact standing wave pressure due to the collision of the reflected and incident waves is closely related to wave celerity and run-up height (Mizutani and Imamura, 2001). The equations to estimate the maximum values of kinetic, quasi-static, impact standing, and overflowing wave pressure proposed in their study are the following:

Maximum kinetic wave pressure: $$\frac{p_{dm}}{\rho_w g h} = K\frac{c^4}{g^2 H h} \qquad (3.11)$$

where p_{dm} is the maximum kinetic wave pressure, c the wave celerity, h the initial water depth, H the incident wave height, ρ_w the density of seawater, g the acceleration of gravity, and K the kinetic wave coefficient. Although Fukui et al. (1962b) proposed $K = 0.33 \sim 0.51$, it is recommended that $K = 0.12$ be used. (Mizutani and Imamura, 2001)

Quasi-static wave pressure: $$\frac{p_{sm}}{p_{dm}} = 0.14(2 + \cos\theta_1)\frac{c^2}{gH} \qquad (3.12)$$

where p_{sm} is the maximum quasi-static wave pressure and θ_1 is the angle of a sloping board. The maximum quasi-static wave pressure, p_{sm} can be considered to be related

to the maximum kinetic wave pressure, p_{dm}, rather than the wave period from the result of Mizutani and Imamura's (2001) study.
Impact standing wave pressure:

Mizutani and Imamura's (2001) observations suggest that the impact of standing wave pressure is closely related to the collision of reflected and incident waves, and also that the important parameter for reflected waves is run-up height, and for incident waves is wave celerity. Therefore, they state that a close relationship among run-up height and quasi-static wave pressure, wave celerity and kinetic wave pressure can be found. The sum of maximum kinetic wave pressure, p_{dm}, maximum quasi-static wave pressure, p_{sm}, and maximum impact standing wave pressure, p_{im}, has the following relationship

$$\frac{p_{im}}{p_{dm}+p_{sm}} = 0.5\ (\frac{g(h+H)cot\theta_1}{c^2} < 1.1) \quad \ldots\ldots\ldots\ldots\ (3.13)$$

$$\frac{p_{im}}{p_{dm}+p_{sm}} = 10cos\theta_1 - 6.6 \begin{pmatrix} Fr=\frac{c}{\sqrt{g(h+H)}} \leq 1.13 \\ \frac{g(h+H)cot\theta_1}{c^2} \geq 1.1 \end{pmatrix} \ldots\ldots\ldots\ (3.14)$$

The difference of (3.13) and (3.14) is caused by the collision of reflected and incident waves and its duration. The small collision occurs for a relatively longer time in the case of (3.13), whereas the large collision takes place for an extremely short time in the case of (3.14) (Mizutani and Imamura, 2001).

Overflowing wave pressure:

The maximum overflowing wave pressure occurs when the overflowing wave collides on the back of the structure (Mizutani and Imamura, 2001). The relationship between the maximum overflowing wave pressure and these parameters is obtained by the law of momentum conservation; this is expressed in the following relationship:

$$\frac{p_{om}}{\rho g H'_d} = A\frac{V_m H_w}{L}\frac{t_0}{t}\sqrt{\frac{2}{gH'_d}}sin\theta_2 \ \ldots\ldots\ldots\ (3.15)$$

Where p_{om} is the maximum overflowing wave pressure, V_m is the maximum velocity, the water depth on the crest is H_w, the angle of the back slope is θ_2, and the height of the models is H'_d. A is the non-dimensional overflowing pressure coefficient, $\frac{t_0}{t}$ the ratio of the time of falling water touched on the bottom after passing the top of the structure, t_0 , the duration time acting of the maximum overflowing wave pressure, t, L, the length acting of the maximum overflowing wave pressure. They also recommend that the coefficient A = 0.003.

Sea walls and bulkheads can be damaged or destroyed and Iwasaki and Horikawa (1960) noted that a quay wall at Ofunato, Japan, failed because of scouring of the backfilling, and that a concrete sheet-pile quay wall at Hachinohe, Japan, collapsed because of a lack of interlocking strength after backfilling was washed away. They

also indicated receding water may seriously scour the sea ward base of a revetment or seawall. The combination of scouring and increased hydrostatic pressure from overtop ping may cause failure. A concrete seawall between Hadenya and Mitobe, Japan, collapsed seaward. Similar failures occurred along a highway on Onagawa Bay and along a quay wall at Kamaishi, Japan. Matuo (1934) mentions a concrete retaining wall which was overturned seaward by the 1933 Sanriku tsunami. Magoon (1962) noted that scour contributed to the partial failure of a steel sheet-pile retaining wall at Crescent City, California, in 1960. The 1960 tsunami washed out concrete seawalls a meter high and created a gully about three meters deep and 27 meters wide in a highway at Hilo, Hawaii. Large stones from a seawall, weighing up to 20 metric tons, were carried inland (Eaton et ai, 1961).

Wiegel (1970) provides an empirical formula for volume of overtopping in cases where tsunamis overtop seawalls or protective dikes. The overtopping volume, V, is de fined as

$$V = 0.287 \int_{t_1}^{t_2} (\frac{1}{2} h_s \cos\frac{2\pi t}{T} - h_w)^{3/2} dt \quad \ldots\ldots\ldots (3.16)$$

where h_s is the tsunami height at the shoreline in meters, T is the wave period, t_1 and t_2 define the time interval where overtopping occurs, and h_w is the elevation of the top of the wall measured from sea level at the time the tsunami occurs; i.e., the value of h_w decreases as the tide stage increases. Caisson type structures are fairly common in the coastal zone, particularly for breakwaters in deeper water (e.g., Matsumoto and Suzuki, 1983). Common design practice for such coastal structures is usually based on static loading; i.e., if the resultant force on the structure is sufficient to cause motion, it is assumed that the structure will fail. Actual motion of a structure may or may not lead to failure. When a tsunami impacts on a structure, three different conditions are possible: the force of the tsunami may be insufficient to move the structure; the force may be sufficient to cause some rocking motion, but not failure; or the force may cause sufficient rotation for structural overturning. An initial static analysis can easily determine if incipient motion occurs (Tanimoto, 1983). If motion will occur for a given magnitude of tsunami force, it is then necessary to analyze possible motion to determine if such motion will lead to failure (Camfield, 1991).

Sumer et al. (2007) describe methods for calculating tsunami impact on marine structures directly and indirectly through harbor resonance. For tsunami forces on sea walls, they suggest the existing methodology following the classic work of Cross (1967). The force expression has two components, one is hydrostatic, the other depends on a force coefficient $C_f = 1+\tan^{1.2}\theta$, where θ is the slope of the front face of the bore. It is given by:

$$Fwall = (1/2)\,\rho\, gb\, \eta 2(x_w, t) + C_f\, \rho\, b\, \eta(x_w, t)\, C^2 \quad \ldots\ldots\ldots (3.17)$$

Where $\eta(x_w, t)$ is the wave height at the wall (distant x_w from the shoreline) and b is the width, while C is the bore speed or surge velocity. $\eta(x_w, t)$ is calculated as if the wall was not there, so presumably one solves the field equations and identifies $\eta(x_w, t)$ as the wave passes through x_w where the wall stands.

A further approach was offered by Ramsden and Raichlen (1990) as a Ph.D. study in California Institute of Technology. They performed laboratory experiments and measured the forces on a vertical wall due to the impact of a bore being triggered by a broken solitary wave. The measured force was compared with the force calculated from

$$\frac{F_T}{\frac{1}{2}\gamma b(H_1+d_w)^2} = \left(\frac{\eta+d_w}{H_1+d_w}\right)^2 + 2C_F N_F^2 \frac{\eta H_1}{(H_1+d_w)^2} \quad \ldots\ldots\ldots (3.18)$$

Where F_T is the total force on the vertical wall, η is surge profile, H_1 is the surge height, b is width of vertical wall, d_w is water depth at the wall, C_F is the force coefficient calculated as $C_F = 1 + \tan\theta^{1.2}$ and generally suggested between 1.4 and 2.1, and $N_F = \frac{c}{\sqrt{gH_1}}$ where c is the measured incident bore velocity. Ramsden and Raichlen's (1990) approach is valid if the solitary waves are triggering the tsunami break. However, since the existing numerical models do not simulate breaking well, the relations and results in their approach cannot be compared with numerical studies.

3.2.2 Other Structures

In Shuto (2009), examples of damages to coastal structures caused by tsunami-induced current are collected from documents in Japan, and classified into four types. First one is that the soil embankments near underpasses or bridge abutments are eroded by concentrating water current. Second, currents parallel to long structures can develop strongly enough to scour the structures toe and destroy them. Third, embankments made of soil are easily eroded by overflowing water of tsunamis. Finally, the toe of quay walls is unprotected against the waterfall that occurs when landed water returns and hits the nearly exposed sea bottom as tsunamis recede. When it comes to breakwaters, he states that after the 1960 Chilean Tsunami, breakwaters at Hachinohe Port were extended to narrow the entrance and limit the tsunami inflow into the harbor. When the 1968 Tokachi-Oki tsunami hit, this narrow entrance effectively decreased tsunami height in the harbor but increased the difference between water levels outside and inside the harbor. When the water level in the harbor was low by the former ebb, the next wave came to overflow the top of caissons to a water depth of about 50 cm. Violently hit by this falling water and pushed by seepage flow, the rear mound became unstable and disturbed. Then the caissons were slid or overturned under a high pressure difference that was not considered in design forces.

Docks can be damaged by a number of factors. In addition to the direct force of the tsunami and possible scour around pilings and quay walls, docks may be damaged by the uplift of moored vessels and by vessels being carried onto the docks. The 1964 tsunami damaged a dock at Crescent City, California, when the water elevation increased to two meters above the dock elevation, uplifting a large lumber barge moored to the dock (Wilson and Torum, 1968; Tudor, 1964). The buoyant force on the barge was transmitted through the mooring lines into an uplift force on the dock structure.

Earthen embankments can be destroyed if overtopped by tsunamis. Matuo (1934) reported that an earthen embankment at Yosihama, Japan, which had been constructed to protect a section of coastline, was swept away flush with the original ground level by the 1933 tsunami. Iwasaki and Horikawa (1960) indicated that a sea dike at Kesennuma Bay, Japan, failed during the 1960 tsunami because incident waves overtopped the dike and caused extensive damage at a gap in the dike when receding water gradually widened the gap. Shepard et ai (1950) mention a case where waves overtopping sand dunes cut a channel 30 meters wide and 5 meters deep.

Damage from a tsunami may also occur to *structures located at the shoreline or along river channels near the shoreline.* Bridges may be damaged by the force of the tsunami against the structure, or by scouring of the channel bottom near bridge piers. The 1964 tsunami at Seaside, Oregon, destroyed a bridge over the Necanicum River and a railroad trestle over Neawanna Creek (Spaeth and Berkman, 1972; Wilson and Torum, 1968). Shepard et al. (1950) discuss the damage to bridges and trestles from the 1946 tsunami in Hawaii. Iwasaki and Horikawa (1960) show a case in Mangoku, Japan, where a bridge support slumped almost one meter due to heavy scouring of the channel bottom.

3.3 Model tests on tsunami-induced loading

Several experiments have been performed in order to understand the performance of structures on the coast (coastal protection structures and buildings) under tsunami loads. Many of the experiments use solitary wave and bores using wave generators in long channels. These experiments are usually performed to understand the forces on the structures generated by the tsunami wave. After 2011 GEJE tsunami, it is observed that many of the failures were due to the overflow. The overflow phenomena is modelled by utilizing pumps which ensures that accurate flow depth at the structure and the duration of the overflow is being represented. These experiments are usually used to understand the failure mechanisms in case of overflow on the protection structure. Key information on some of the tsunami experiments are given in Table focusing on the aim, channel characteristics, wave generation and structure types.

Table 3.2 Summary of model test on tsunami-induced loading

Source	Aim	Channel (m)	Model Scale	Wave Generator Type	Structure Type	Wave Type
Ramsden, 1996, USA	To measure forces and overturning moments on a vertical wall	36.6*0.396*0.61	-	Piston Type	Vertical wall	Turbulent bore
Miles, 2007, USA	To test a model house under surge loading and record the uplift and compression forces	-	1/36 and 1/6	-	Scaled wooden house	Breaking waves and bores
Young et al., 2008, USA	To investigate the liquefaction potential of planar fine sand slopes during tsunami runup and drawdown	48.5*2.16*2.1	-	Tsunami Wave Basin	Fine sand beach	Breaking waves and bores
Lukkunaprasit et al., 2008, Thailand	To investigate tsunami forces on a Reinforced concrete (RC) buildings	40*1*1	-	by a sudden release of water through a controlled gate at the bottom of the water tank	Reinforced concrete (RC) buildings	-
Robertson et al., 2008, USA	To determine the effect of	48.8 x 26.5 x 2.1	-	Piston Type	A wall/flo	Generating clean

	tsunami bores on coastal and near- shore structures				or system	solitary waves
Palermo et al., 2009, Canada	To advance the existing understanding of the complex interaction between hydraulic forces and the impacted structures	10*2.7*1.4	Large Scale	Pumps with variable discharge flow	Square and circular sections	Turbulent bores due to a typical dam break phenomenon
Fujima et al., 2009, Japan	To estimate tsunami wave force acting on rectangular onshore structures	11*7*1.5	-	Piston Type	Vertical wall	A wave paddle was programmed to move back and forward slowly
Mizutani et al., 2009, Japan	To investigate drifted vessel due to a tsunami and the reflection of the tsunami from a quay wall	30*0.7*0.9	1/40	Piston Type	A quay wall	Generated as half-sinusoidal waves
Kato et al., 2011, Japan	To investigate coastal dike failures caused by the Great East Japan Earthquake failure from scouring at the landward toe is the	40*2*1.5	1/25	Overflow with pump	Dike	-

	dominant failure pattern.					
Hanzawa et al., 2011, Japan	To discuss the stability of wave-dissipating blocks of detached breakwater against solitary tsunami waves	30*0.5*1	-	Piston Type	RMB Tetrapods	-
Linton et al., 2013, USA	To observe hydrodynamic conditions and structural response for a range of incident tsunamis	104*3.66*4.57	Large Scale	Piston type wave maker with 4 m stroke	A full-scale light-frame wood wall	Idealized solitary waves
Arikawa et al., 2012, Japan	To investigate the failure modes of Kamaishi Breakwater	70*3.5*5	1/20	Overflow with pumps	Composite Breakwater	
Arikawa et al., 2013, Japan	To investigate the failure modes of Hachinohe Breakwater		1/25	Overflow with pumps	Vertical Breakwater	

3.4 Summary

Building codes do not generally explicitly consider tsunami loading, as it is assumed that inland structures can be protected by proper site planning. However significant amount of damage has been observed during 2011 GEJE tsunami which put an emphasis on proper planning of buildings under tsunami flow. Additionally, many of the coastal protection structures are designed by considering the tsunami wave height focusing on the overflow conditions. However, 2011 GEJE tsunami event showed that the forces associated with tsunami is also important in the case of sliding failure.

Additionally, once the overflow happens many additional failure modes are initiated which causes further damage to the structures. Thus it is important to consider different forces and failure modes in the design of land and coastal structures in the design phase.

Three parameters are essential for defining the magnitude and application of these forces: (1) inundation depth, (2) flow velocity, and (3) flow direction. The parameters mainly depend on: (a) tsunami wave height and wave period; (b) coastal topography; and (c) roughness of the coastal inland. The extent of tsunami-induced inundation depth at a specific location can be estimated using various tsunami scenarios (magnitude and direction) and numerical tools described in previous section. However, the flow velocity and direction is generally more difficult to estimate. Flow velocities change in magnitude, while flow direction varies due to onshore topography, soil cover, buildings and obstacles. Forces associated with tsunami consist of: (1) hydrostatic force, (2) hydrodynamic (drag) force, (3) buoyant force, (4) surge force and (5) impact of debris. Many of the proposed formulas (Table 3.3) include empirical coefficients thus there is a range of values for forces. Additionally, different design codes use different versions of the formulas when calculating the tsunami forces.

In the case of hydrostatic force, velocity head is not always included in the calculations especially when tsunami bore is expected to develop due to the fact the other forces are much more significant. Buoyant force is very important – uplift causes buildings to relocate under tsunami loading. However it is not explicitly considered at many locations to mitigate possible tsunami inundation. Hydrodynamic forces cause of breakage of several different structural parts during a tsunami event. However, the calculations depend on the area and shape of structure as well as accurate representation of tsunami wave. There exists uncertainty due to drag coefficient which depend on shape of structure such as the structure of the columns as well as reliable tsunami velocity estimation. Tsunami velocity at different locations under inundation is one of the topics that has to be further studied to increase the force calculations in the design of structures. The proposed formulas all have empirical coefficients thus there is a range of values for numerical prediction of tsunami velocity. One can either use conservative values – or work with range which actually gives 100% difference in terms of velocities. Additionally, the effects of run-up, backwash and direction of velocity are not addressed in current design codes.

Table 3.3. Summary of the Reviewed Tsunami Loads

Source	Type of Load	Formula
City and County of Honolulu Building Code (CCH) Alternatively, FEMA 55	The hydrostatic force	$F_{HS} = \frac{1}{2}\rho g\,(ds + \frac{up^2}{2g})^2$
CCH (2000), FEMA 55 (2003)	The buoyant force	$F_B = \rho g V$
CCH (2000), FEMA 55 (2003)	The drag force	$F_D = \frac{\rho\, C_D A\, u^2}{2}$
FEMA 55 (2003)	Bore velocity	$u = C\sqrt{g d_s}$
Dames and Moore (1980), CCH (2000)	The surge force	$F_S = 4.5\rho g h^2$
Asakura et al. (2000),Okada et al., 2005	Tsunami wave pressure	$qx = \rho g(3h - z)$
FEMA 55 (2003) and CCH (2000)	Debris impact force	$Fi = m_b\frac{du_b}{dt} = m\frac{u_i}{\Delta t}$
Keulegan (1950)	Surge velocity	$u = \sqrt{2gh}$
Fukui (1963)	Surge velocity	$u = \sqrt{1.83(gh)}$
Nasu (1948)	Current velocity	$u^2 < \frac{h_v + 0.89b}{0.0358}$
Mizutani and Imamura (2001)	Maximum kinetic wave pressure	$\frac{p_{dm}}{\rho_w g h} = K\frac{c^4}{g^2 H h}$
Mizutani and Imamura (2001)	Quasi-static wave pressure	$\frac{p_{sm}}{p_{dm}} = 0.14(2 + \cos\theta_1)\frac{c^2}{gH}$
Mizutani and Imamura (2001)	Impact standing wave pressure	$\frac{p_{im}}{p_{dm} + p_{sm}} = 0.5\ (\frac{g(h+H)cot\theta_1}{c^2} < 1.1)$
Mizutani and Imamura (2001)	Impact standing wave pressure	$\frac{p_{im}}{p_{dm} + p_{sm}} = 10cos\theta_1 - 6.6\begin{pmatrix} Fr = \frac{c}{\sqrt{g(h+H)}} \le 1.13 \\ \frac{g(h+H)cot\theta_1}{c^2} \ge 1.1 \end{pmatrix}$

Mizutani and Imamura (2001)	Overflowing wave pressure	$\frac{p_{om}}{\rho g H_d'} = A\frac{V_m H_w}{L}\frac{t_0}{t}\sqrt{\frac{2}{gH_d'}}\sin\theta_2$
Wiegel (1970)	Overtopping volume	$V = 0.287\int_{t_1}^{t_2}(\frac{1}{2}h_s\cos\frac{2\pi t}{T} - h_w)^{3/2}dt$
Sumer et al (2007)	Tsunami force on sea walls	$Fwall = (1/2)\rho\, g b \eta 2(x_w t) + C_f \rho\, b \eta(x_w t) C^2$
Ramsden and Raichlen (1990)	Tsunami force on a vertical wall	$\frac{F_T}{\frac{1}{2}\gamma b(H_1+d_w)^2} = (\frac{\eta+d_w}{H_1+d_w})^2 + 2C_F N_F^2\frac{\eta H_1}{(H_1+d_w)^2}$

The applicability of the presented formulas depend on the data that the respective researcher has worked with. Thus, detailed information can be found in the referenced documents. The formulas related with tsunami impact on coastal structures given above are the ones available in literature by the time of 2014 (time of deliverable D1 publication). These should be modified following the FEMA publications (expected in 2016) and Japanese guidelines in late 2015.

There is significant uncertainty of the calculation of surge force exerted on structure (walls) due to limited number of research. A combination of hydrostatic and drag forces for each specific situation has to be performed for more reliable calculations. There are some model tests to verify the proposed formulas. However it is seen that formulas might be very conservative. Surge force also depends on tsunami velocity which requires further study as mentioned before.

Considering tsunami loads on coastal structures such as breakwaters, the available design codes do not integrate tsunami loads explicitly. Thus the performances of these structures are assessed in the field as in the case of 2011 tsunami. The main function of coastal structures against tsunamis is to prevent overflow. Thus most of the time the design consideration is based on historical events or model results from possible tsunami scenarios. However, tsunami loads can cause damage on the structure (e.g. slope instability) and in return initiate overtopping during later stages due to long duration of tsunami waves. Additionally, once overflow occurs, other types of failure modes can be seen such as scouring which further increases the damage. Design codes for coastal structures such as breakwaters are focused on wind waves and storm surges since the tsunami events does not occur frequently. Since experiments on the performance of coastal structures under tsunami loading and overflow have gained attention recently, most of the information on failure modes are based on the observations and field surveys of the latest tsunami events. However, the exact sequence of many of the damages observed has not been understood yet. Also not every type of coastal structure has been analyzed in detail for every type of failure mode. Thus it is very important to further investigate the performance of

coastal structures and derive relationships that can be included in the design codes as future work.

4 Failure Modes

4.1 Introduction

Events such as the 2011 Great East Japan Earthquake Tsunami or the 2004 Indian Ocean Tsunami are important for future tsunami preparation to classify various modern counter measures against mega-tsunamis. For example, the 2011 Tōhoku Earthquake and Tsunami was the first case where modern, well-developed tsunami countermeasures were put to the test for such an extreme event. One of the most important issues in the natural sciences, engineering, and social sciences is to understand the relationships between inputs (local tsunami occurrence) and outputs (local damage). For future improvement of tsunami disaster countermeasures, much can be learned from such kinds of catastrophic events. Therefore, field surveys are important for understanding the event and for planning future tsunami-disaster reduction. Many surveys were conducted after these events by several researchers in collaboration with universities, institutes and other organizations consisting of members from different fields of the natural sciences, tsunami engineering, coastal engineering, and tsunami-related research throughout both Japan and other countries to understand the collapse phenomenon of coastal structures and to clarify the mechanism of their failures related with tsunamis in particular.

The frequent occurrence of typhoons, storm surges and tsunami led to the development in Japan of some of the most extensive coastal defences in the world. Typical coastal structures of jetties, groins, and breakwaters (both detached and submerged) may be seen along the coastline, in addition to significant land reclamation projects. Fraser et al. (2013) presented observations of damage to buildings (including vertical evacuation facilities) and coastal defences in Tōhoku due to the March 11th 2011 Great East Japan earthquake and tsunami event following investigation by a post-tsunami field mission, Earthquake Engineering Field Investigation Team (EEFIT), at 10 locations in Iwate and Miyagi Prefectures. The rupture process resulted in significant deformation of the sea bed over a large area and that generated the tsunami. This deformation occurred as close as 70 km to the Tōhoku coastline, leading to relatively short tsunami arrival times in the three worst-affected prefectures: Iwate, Miyagi, and Fukushima. Observations show that many sea walls and breakwaters were overtopped, overturned, or broken up, but provided some degree of protection. They show the extreme variability of damage in a local area due to inundation depth, flow direction, velocity variations and sheltering.

Some researchers from different universities and institutions prepared a knowledge note series in 2012 which is a product of the staff of The World Bank with external contributions as the outcome of the Learning from Megadisasters project of the Government of Japan and the World Bank Group. Based on their first knowledge

note which covers structural measures against tsunamis, dikes are both necessary and effective in preventing ordinary tsunamis, which are relatively frequent, but they are of limited use against the extreme events that occur less frequently. Japan's Tohoku region built 300 kilometers of coastal defense over the course of 50 years. (World Bank Knowledge Note 1-1, 2012). During the GEJE (Great East Japan Earthquake), the defensive structures along the coast suffered unprecedented damage: 190 of the 300 kilometers of coastal structures collapsed under the tsunami. In some areas they did serve to delay the arrival of the waves, buying extra minutes for people to evacuate. Certain breakwaters were also effective in mitigating damage from the tsunami. The breakwater at the mouth of Kamaishi Bay in Kamaishi City, Iwate, was the world's deepest breakwater. Although destroyed by the GEJE tsunami, it reduced its force, and therefore its height, by about 40 percent and delayed its arrival by some six minutes, allowing more time for people to evacuate to higher ground.

4.2 Seawalls and revetments

Coastal populations of Tōhoku were among the best prepared in the world with respect to tsunami, with extensive sea defences including sea walls constructed specifically for protection against tsunami. With wave heights sufficient to overtop and breach coastal defences, the 2011 tsunami caused extensive damage to residential areas, commercial and industrial facilities, agricultural land and infrastructure.

Fraser et al. (2013) presented their field observations of damage to coastal defences in Tōhoku due to the March 11th 2011 Great East Japan earthquake and tsunami. Sea walls designed for tsunami and standing 10 m high dominate the landscape of Taro and they were almost all toppled from their positions and the only parts of the wall left standing were some buttress supports and blocks around the gates (The 2011 Tōhoku EarthquakeTsunami Joint Survey Group 2011). The coastline in Sendai City has the main defence being concrete block revetments along Arahama Beach. The concrete defences at Arahama Beach had failed in several places and the sand infill had been washed out, while concrete blocks had been removed and washed up to landward into the coastal pine forest. The beach in Yamamoto Town had also a concrete block revetment. Both sides of the revetment comprised a concrete lattice in-filled with concrete blocks and natural vegetation. At several locations along the revetment, there were breaks in the reinforced lattice and most of the concrete blocks were missing. Scour on the leeside was a main cause of embankment failure.

Hydraulic control structures and seawalls in Otsuchi village along the Sanriku ria coast were completely overtopped during the inundation. (Mori et al, 2013).

Jayaratne et al. (2013)'s study is another one which highlighted critical failure mode of coastal structures due to the 2011 Great Eastern Japan Earthquake Tsunami. A curved 2.5 m high concrete seawall in the east side of Ishinomaki port was one of the damaged structures found in the field survey. Two large scour profiles at the leeward slope extended about 60.0 m in length along the seawall. The massive concrete platform placed at the toe of the leeward slope disappeared due to the tsunami,

leading to two scour holes being created. The destructive mechanism in the east side of Ishinomaki was quite similar to that at the west side, though the degree of damage in the leeward slope appears to be dependent on the size and shape of structural elements.

Yeh et al. (2012) is another study of tsunami effects on coastal infrastructure and observed several failure patterns of coastal structures (seawalls) along the Sanriku coast due to the 2011 East Japan Earthquake and Tsunami. As they state, flow induced suction pressure near the seawall crown could have caused the failure of concrete panels that covered the infill. Remarkable destruction of upright solid-concrete type seawalls was closely related with the tsunami induced scour and soil instability. They found that soil instability played a major role in the failures. For the mound-type seawall in Kanahama, the centrifugal pressure force induced by the overtopping flow is capable of removing the concrete panels covered the rear face of the seawall. Furthermore, the fast flow velocities with intense turbulence resulted in severe undermining damage in the rear face of the seawall, as well as formation of a large scour hole behind. The solid upright type seawall in Kirikiri was destroyed during the tsunami's return-flow phase. Scouring and undermining actions are the primary cause of the failure. The similar upright type in Hakozaki was found to be almost undamaged. Unlike the one in Kirikiri, the seawall toes in both front and rear sides are protected with 2-m wide concrete flanges. These concrete flanges must have prevented the toes (especially the rear side) from being undermined. Regardless of the type of seawall, protection of the rear-side surface and the toe appears to be critical for avoiding failure when and if tsunamis overtop a seawall.

Earthquake Engineering Research Institute (EERI) published a report on the effects of Japan Tsunami of 2011. The American Society of Civil Engineers (ASCE) has sponsored several reconnaissance teams to survey effects of the great East Japan earthquake and Tōhoku tsunami. The performance of coastal defensive structures during the 2011 Tōhoku event was analyzed together with several other subjects. First of all, as stated in the report, irrespective of population, the majority of coastal communities north of Sendai had seawalls to mitigate tsunami effects. The seawalls were constructed at different times and in different ways. The height of the recent tsunami was greatly affected by the coastal bathymetry and local topography and, in all cases surveyed, it exceeded the design height of the tsunami defensive walls and gates by a significant margin—sometimes up to twice their height. The overtopping frequently created a breaching failure, resulting in nearly complete destruction of most low-rise buildings in low-lying communities. However, it appeared that there could have been even greater spatial damage had there been no seawall protection at all. A common tsunami protection wall consisted of a compacted earth dike protected by concrete slabs on both the offshore and onshore slopes. During overtopping, the concrete panels were often stripped from the earthen dike, which then eroded rapidly to allow free passage of the inbound and outbound tsunami flow. The concrete panels were often carried inland by the flow, leading to impact damage to the buildings they were meant to protect. Another common seawall construction consisted of massive gravity walls constructed of monolithic concrete blocks. There were no signs of

continuity between adjacent blocks, so the design relied on each block acting as a separate gravity wall segment. Many of these walls failed due to massive scour of the onshore toe of the foundation caused by overtopping. In some cases the concrete gravity seawalls were overturned by return flow rather than by the incoming tsunami. Notable exceptions to the above failures were seawalls using reinforced concrete construction with sound foundations. Although these walls had a moderate amount of overtopping, they did not fail structurally, so were able to provide a pronounced mitigating effect on tsunami damage behind them.

4.3 Sea Dikes

According to Jayaratne et al. (2013), the south side of the sea dike at Higashimatsushima was partially damaged as a result of the 2011 event and was temporarily protected by a plastic blanket. There was some trace of scour failure at the leeward slope and toe at the south of Higashimatsushima and the researchers noticed that under the on-going tsunami recovery process the leeward face of south side had been reinforced with new rock and plastic sheets as a temporary protection cover. They also noticed severe damage to the leeward face and toe of the sea dike at Soma city. Diverse failure patterns were observed from the north to the south side, resulting in partial to total failure of the leeward face due to scour. The slabs that the leeward slope was built were completely removed and scattered over an ample area, creating large scour holes at the toe. It was clear from the failure in the leeward face that this dike was initially designed to withstand storm surge conditions and not tsunami attack. The leeward slope and toe of sea dike at Iwanuma city completely collapsed due to the effects of the tsunami attack. The seaward slope of this dike was covered with tsunami deposit and a vegetation layer at the time of survey and there was no indication of failure of the seaward slope. As stated in the study, it was clear from the initial design that these dikes were built to protect against water overflow under storm surge conditions. The crest of the dike at Yamamoto city was covered with a thick tarmac surface and a sequential collapsing pattern of crest at the leeward end was noticed. It was believed that scour at the under layer of the leeward slope took place by the infiltration of tsunami overflowing water through these sequential holes on the crest. The coastal defences at Watari city consisted of a rubble mound revetment placed directly in front of the sea, and a curved concrete sea dike located about 13.43 m away from the leeward slope of revetment. Jayaratne et al. (2013) measured a 4.06 m deep scour hole at the leeward toe of the curved coastal dike. They believe that the main purpose of having a composite coastal defence scheme in this area was to reduce the inundation distance, particularly by the use of a second structural element (a curved wall). The failure mode of coastal dikes in Watari city appeared to be similar to that at Soma city.

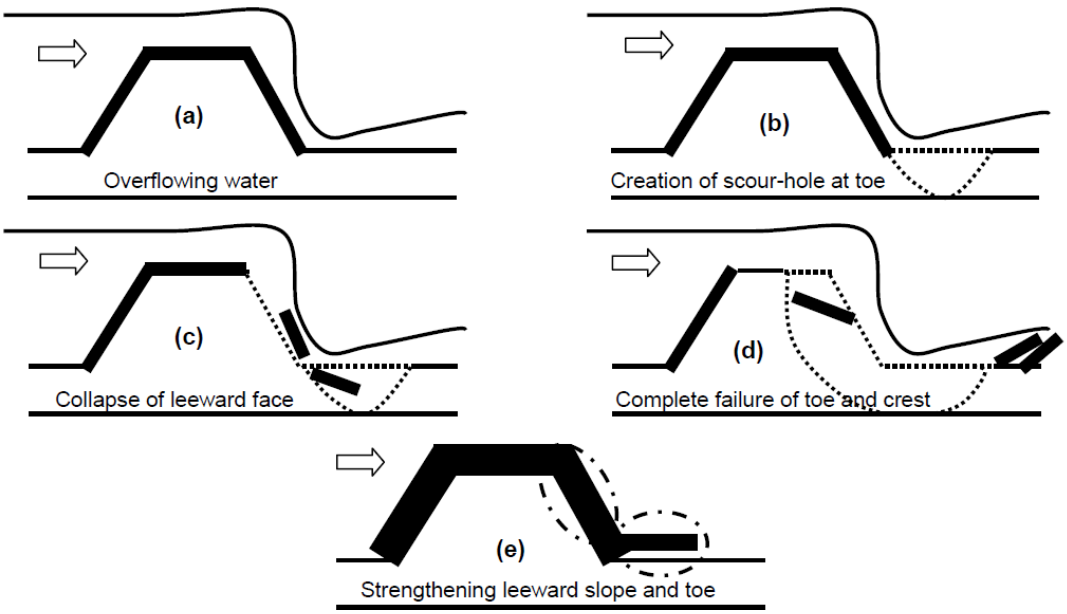

Figure 3.2 Stages of sea dike failure at Miyagi and Fukushima prefectures a) Overflowing water, b) Creation of scour-hole at leeward toe, c) Failure of leeward slope, d) Complete failure of crest, leeward slope and toe, e) Recommended section. (Jayaratne et al., 2013)

Kato et al. (2012) also investigated the failure mechanism of coastal dikes and sea walls induced by the Great East Japan Earthquake Tsunami. Based on the results of their field surveys, they state that coastal dike failures caused by the Great East Japan Earthquake were classified into eight patterns. The results of hydraulic model experiments related to major failure patterns reinforced the proposed failure processes. In addition, the aggregated length of each failure pattern showed that failure from scouring at the landward toe is the dominant failure pattern. They conducted their field surveys along the shoreline in Iwate, Miyagi, and Fukushima Prefectures. They also carried out hydraulic model experiments to understand the failure mechanisms of the coastal dikes. The resulting failure patterns are as the followings:

1. *Failure from scouring at landward toe:* The landward toe of the coastal dike was scoured in many areas where the dike or seawall was not completely washed away and where tsunami run-up induced scouring at the landward toe, resulting in the destruction of landward armor and the dike body. Based on the results of field surveys and physical experiments, the process of failure from scouring at the landward toe can be summarized as shown in *Fig.3.3* according to the authors.

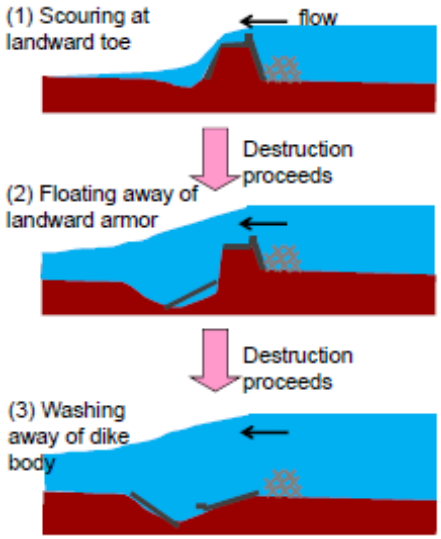

Fig.3.3. Failure process originating from scouring at landward toe (Adapted from: Kato et al., 2012)

2. *Failure from the crown or the top of landward armor:* Failure of the landward slope or crown armor was observed by the team even where the landward toe was not scoured. On the Kanahama Coast, the upper part of the landward armor floated away, while no obvious scouring was seen on the landward side of the coastal dike whereas on the Omagari Coast, the crown armor was washed away, but there was no damage to the seaward and landward armor. One of the main factors related to this pattern is negative force acting on the landward armor during tsunami runup. This negative force might be caused by fast flow at the top of the landward slope.

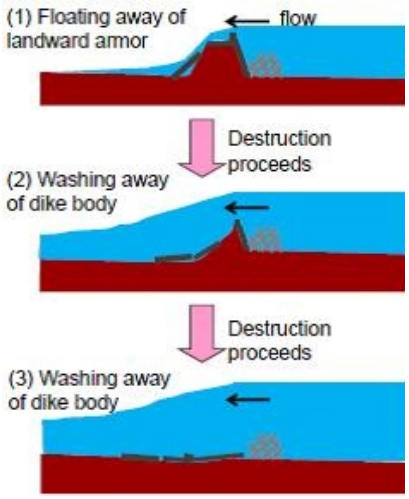

Fig. 3.4. Process of failure from the crown slope or the top of the landward armor (Adapted from: Kato et al., 2012)

3. *Parapet failure induced by tsunami run-up:* Concrete parapets were installed along the shoreline to mitigate wind-wave overtopping, but some of the parapets were broken by tsunami run-up. This pattern may occur if shear stress induced by the wave force acting on the parapet during tsunami overtopping is larger than the shear strength of the parapet joints.

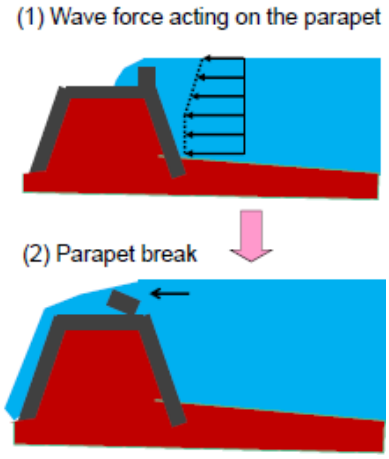

Fig. 3.5. Process of parapet failure induced by tsunami run-up (Adapted from: Kato et al., 2012)

4. *Failure from scouring at seaward toe:* Seaward flow over the coastal dike may cause scouring at the seaward toe of the dike as also pointed out in previous studies (e.g., Noguchi et al. 1997). On the Mizuumi Coast, Iwate Prefecture, the seaward armor of the coastal dike was broken and the dike body was washed away. Seaward flow during tsunami drawdown caused scouring at the seaward toe of the coastal dike and revetment. Scouring at the landward toe affected the stability of the seaward armor, resulting in floating away of seaward armor and breaching of the dike.

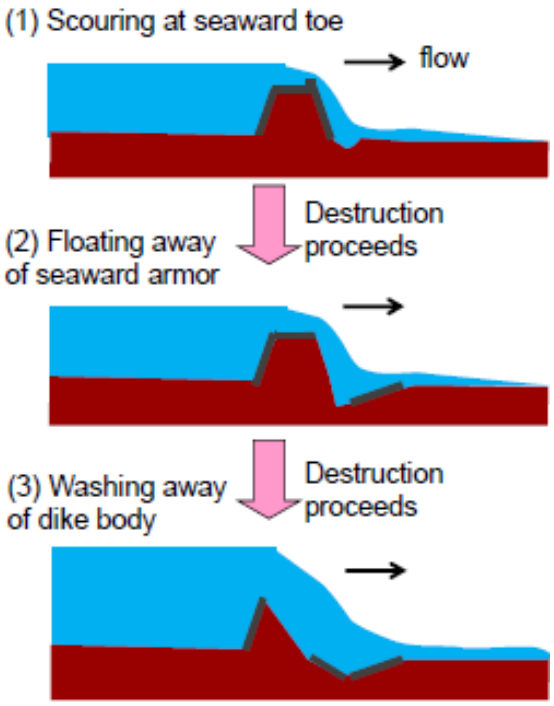

Fig. 3.6. Process of failure from scouring at seaward toe (Adapted from: Kato et al., 2012)

5. *Parapet failure induced by tsunami drawdown:* Similar to tsunami run-up, tsunami drawdown also results in wave forces acting on the parapet leading to parapet failure. Parapets are designed not for tsunami forces from the land but for wave forces from the sea.

6. *Seawall overturning by tsunami run-up:* Overturning of a seawall which was observed on the Ryoishi Coast, Iwate Prefecture may occur if the overturning moment induced by the wave force on the seawall during tsunami runup or drawdown is larger than the resistance moment due to the weight of the seawall.

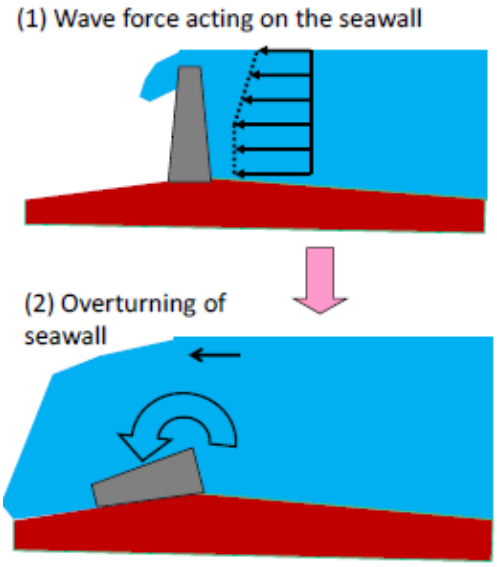

Fig. 3.7. Process of seawall overturning (Adapted from: Kato et al., 2012)

7. *Seawall overturning by tsunami drawdown:* Wave forces act on the seawall also during the tsunami drawdown stage. As with the previous pattern, seawall failure may occur due to the overturning moment.

8. *Mainly by seismic motion:* Tsunami was the dominant force for coastal dike failure in the earthquake; however, some coastal dikes and revetments were damaged mainly by seismic motion and ground liquefaction. However, on the coasts where tsunami waves were relatively high, the damage caused by seismic motion would likely be hidden by tsunami damage after the earthquake.

Kortenhaus et al., 2002 also performed a detailed analysis of failure modes for sea dikes and derived a complete set of limit state equations for the description of failure scenarios of sea dikes. They then used these models and equations to calculate the respective failure probabilities and the overall failure probability by fault tree approach. They give the failure mechanisms that have been identified by them as those may lead to breaching of sea dikes based on the results of a failure analysis of sea and estuary dikes (Oumeraci and Schüttrumpf, 1999). The procedures are as the following for the seaward and the shoreward sides.

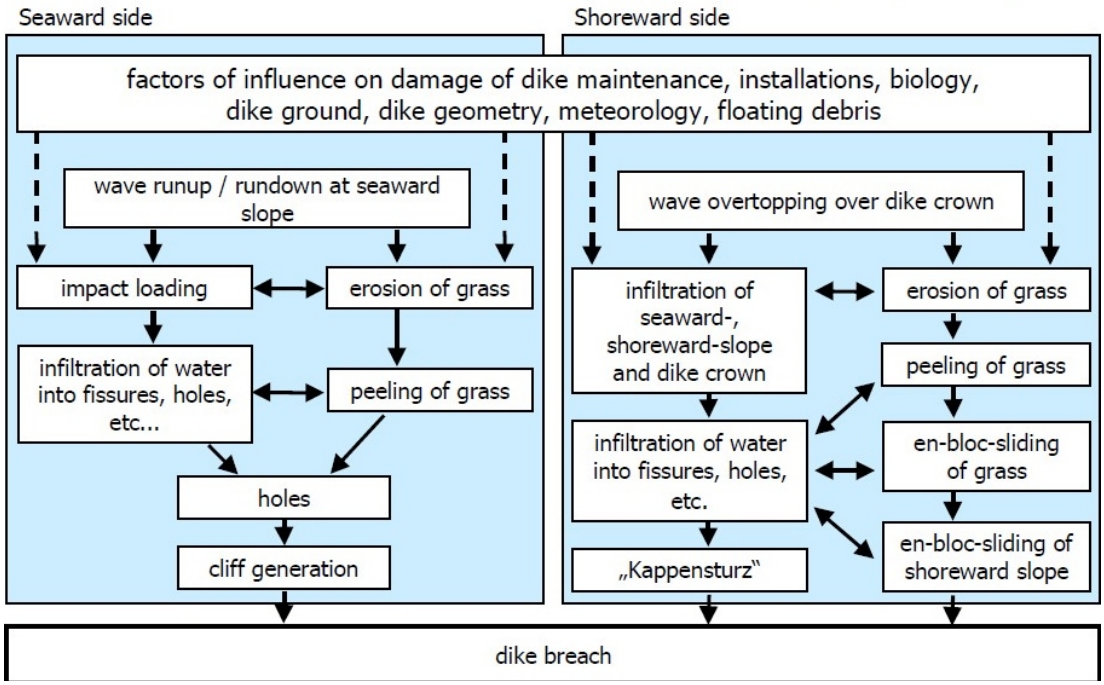

Fig. 3.8. Failure modes of sea dikes eventually leading to dike breaching (adapted from Kortenhaus et al., 2002).

4.4 Breakwaters

On March 11th a total of 8,500 m of breakwaters collapsed (Yagyu 2011), including the newly-completed tsunami breakwater in Kamaishi City designed to withstand a tsunami of 5–6 m. They were not effective in stopping the waves from overtopping, and in many situations suffered catastrophic failure. Takahashi et al. (2011) suggested that in future, rather than building even bigger structures, coastal defences should remain of similar size, but with special attention given to their stability in order that they survive even a huge tsunami despite being overtopped. The rationale for this is that a defence that is overtopped but survives is better than no defence at all.

Fraser et al. (2013) states that, despite the fact that the breakwaters were severely damaged, it is estimated that the breakwater in Kamaishi City reduced the height of the tsunami by 40% (from 13.7 to 8 m), delayed the tsunami arrival time onshore by 6 min allowing more time for evacuation, and reduced run-up from (a simulated height of) 20.2 m to the observed 10 m (Kazama 2011). In Ōfunato City, Iwate Prefecture, and prior to the tsunami, there were also two breakwaters at the mouth of the bay, 540 m in combined length, which collapsed completely on March 11th (Yagyu 2011). Onagawa Town had two breakwaters situated eastside of the harbour at the mouth of the bay; post-tsunami aerial photographs indicate that the breakwaters were destroyed by the tsunami and only a few caissons remain visible above water level on the south section.

Arikawa et al. (2012) and Arikawa and Shimosako (2013) have studied the failure mechanisms of breakwaters of Kamaishi (composite breakwater) and Hachinohe (vertical breakwater). They have modelled both of the breakwaters and studied the safety factor related to overturning, sliding, scour at the toe (leeside) and bearing capacity failures due to tsunami overflow. They have showed that for the cause of Kamaishi breakwater failures where many of the caissons had slided and/or overturned, were several: [1] Dynamic water pressure as wave force, [2] Water level difference between the outside and inside of the harbor, [3] Scouring of the foundation mound caused by overflowing and joint flow velocity and [4] Decline of bearing capacity caused by increase of pore water pressure. They assumed that dynamic wave pressure was less significant and focused on water level difference (overflow) and the scouring for model tests. The test results showed that major cause of the collapse of the breakwater at the Kamaishi Harbor mouth is the water level difference, and that the fall of the back surface pressure during overflow and rise of instability of the mound by scouring made them more vulnerable to collapse at the same time as it scattered their collapse. For the case of Hachinohe breakwater, it was revealed that the failure modes are sliding mode, which occurs when friction resistance is exceeded by external force, overturning mode caused by rotation moment, and bearing capacity failure mode in which the foundation is destroyed by caisson load. However, in the case where scouring of the foundation part in particular has reached the caisson bottom, this causes the caisson to overturn. And this is called foundation scouring mode.

Mori et al. (2013) also studied 2011 Tōhoku Earthquake, tsunami damage and its relation to coastal protection along the Sanriku Coast. They emphasize that tsunami barriers (onshore and offshore breakwaters and natural tsunami barriers) were severely damaged, and the extent of inundation was underestimated in several areas. The coastal area in Otsuchi village was completely destroyed as the tsunami destroyed the breakwater and propagated inland along the Otsuchi and Kotsuchi Rivers. Hydraulic control structures and seawalls were completely overtopped during the inundation.

According to Jayaratne et al. (2013)’s study, large concrete armour units had been placed in front of the seaward slope of the breakwater at Ishinomaki Port. It was found that the primary armour units on the seaward slope were displaced and scattered in front of the breakwater, and some units were buried under tsunami deposits, though there was no indication of damage to the front slope. The reason for this destructive pattern could be due to the overflowing pressure acting on the crest and leeward slope of the structure.

Esteban et al. (2013) states that field surveys of recent events such as the 2011 Great Eastern Japan Earthquake Tsunami and 2004 Indian Ocean Tsunami have shown flaws in the design of protection structures. In Esteban et al.’s (2013) work, the authors have set out to improve the accuracy of the formula of Esteban et al. (2012) by expanding the analysis to a number of other ports that were affected by the 2011 Great Eastern Japan Earthquake Tsunami and the 2004 Indian Ocean Tsunami.

The 2011 Great Eastern Japan Earthquake and Tsunami disaster was so large that it has prompted considerable re-thinking amongst the Japanese Coastal Engineering Community, which has now started to classify tsunami events into two different levels (Shibayama et al., 2013), according to their level of severity and intensity. Level 1 Events would have a return period of several decades to 100+ years and be relatively low in height, typically with inundation heights of less than 7-10m. Level 2 Events on the other hand would be less frequent events, typically taking place between every few hundred to a few thousand years. To derive a formula for the design of breakwater armour units the authors (Esteban et al., 2013) used real-life failures of armour units at several locations along the South West of Sri Lanka (for the 2004 Indian Ocean Tsunami) and northern Japanese (for the 2011 Great Eastern Japan Earthquake and Tsunami) coastlines. Firstly, they surveyed the damaged ports in Sri Lanka which was hit by a massive tsunami triggered by a 9.0 magnitude earthquake off the coast of Sumatra on 26 December 2004. Then, they analysed the damage in Japanese Ports and during the field surveys, it appeared that composite breakwaters (those protected by armour units such as Tetrapods) were far more resilient than simple caisson breakwaters. It appears that the armour behaved as designed at dissipating the impact of the tsunami wave forces on the seaward side of the caisson, although damage to armour units was also recorded for several composite breakwaters. Also, evidence from the failure of coastal dykes appear to indicate that many structures fail due to the overtopping effect of the tsunami, which can cause scour at the landward side of these structures. Similarly, rubble mound structures might be more vulnerable to this scouring at the back than caissons, which are more massive and can resist this effect, provided that the toe of the structure does not fail. As the authors judging from video footage of the 2011 Great Eastern Japan Earthquake and Tsunami, wave overtopping is a complex phenomenon, which might actually represent the defining failure mode. A prolonged overflowing effect would generate a very intense current, and many structures along the Tohoku coastline appeared to have failed due to erosion of the landside toe of the structure. This has led some researchers (Kato et al., 2012; Sakakiyama, 2012; Hanzawa, 2012) to state that the failure mode is directly related to this overflowing current. Nevertheless, the initial impact of the wave also has an effect on the breakwater armour, and it would appear logical that once this initial wave shock has been absorbed, the overflowing current would probably have no effect on the armour units. The exact failure mechanism for each of the breakwater types is still unclear, and whether armour units were displaced by the incoming or the outgoing wave could not be easily established for any of the field failures recorded. Therefore, the authors carried out some preliminary laboratory experiments which appear to indicate that although the incoming tsunami wave can cause some movement to the caisson, the major failure mode of the armour could occur as a result of the outgoing wave and the situation in their experiments can be seen below:

Fig.3.9. Overtopping of a composite breakwater by incoming tsunami wave (note no armour damage) Adapted from: (Esteban, Miguel, et al., 2013)

Fig.3.10. Overtopping of a composite breakwater by outgoing tsunami wave (note the heavy damage) Adapted from: (Esteban, Miguel, et al., 2013)

Following the 2011 Great Eastern Japan Earthquake and Tsunami, there is a general perception that tsunami counter-measures must be designed to fail in a non-catastrophic way, even against Level 2 events. Therefore, it is recommended by Esteban et al. (2013) that partial failure should be accepted when designing important structures against the more extreme Level 2 tsunami events. However, only limited damage should be required for the smaller and more frequent Level 1 events.

4.5 Other Structures and Coastal Protection Elements

According to Fraser et al. (2013)'s study regarding their field observations on the 2011 event, the tsunami at Kesennuma flowed north up the bay, arrived at the harbour as a fast-flowing rising tide (Japan Coast Guard 2011) and overtopped harbor walls and river defences. Significant damage was sustained along the western shore of the bay (on the eastern side of the river) and in the northern area of the city at the head of the bay. Embankments provided a large degree of protection to some parts of the survey area as no scour or slope failure was observed at these embankments and in both cases tsunami damage to buildings behind the embankments was substantially lower than in front. The impact of embankments was entirely related to their position and height relative to tsunami inundation depth; however, as stated in the study, these observations provide evidence that in low to moderate inundation depths, placement

of infrastructure on embankments can limit damage to both infrastructure and structures in the lee of the embankment. The coastal defences in Minami-Sanriku Town consisted of two flood gates across the two river channels; the concrete pillars of these gates remain standing although the attached steel operating components were washed away (Fraser et al, 2013). The beach in Yamamoto Town had pine coastal forest immediately inland. Pine trees of the coastal forest were largely destroyed by the tsunami: they had bent over and trunks were snapped very close to the base. The coastal forest provided substantial amounts of debris which was seen to cause structural damage to a steel frame agricultural building located 1 km inland.

Mori et al. (2013) analyses three different bays—Rikuzen-Takata, Otsuchi, and Kamaishi—along the Sanriku ria coast. They give information about Rikuzen-Takata which had a natural sandy beach with 80,000 pine trees as a part of a coastal protection plan. Because of the reliance on the pine trees and sandy beach as a natural buffer, the coastline of Rikuzen-Takata was protected by a breakwater of relatively low height (5 m) compared to other regions. However, this natural protection was completely destroyed except for one pine tree. There was more than 100 m of shoreline loss due to a combination of subsidence and erosion from the tsunami.

Nagasawa and Tanaka (n.d.) studied damage of the civil structures with massive geomorphic change caused by Tōhoku-Pacific Ocean Earthquake and Tsunami in 2011. In addition to that the strong wave power and flow generated by the run-up of it has destroyed many sea and river embankments and buildings in coastal area, they caused a large-scale geographical variation. According to their field survey, after 2011 tsunami, the shore protections in Oisehama beach were entirely collapsed and the parts of it moved seaward and the sand of beach were also washed away. At the result, the coastal-line moved landward about from 50 to 200m. There were coastal forest and rice fields, and houses along the street behind the beach. But almost all of those in inundated area were washed away due to the tsunami. They state that as it is understood from the aerial photographs of the Oisehama beach area, almost all shore protections, except the east part, were destroyed and washed away. And the coast-line is moved landward from revetment normal before disaster. The objects like island in the sea are parts of destroyed revetment. Therefore, it is thought that the destroyed revetments were moved seaward by tsunami flow. They estimate that the tsunami external force acted on the revetments seaward and the revetment fell down seaward and destroyed. The length of coastline along which the revetments were destroyed due to tsunami flow is about 1km in Oisehama beach, and the sands of the beach were eroded seriously. But one important thing is that the serious erosion did not occur at the east end of the beach whose shore protection was not destroyed. As a result, the places where the structural damages with massive geomorphic change due to tsunami occurred were low-lying area and river mouth in which the tsunami flooded in large and deeply and the flow concentrated on the low-lying point such as old flow paths and small channels when the tsunami rushed out to sea. Also, it is thought that the tsunami rushing back out to sea associated with massive overflow and front scours of the shore protection caused the collapse of the shore protection. However, they state that, it is necessary to study in detail when the revetment have

actually collapsed, because of that the tsunami have attacked the coast area repeatedly.

4.6 Failure Mode Matrix

The previous sections have described several failure modes reported from different authors. In the following, an overview of the different failure modes will be given with a short example, the source of information, and further details.

For Table 4.1:
1-A, 2-A, 3-A *Overflow - Functional Failure:* The coastal area in Otsuchi village was completely destroyed as the tsunami destroyed the breakwater and propagated inland along the Otsuchi and Kotsuchi Rivers. Hydraulic control structures and seawalls were completely overtopped during the inundation. (Mori et al. (2013)

1-J *Revetments – Sliding:* Nagasawa and Tanaka (n.d.) estimate that the tsunami external force acted on the revetments seaward and the revetment fell down seaward and destroyed.

1.1-B *Concrete Seawalls – Scour:* Two large scour profiles at the leeward slope of the curved 2.5 m high concrete seawall in the east side of Ishinomaki port extended about 60.0 m in length along the seawall. The massive concrete platform placed at the toe of the leeward slope disappeared due to the tsunami, leading to two scour holes being created. (Jayaratne et al., 2013)

1.1-H *Concrete Seawalls – Overturning:* In some cases the concrete seawalls were overturned by return flow rather than by the incoming tsunami. (Earthquake Engineering Research Institute, EERI, 2011)

1.2-B, 1.2-C *Solid-Concrete Seawalls – Scour:* Yeh et al. (2012) conducted surveys along the Sanriku coast after 2011 event and state that remarkable destruction of upright solid-concrete type seawalls was closely related with the tsunami induced scour.

1.2-E *Seawalls – Soil Instability:* Remarkable destruction of upright solid-concrete type seawalls was closely related with also soil instability. The rapid decrease in inundation depth during the return-flow phase caused soil fluidization down to a substantial depth and this mechanism explains severely undermined foundations observed in the area along the Sanriku Coast of low flow velocities. They found that soil instability played a major role in the failures. (Yeh et al., 2012)

1.2-H *Seawalls – Overturning*: Overturning of a seawall which was observed on the Ryoishi Coast, Iwate Prefecture induced by the Great East Japan Earthquake Tsunami may occur if the overturning moment induced by the wave force on the seawall during tsunami runup or drawdown is larger than the resistance moment due to the weight of the seawall. (Kato et al., 2012)

1.3-B *Mound-type Seawalls – Scour:* The fast flow velocities with intense turbulence resulted in severe undermining damage in the rear face of the mound-type seawall in Kanahama, as well as formation of a large scour hole behind. (Yeh et al., 2012)

2.2-B *Dikes – Scour (Leeward):* Jayaratne et al. (2013) noticed severe damage to the leeward face and toe of the sea dike at Soma city. Diverse failure patterns were observed from the north to the south side, resulting in partial to total failure of the leeward face due to scour.

2.2-C *Dikes – Scour (Seaward):* Seaward flow over the coastal dike may cause scouring at the seaward toe of the dike as also pointed out in previous studies (e.g., Noguchi et al. 1997). Seaward flow during tsunami drawdown caused scouring at the seaward toe of the coastal dike and revetment. Scouring at the landward toe affected the stability of the seaward armor, resulting in floating away of seaward armor and breaching of the dike. (Kato et al., 2012)

3.1-B, D& E *Breakwater – Scouring, Sliding and Soil Failure:* All these failure modes due to tsunami overflow was observed in Kamaishi and Hachinohe Breakwaters. Both breakwaters were modelled in laboratory and several experiments were performed to determine factor of safety regarding sliding and overturning considering the scour at the leeward (at the foundation level) as well as bearing capacity failure (soil failure). (Arikawa and Shimosako, 2013)

3.2-G *Breakwater – Slope Failure (Seaward):* Large concrete armour units had been placed in front of the seaward slope of the breakwater at Ishinomaki Port. It was found that the primary armour units on the seaward slope were displaced and scattered in front of the breakwater, and some units were buried under tsunami deposits, though there was no indication of damage to the front slope. (Jayaratne et al., 2013)

3.3-F *Composite Breakwaters – Slope Instability (Leeward):* Esteban et al., 2013 states that the exact failure mechanism for each of the breakwater types is still unclear, and whether armour units were displaced by the incoming or the outgoing wave could not be easily established for any of the field failures recorded. Therefore, they carried out some preliminary laboratory experiments which appear to indicate that although the incoming tsunami wave can cause some movement to the caisson, the major failure mode of the armour could occur as a result of the outgoing wave.

3.3-H *Composite Breakwater – Overturning:* In Kamaishi City, the tsunami on March 11th overturned the north section (990 m in length) of the newly completed offshore breakwater and although the south section (670 m in length) survived mostly intact, it was left inclined (Yagyu 2011, retrieved from Fraser et al., 2013).

4.1-I *Parapet, Crown Walls – Run-up & Drawdown Failures:* Concrete parapets were installed along the shoreline to mitigate wind-wave overtopping, but some of the parapets were broken by tsunami run-up. This pattern may occur if shear stress

induced by the wave force acting on the parapet during tsunami overtopping is larger than the shear strength of the parapet joints. Similar to tsunami run-up, tsunami drawdown also results in wave forces acting on the parapet leading to parapet failure. Parapets are designed not for tsunami forces from the land but for wave forces from the sea. (Kato et al., 2012)

4.2-A *Harbour Walls – Functional Failure:* The tsunami at Kesennuma flowed north up the bay, arrived at the harbour as a fast-flowing rising tide (Japan Coast Guard 2011) and overtopped harbour walls and river defences. Harbour walls at the Yuriage Port show also functional failure (overtopped). (Fraser et al., 2013).

5-B *Embankments – Scour:* Scour on the leeside was a main cause of embankment failure due to 2011 Tōhoku Earthquake, Tsunami in Yamamoto Town. (The 2011 Tōhoku EarthquakeTsunami Joint Survey Group 2011, http://www.coastal.jp/tsunami2011/index.php?Fieldsurveyresults)

6-A *Tsunami Gates – Functional Failure:* Most seawalls had openings to allow vehicular traffic to pass through the wall, with heavy steel gates to close the openings when a tsunami warning was announced. It appeared that (during 2011 Tōhoku event analysis of EERI Teams), such gates had been successfully closed prior to the tsunami inundation, and that the majority of the gates resisted well the incoming flow, but often failed during the outward return flow, for which they had not been designed. (EERI, 2011)

6-H *Tsunami Gates – Overturning:* Many tsunami gates designed to reduce flooding along rivers were overturned by the Great East Japan Earthquake and tsunami. (World Bank Knowledge Note 1-1, 2012)

Many of the failure modes presented in this report are aimed to cover several types of failures since exact process of many of the failure modes have not been determined yet. Observations are almost always after the event, thus, they can only give information on the total failure or the most governing failure mode. For example, many of the dikes have failed due to scour however it is also seen that after scour at the base of the structure, removal of concrete slabs, washout of sand fill or erosion of inner slopes have occurred which contributed to the overall failure of the structure. For example, slope instability on the leeward side has been developed to cover all of the secondary processes (removal of concrete slabs, washout of sand fill, etc) that is mentioned above. Similarly, removal of blocks in case of rubble mound structures or seaward protection of vertical structures are covered by failure mode named as slope instability on the sea side. Certainly, it is possible to reorganize the presented matrix with more detailed failure types and this is one of the objectives of RAPSODI project.

Using these field observations, the initiating drivers for all failure modes may be categorised into two main processes: (1) Water level difference across the structure, and (2) tsunami wave-induced forces. In Tab. 4.1 an overview of the observed failure

modes for each of these processes is provided for all coastal structures which were investigated.

Table 4.1 Failure Mode Matrix

COASTAL STRUCTURES FAILURE MECHANISMS			FAILURE MODES INDUCED BY TSUNAMI LOAD CONDITIONS																			
			WATER LEVEL DIFFERENCE ACROSS THE STRUCTURE		A	B	C	D	E	F		G	H	I	J	K						
					Overflow (functional failure)	Scour - Foundation Undermining (Leeward)	Scour - Foundation Undermining (Seaward)	Sliding	Soil Failure (Settlement, Seepage, Liquefaction)	Slope Failure (Leeward)	WAVE FORCE	Slope Failure (Seaward)	Overturning	Parapet/Crown Wall failures due to tsunami runup&drawdown	Sliding	Scour						
COASTAL PROTECTION STRUCTURES	1	Seawalls and Revetments																				
	1.1	Concrete Block			v	v							v		v							
	1.2	Composite (solid-concrete)			v	v	v		v				v									
	1.3	Mound			v	v			v													
	2	Sea Dikes																				
	2.1	Mound																				
	2.2	Concrete armored			v	v	v															
	3	Breakwaters																				
	3.1	Block Type			v	v		v	v													
	3.2	Rubble Mound			v							v										
	3.3	Composite (caisson and mound)			v	v				v			v		v							
	4	Walls																				
	4.1	Parapet/Crown Walls												v								
	4.2	Harbour Walls			v																	
	4.3	Quay Wall							v													
	5	Embankments				v																
	6	Sluices, Tsunami Gates			v								v									

Another failure mode matrix, Table 4.2, is being prepared for buildings by analysing the model tests, observations and field data. The matrix and the corresponding examples are given below. Similar to the coastal structures matrix, the failures are grouped into two according to the main driving processes: impulsive tsunami loading and standing tsunami pressure. The structures are also grouped according to the available protection measures taken against tsunami impact, construction type and individual parts of the structures. However, it should be noted that this matrix is a preliminary result and requires additional work.

For Table 4.1:
2.1.1 – A; 2.1.2 – B,M: Arikawa (2009) examined the failure mechanisms of wooden walls and reinforced concrete walls with different thicknesses and strength under a high-intensity tsunami attack (i.e. 2011 Great East Japan Earthquake and Tsunami). He found out that the wooden wall was destructed at the moment that water hit the wall and the failure was explosive. However, the destruction and the failure mechanism of concrete walls depended on the thickness and the strength. He stated that the bending or punching shear failure occurred when the concrete was low-strength whereas the failure mode shifted local failure to whole destruction when the concrete is high-strength.

2.2.2: Arnason et al. (2009) investigated tsunami-structure interaction with laboratory experiments carried out on vertical acrylic columns of different cross-sections by generating bore-like flow of a broken tsunami wave. They measured the water-surface variations, velocity flow fields, and forces on columns but no information exists on the failure mechanism of the structures. It is not even mentioned if the structures are failed in some conditions or not.
1.1, 1.2, 1.3 – L; 1.3.1 – H; 2.1.3, 2.1.4, 2.1.5 – L; 2.1.4 – K; 2.2.1 – L; 2.3 – K; 2.4.1 – H, I:

Asai et al. (2012) surveyed the Tohoku area (from Hachinohe city in Aomori Prefecture to Soma city in Fukushima Prefecture) after the Great East Japan Earthquake and Tsunami to investigate structural damage and inundation depth in the area to assess the design load for tsunami shelters. Their investigation consists of more than 130 structures including (a) buildings with simple configuration, (b) fence walls, (c) RC or masonry columns (bridge piers, gate piers, etc.), (d) stone monuments, (e) seawalls, and (f) steel fences. They give relationship between equivalent tsunami pressure, flow velocity, Froude number and structure's damage and four different failure modes for different types of structures as rebar yielding, rebar fracture, sliding and overturning observed in the survey area.

3.1 – E, F, G, N, O; 3.2 – E, H, M, P: Building Research Institute and National Institute for Land and Infrastructure Management and Ministry of Land, Infrastructure, Transport and Tourism jointly carried out site investigation for building damages affected by tsunami in 6 cities for Iwate prefecture (Miyako, Yamada, Otsuchi, Kamaishi, Ofunato, and Rikuzen-Takata), and 9 cities for Miyagi prefecture (Kesennuma, Minami-sanriku, Onagawa, Ishinomaki, Sendai, Natori,

Iwanuma, Watari, and Yamamoto). Fukuyama et al. (n.d.) stated their observations as the following seven types of damage patterns of reinforced concrete buildings as; pancake collapse, 1st story collapse, overturning and movement, tilting and drifting by scouring, sliding, fracture of wall (opening) and debris impact provided with examples. For the steel buildings; main patterns are washout by fracture of exposed column base and capital connection, overturning, large residual deformation and debris impact.

2.3.1, 2.3.2 – C: Meyyappan et al. (2013) conducted laboratory experiments to investigate the effect of a sequence of waves (tsunami 'blows') before failure and the shape of the building to its ability against tsunami. The failure mechanism that they observed is overturning on those model testing and they state that the number of tsunami 'blows' is an essential parameter in the design of tsunami resistant structures. Circular buildings are found to be better than rectangular/square shaped buildings and of the two non-circular building models considered in the study, square shaped building showed better performance.

All – J; 2.3, 2.1.1, 2.4.2 – E:
Yalciner et al. (2011) reported their findings from a field survey performed in the tsunami hit areas of Great East Japan Tsunami as the Sendai Airport, Yuriage, Natori, and Sendai port, Taro, Miyako, Yamada, Kamaishi, Rikuzentakata, Ofunato and Kesennuma. According to Yalciner et al. (2011), it was clearly observed that tsunami energy is focused in narrow long bays and when arrived coastal areas it propagated inland along rivers. They presented building damage and possible reasons of building damage. According to their findings, large scale erosion was observed around the concrete structures and in some cases causing overturning. Scouring occurred as expected during tsunami attacks (Sumer, 2007). They also stated that almost all wooden structures were either destroyed by debris impact or carried away due to strong currents - few out of thousands of buildings survived. They presented an example of the tsunami damage of an elementary school in Arahama. The entire stage of the school was covered with mud and debris, while two cars had been carried into the building.

1.2.1, 2.2.1 – E:
Ghobarah et al. (2005) conducted a field investigation of the 26 December 2004 south east Asia earthquake- and tsunami-affected areas in Thailand and Indonesia. They stated in their report that many reinforced concrete columns failed due to the impact of large and heavy objects in the debris such as boats and cars. They suggest that the inclusion of redundancies in the design may ensure that the structure will not collapse due to the failure of one or two columns.

Tab.4.2 Preliminary failure matrix for land structures (buildings)

LAND STRUCTURES FAILURE MECHANISMS			FAILURE MODES INDUCED BY TSUNAMI LOAD CONDITIONS																		
			IMPULSIVE TSUNAMI LOADING	Total Failure (explosive)	Bending and/or punching shear failure	Overturning	Sliding	Debris Impact	1st story collapse	Pancake Collapse	STANDING TSUNAMI PRESSURE	Overturning	Sliding	Scour	Rebar Yielding	Rebar Fracture	Wash-away due to sustained force	Tilting and Drifting by scouring	Fracture of Wall (Opening)	Large residual deformation
				A	B	C	D	E	F	G		H	I	J	K	L	M	N	O	P
LAND STRUCTURES	1	**Structures with protection**																		
	1.1	**Walls**																		
	1.1.1	Concrete-Block Fence Wall												√		√				
	1.2	**Columns**																		
	1.2.1	RC Column						√								√				
	1.2.2	Concrete-Block Column														√				
	1.3	**Other**																		
	1.3.1	Stone Monuments										√								
	1.3.2	Railway Bridge												√		√				
	2	**Structures without protection**																		
	2.1	**Walls**																		
	2.1.1	Wooden Wall		√				√												
	2.1.2	Concrete Wall			√									√			√			
	2.1.3	Concrete-Block Wall												√		√				
	2.1.4	RC Fence Wall												√	√	√				
	2.1.5	Concrete-Block Fence Wall												√		√				
	2.2	**Columns**																		
	2.2.1	RC Column						√								√				
	2.2.2	Vertical Column (acrylic)																		
	2.3	**Buildings**													√					
	2.3.1	Circular Buildings						√												
	2.3.2	Rectangular / Square Shape Buildings				√		√						√						
	2.4	**Other**																		
	2.4.1	Stone Monuments										√	√							
	2.4.2	Wooden Structures						√												
	3	**Structures with no Information on Protection**																		
	3.1	**RC Buildings**						√	√	√				√				√	√	
	3.2	**Steel Buildings**						√				√		√			√			√

4.7 Summary

Two matrices have been prepared to summarize tsunami impact on coastal structures and buildings based on the observations and experiments provided in the literature.

The first matrix (Table 4.1) gives insight into the failure modes of different types of structures due to water level differences where overflow occurs and due to tsunami wave loadings. Many of the structures given in the table describes the types of structures located in Japan considering the vast amount of information collected after 2011 GEJE tsunami. Functional failure of the structures (overflow) mainly occurs to water level differences across the structure during the tsunami wave. On top of the functional failure, the structures are observed to become damaged or totally collapse due to water level differences. Most of the time it is seen that several of the failure modes took place consecutively to generate the final damage observed. However, the

exact sequence of the failure modes for many of the failures require more experiments and/or real time observations to accurately understand the overall damage caused by tsunami. Additionally, not all the failure modes presented in the matrix have been observed for every type of the structures. This could either mean that that particular type of failure is not possible or the failure mode requires more research in order to reach a conclusive outcome.

Most of the missing information is about performance of rubble mound breakwaters since they are not common in Japan. Additionally, failure modes due to wave impact has not been investigated much in the literature. One reason could be due to the fact that tsunami waves are solitary waves and if there exists no overtopping, damage is usually insignificant for large structures. However, the exact amount of damage that could be caused by tsunami wave force would be important in case of maintenance as well as possible decrease in the resilience of the structure under cyclic loading such as storms. Another important outcome of the failure matrix is that soil conditions and soil-structure interaction is very important in the case of overflow. Much of the observed failures were based on scouring on either side of the structures occurred during the tsunami event. Additionally, some of the failures were due to the tsunami drawdown (outflow) which was not considered in the design of these structures before 2011 observations.

Another failure modes matrix (Table 4.2) showing failure mechanisms of different land structures such as reinforced concrete and steel buildings, walls, columns, wooden structures is presented. An analysis of both experimental studies and post-event surveys has been performed and findings are roughly categorized according to the tsunami loading condition which is either tsunami impact pressure or the standing tsunami pressure. Debris impact is commonly observed in wooden structures and buildings whereas overturning, bending and punching shear failure and 1st story collapse are the other failure modes seen under impulsive tsunami loading. In case of standing tsunami pressure, scour and rebar fracture are the most common ones and overturning, rebar yielding and wash-away due to sustained force are the other present forms of failure. The analysis shows that the static and dynamic effects of debris on structures is significant in addition to tsunami pressure. Also, the design approaches against erosion around concrete structures should be improved and extended since it occurs in most of the cases. Finally, some design strategies could be developed such that buildings do not collapse as a result of one or two column failures.

5 Vulnerability Assessment

A recent increased interest in tsunami risk is probably due to a trend in natural hazard science where hazard-oriented approaches are shifted to risk approaches. Likewise, the turning point in tsunami risk research was recent tsunami events with severe consequences (e.g. the Indian Ocean tsunami on December 26, 2004, the Java tsunami in July 2006, the Solomon Islands tsunami in April 2007 or the 2011 Tohoku Earthquake and Tsunami). Løvholt et al. (2014) provide an overview on the achievements made in tsunami risk reduction since 2004.

It is expected that future tsunamis can have a higher impact due to the increasing number of people, buildings and infrastructure that are being exposed to natural hazards as the pressures for urban development extend into areas of higher risk. To avoid or mitigate future tsunami events, it is necessary to study and understand this phenomenon in detail. Knowledge about exposed elements, and their susceptibility, coping and adaptation mechanisms is a precondition for the development of people-centered warning structures (Post et al., 2008). Overall, risk assessment has two dimensions as the hazard assessment and the assessment of vulnerability. Both components have a significant influence on the level of tsunami risk and provide the basis for the tsunami risk assessment. Vulnerability assessment as the second dimension of risk assessment plays a crucial role in tsunami disaster reduction strategies. Vulnerability can be defined as “The conditions determined by physical, social, economic, and environmental factors or processes which increase the susceptibility of a community to the impact of hazards” (ISDR, 2004). With respect to this definition, vulnerability is trans-disciplinary and multi-dimensional, covering social, economic, physical, political, engineering and ecological aspects and dimensions (Post et al., 2009). Risk and vulnerability assessment is also an integral part in the development of an effective end-to-end early warning system, which significantly contributes to disaster risk reduction to low-frequency but extreme events like tsunamis. Actually, there is no general agreement between different disciplines on the definition of risk and the same can be said for tsunami risk applications. Tsunami risk is generally expressed as the product of hazard and vulnerability (e.g. Rynn and Davidson, 1999); some scientists also use the extended expression such as the product of hazard, vulnerability and economic value (e.g. Papadopoulos and Dermentzopoulus, 1998), or simply hazard and consequences or exposure (Clague et al. 2003).

There are numerous methods that have emerged to evaluate risks, and these range from highly technical, statistical, quantitative assessments to simple, qualitative assessments. The best assessments would combine these methods, treating each hazard separately, as well as incorporating considerations for multiple and cumulative hazards occurrences into the overall assessment framework and methodology.

5.1 General Tsunami Vulnerability Assessment Approaches

To begin with the general approaches regarding tsunami vulnerability assessment, the UN International Decade for Natural Disaster Reduction (IDNDR) project "Contemporary Assessment of Tsunami Risk and Implication for Early Warnings for Australia and its Island Territories" was a pilot project which aimed to assess tsunami risk, in qualitative and quantitative terms (Rynn and Davidson, 1999). In the project, vulnerability is defined in qualitative terms as high, medium and low level for the built and natural environment. The recently published report Natural hazards in Australia: Identifying risk analysis requirements (Middelmann, 2007) contains also a chapter on tsunamis. In their report, the general approach to estimating tsunami risk involves five key sequential stages. Vulnerability model is the fourth stage for estimating tsunami risk. The model is to characterize the nature and magnitude of the damage from a wave of given velocity. The structural and human vulnerability are considered and if possible must be estimated.

A contribution from Thailand to tsunami risk assessment is the CRATER project (Coastal Risk Analysis of Tsunamis and Environmental Remediation) (Cavalletti et al. 2006). In the project, vulnerability parameters are categorized into the four groups; population, built environment, socio-economic aspects and environment. For each parameter a list of impact elements is prepared. The total vulnerability is a sum of impact elements based on a weighting factor. The risk value is calculated for each vulnerability parameter and the final outcome is so-called thematic risk maps (i.e. population risk map, socio-economic risk map or building risk).

Another interesting example from Greece can be found in Papathoma and Dominey-Howes (2003) and Papathoma et al. (2003). The authors used a new vulnerability approach for the estimation of the cost of a hypothetical tsunami impact in two coastal villages in the Gulf of Corinth and for the city of Heraklion. The authors demonstrate the importance of the vulnerability component in tsunami risk assessment as a very dynamic factor dependent on a number of parameters relating to the built environment, sociological, economic, environmental and physical data. The vulnerability parameters are ranked according to their importance and a weighting factor is applied. The tsunami source and off-shore bathymetry are neglected in this approach. This so-called "Papathoma method" is divided into the following steps:

1) Identification of the inundation zone and inundation depth zones. The inundation zone is considered between the coastline and the 5 m contour based on probability studies of historical tsunamis, where the greatest wave height was 5 m (from 1963).
2) Identification of factors that affect the vulnerability of buildings and people. For the built environment the following parameters are considered: number of stories of each building, description of ground floor, building surroundings, material, age and design. Population density and number of people per building are basic sociological parameters.

3) Calculation of the vulnerability of individual buildings (BV) within the inundation zones using a multi-criteria evaluation method:
   $BV = (7 \times a) + (6 \times b) + (5 \times c) + (4 \times d) + (3\times e) + (2 \times f) + (1\times g)$
   Where, a-g = Standardized scores that are related to the material of the building, row of the building, numbers of floors, building surroundings, condition of the ground floor, sea defence and width of the inertial zone, respectively.
   Human vulnerability (HV) of each building is calculated by:
   $HV = BV \times P$
   Where, P is the population.
4) Display of building vulnerability and human vulnerability for example in a GIS environment. Since this approach particularly focuses on vulnerability assessment, the other risk components are generalized or simplified, i.e. the tsunami sources are not considered and the inundation zone is just defined as the area between the coastline and the 5 m contour. The cost of a future hypothetical tsunami is estimated for the affected properties (such as buildings, households, businesses, etc.) and the results are presented in Euros.

The ‘‘PTVAM’’ Papathome Tsunami Vulnerability Assessment Model [Papathoma and Dominey-Howes, 2003, Papathoma et al., 2003] is a dynamic model that incorporates multiple parameters (attributes) that are known to influence vulnerability to tsunami loss and damage. The model is dynamic in that the attribute data contained within the primary database, may be modified and updated allowing investigation of vulnerability both spatially and temporally. The PTVAM is organized and presented within a GIS framework thus allowing rapid data entry and visualization of changing vulnerability (through the production of new maps). Based on an analysis of multiple post-tsunami field surveys, Papathoma (2003) identified a suite of attributes (parameters) that are reported to affect the degree of damage from, or protection to, tsunami flooding for individual buildings and structures. These attributes were then classified into ‘major classes or groups’ (e.g. built environment, sociological data, economic data and environmental/physical data) and variations (values) in the degree or range of these attributes were identified together with a vulnerability descriptor for each attribute. These vulnerability classes/groups, parameters, values and descriptors are given in Table 5.1.

Table 5.1. Vulnerability classes/groups, attributes, values and descriptor as outlined in the PTVAM framework

Major class	Parameter (attributes)	Value	Vulnerability descriptor
The Built Environment	Number of stories in each building	Only one floor	High vulnerability
		More than one floor	Low vulnerability
	Description of ground floor	Open plan with movable objects, e.g. tables and chairs	High vulnerability
		Open plan or with big glass windows without movable objects	Moderate vulnerability
		None of the above	Low vulnerability
	Building surroundings	No barrier	Very high vulnerability
		Low/narrow earth embankment	High vulnerability
		Low/narrow concrete wall	Moderate vulnerability
		High concrete wall	Low vulnerability
	Building material, age, design	Buildings of fieldstone, unreinforced, crumbling and/or deserted	High vulnerability
		Ordinary masonry brick buildings, cement mortar, no reinforcement	Moderate vulnerability
		Precast concrete skeleton, reinforced concrete	Low vulnerability
	Movable objects	Movable objects present	High vulnerability
		No movable objects present	Low vulnerability
Sociological data	Population density	Population density during the night	Vulnerability may be high *or* low
		Population density during the day	Vulnerability may be high *or* low
		Population density during the summer	Vulnerability may be high *or* low
		Population density during the winter	Vulnerability may be high *or* low
	Number of people per building	Many	High vulnerability
		Few	Low vulnerability

Table 5.1. Continued

Major class	Parameter (attributes)	Value	Vulnerability descriptor
Economic data	Land use	Business (shops, taverns, hotels etc.)	No value required
		Residential	No value required
		Services (schools, hospitals, power stations etc.)	No value required
Environmental/physical data	Physical or man-made barriers/sea defence	Natural (sandy beach or marsh offering low protection)	High vulnerability
		Soil embankment (offers moderate protection against flooding)	Moderate vulnerability
		Concrete stone wall (offers high protection against flooding)	Low vulnerability
	Natural environment	Wide intertidal zone	Low vulnerability
		Intermediate intertidal zone	Moderate vulnerability
		Narrow intertidal zone	High vulnerability
	Land cover (vegetation)	No vegetation cover	High vulnerability
		Scrub and low vegetation	Moderate vulnerability
		Trees and dense scrub	Low vulnerability

Dunbar and Weaver (2008) presented an exposure and vulnerability assessment module within the scope of "U.S. States and Territories National Tsunami Hazard Assessment: Historical Record and Sources for Waves" prepared by a collaboration of National Oceanic and Atmospheric Administration (NOAA) and U.S. Geological Survey (USGS). After the tsunami hazard has been characterized, the next step is to determine who and what is actually exposed to tsunami inundation and runup. This requires an assessment of the people, homes, commerce, industry, natural resources, etc., that are in the tsunami inundation zones for a given event. However, exposure does not equal vulnerability—the susceptibility to harm or damage during tsunami inundation. The vulnerability of a physical structure would be influenced by factors such as structural design, material, condition of structure, and distance from shoreline whereas the factors that would control the vulnerability of a person would include age, gender, education, mobility, and physical health (Dunbar and Weaver, 2008).

According to the three pillars of sustainable development, Post et al. (2007) developed and presented indicators for the socio-economic and physical dimensions of vulnerability. The main task is an assessment of vulnerability and coastal risk towards tsunami threats and their study is embedded in the German-Indonesian Tsunami Early Warning System (GITEWS) project. Products of the three years project include new physical and socio-economic vulnerability assessments, vulnerability and risk maps and guidelines for decision makers how to monitor and conduct continuous vulnerability assessment for effective early warning and the disaster mitigation strategies. If looked at their conceptual framework, their research is focused on "who and what is vulnerable" meaning that the socio-economic spheres ("who" including e.g. social groups and institutions) have to be linked with the physical-natural spheres ("what" in a sense of e.g. built environment, critical infrastructures, economic sectors. The vulnerability assessment approach that conducted and operationalized in the project is based on the BBC-framework (Birkmann, 2006). It encompasses the identification and assessment of the vulnerability of the population exposed (different social groups), basic infrastructure services and physical structures within coastal communities. The BBC framework emphasizes the fact that vulnerability is defined through exposed and susceptible elements on one hand, and the coping capacities of the affected entities (for example social groups) on the other.

Furthermore, the underlying concepts and applied methods in the GITEWS project are also explained in Strunz et al. (2011). The vulnerability assessment starts with exposure estimation. The approach for exposure estimation, which has been developed in GITEWS, is based on a combined approach using in-situ assessment and remote sensing. In a first step, a detailed assessment based on the selection of some representative buildings ("stratified sampling") is made. Geometrical and structural parameters of these buildings are acquired in an in-situ assessment. According to these parameters the sample buildings are categorized. The approach is based on a decision tree algorithm and on object based image interpretation. The method is described in more detail in Sumaryono et al. (2008). After that comes the assessment of response capabilities and preparedness. Because, the analysis of the

response capabilities and community preparedness to tsunami warnings is an important issue in vulnerability assessment. The assessment has to answer the questions of warning dissemination, anticipated response and evacuation. The detailed methodology is described in (Post et al., 2009).

The Last Mile-Evacuation research project (Taubenböck et al., 2009) aims to develop a numerical tsunami early warning and evacuation information system, particularly for the low-lying, coastal city of Padang, Indonesia. The city is severely at risk regarding earthquake-generated tsunamis. The vulnerability assessment which is one of the key goals of the project provides spatial information with regard to social aspects to improve tsunami disaster risk reduction in terms of disaster management efforts and long-term coastal urban spatial planning. With this regard, they aimed at the assessment of time-specific distribution of various social groups based on the city's physical structure and socio-economic characteristics taking into consideration the tsunami-prone areas (dynamic exposure mapping), the assessment of factors that may cause ineffective and delayed evacuation warning response and root causes for a lack of access to effective early warning dissemination and also the assessment of factors that influence people´s evacuation behaviour such as lack of awareness or knowledge of tsunami risk and preparedness. In the initial phase, a vulnerability framework containing various vulnerability components was developed based on a literature study on vulnerability concepts, early warning and evacuation behaviour. The vulnerability components were divided in main thematic areas according to the relevant planning purpose and potential end-users such as urban planning, disaster management and community development. This process was done in an iterative manner during the course of the research: Criteria for each vulnerability component were derived by means of a literature study and participatory consultations with the local stakeholders. (www.ehs.unu.edu/article/read/last-mile)

Primary data collection was conducted as a combination of qualitative approaches such as semi-structured interviews, participatory rural appraisal (PRA), as well as Focus Group Discussion (FGD) and quantitative approaches such as questionnaire-based surveys. Secondary data was collected from existing statistical and spatial data provided by authorities and derived from remote sensing analysis. Descriptive and multivariate statistical analysis was employed to test the influence of various variables for each component of the vulnerability of people exposed to tsunami risk. The analysis served as a filtering process to select the final sets of indicators. Spatial analysis using GIS tools was carried out to link the social data with the spatial structure of the city. Finally, thematic aggregated vulnerability maps were produced. The applicability of maps and indicators is validated by means of discussions with the local stakeholders and potential main users.

As stated in the fifth cluster of the Learning from Megadisasters Knowledge Notes project of the Government of Japan and the World Bank Group (Sagara, and Saito, 2013), the damage caused by the GEJE far exceeded the predisaster damage estimates, because of the underestimation of the earthquake and tsunami hazards. The number of completely destroyed buildings was about six times the estimated amount,

and the number of human lives lost was more than seven times the estimation. Therefore, they characterize a conventional methodology for estimating damages. A quantitative estimation of the impact was carried out using the relationship between the magnitude of the hazard (seismic intensity, maximum ground velocity, tsunami inundation depth, and so on) and the actual damage (number of destroyed houses, human loss, and so on), which was established based on historical earthquakes. For example, tsunami damage to buildings was estimated using the assumption that a building is completely destroyed if the inundation depth is 2.0 meters or more based on empirical evidence. Human losses caused by tsunamis were estimated based on the tsunami-affected population and historical records of death by tsunami inundation depth and estimated evacuation rates (percentage of people who can obtain warning information and the time it takes for people to evacuate). Furthermore, infrastructure damage was estimated on the basis of the estimated number of destroyed buildings, lifeline failure rates and the number of days required for restoration, for which empirical relationships have been established based on previous disasters. According to them, the underestimation of damage in the case of the GEJE was largely due to an underestimation of the magnitude of the hazards involved. Also, it has been pointed out that some factors such as evacuation rates used for damage estimation purposes were higher than actual rates, which could have further contributed to an underestimate of human losses. At the time of this writing, the damage estimation methodology is being revised.

Structures along the coast are particularly susceptible to a variety of natural hazards. Coastal construction practices, however, as they exist today, may not be sufficient to resist their extreme loads. A 3-tier tsunami vulnerability assessment technique is presented in Ismail et al. (2012). The scope of their assessment is focused on the vulnerability of the physical characteristics of the coastal area of the north-west coast of Peninsular Malaysia, and the vulnerability of the built environment in the area that includes building structures and infrastructures. The assessment was conducted in three distinct stages which stretched across from a macro-scale assessment to several local-scale and finally a micro-scale assessment. On a macro-scale assessment, Tsunami Impact Classification Maps were constructed based on the results of the tsunami propagation modelling of the various tsunami source scenarios. Tsunami heights and flood depths obtained from these maps were then used to produce the Tsunami Physical Vulnerability Index (PVI) maps. The final stage is the development of the Structural Vulnerability Index (SVI) maps, which may qualitatively and quantitatively capture the physical and economic resources that are in the tsunami inundation zone during the worst case scenario event. The results of the assessment in the form of GIS-based Tsunami-prone Vulnerability Index (PVI and SVI) maps are able to differentiate between the various levels of vulnerability, based on the tsunami height and inundation, the various levels of impact severity towards existing building structures, property and land use, and also indicate the resources and human settlements within the study area.

NGI (2011) published a document namely “Analysis of the 2011 Tohoku tsunami” and they have developed a GIS based model to assess tsunami vulnerability and

mortality risk. The model includes exposure analysis and mortality risk analysis based on structural building vulnerability. To account for structural vulnerability a sampled number of buildings have been mapped in the field and four vulnerability criteria were assigned to each of the mapped buildings: (i) number of floors (height), (ii) barriers in place, (iii) material, and (iv) use. To gather a spatial distribution for the whole study area (Bridgetown, Barbados and Batangas Bay, the Philippines) building information was extrapolated to all buildings in the study area using GIS tools. Finally, a weighting scheme was applied to provide vulnerability scores to each building according to the four vulnerability criteria. The model was applied in a pilot study of vulnerability mapping for tsunamis prepared for Bridgetown, Barbados within a two years capacity building program on natural disaster mitigation in the Caribbean (NGI, 2009). See also Deliverable D8 "A GIS tsunami vulnerability and risk assessment model" (NGI 2015).

Dall'Osso and Dominey-Howes (2009) also presented a report which aimed to apply and test a newly developed and highly novel GIS tool to assess the vulnerability of coastal infrastructure to catastrophic marine floods (tsunami). The GIS model calculated a Relative Vulnerability Index (RVI) score for every building in the study area (selected coastal suburbs of Sydney) that would be touched by the water. RVI scores were calculated combining buildings physical features (number of stories, construction material, hydrodynamics and orientation of the ground floor, type of foundation, preservation condition), building surroundings (movable objects that could hit the structures and possible protection offered by other buildings or natural and artificial fences) and exposure to inundation (the expected water depth at the points where buildings are located). An innovative approach based on the Analytic Hierarchy Process was used to weight all the different contributions to the final value of RVI.

Ports and harbors are especially vulnerable to earthquake-related hazards, such as severe ground shaking, soil liquefaction, landslides, and tsunami inundation because of their geographic location. The NOAA Coastal Services Center (NOAA CSC), and the U.S. Geological Survey (USGS) Center for Science Policy have undertaken an initiative to increase the resiliency of Pacific Northwest ports and harbors to earthquake and tsunami hazards. Specific products of this research and planning initiative include a community-based mitigation planning process aimed at ports and harbors and a GIS-based vulnerability assessment methodology (Wood et al., 2002). Working with the local officials, emergency managers, and state and federal agencies, a model planning process was developed and later refined. It consisted of five steps, each with a variety of activities and the third step was the vulnerability assessment. Given agreed-upon scenarios, the assessment includes using GIS and field surveys to identify the exposure of port and harbor infrastructure, facilities, and other resources to earthquake and tsunami hazards; conducting community-based planning workshop with local stakeholders and technical advisors to assess vulnerability from a combined local/technical perspective, using field visits, facilitated brainstorming, and priority-setting techniques.

If continued with the case study examples of tsunami vulnerability assessment, Sinaga et al. (2010) presents a GIS mapping methodology, a case study of the Jembrana Regency in Bali, Indonesia. They describe a GIS-based multi-criteria analysis and use multiple geospatial variables of topographic elevation and slope, topographic relation to tsunami direction, coastal proximity, and coastal shape. They also incorporated expert knowledge by the Analytic Hierarchy Process (AHP) to construct a weighting scheme for the geospatial variables. In order to examine tsunami vulnerability in relation to land use, they overlaid an official land-use map on the tsunami vulnerability map. Buildings as well as residential and agricultural areas were found to be particularly at risk in their study area.

The same GIS mapping methodology is also used in Kameda's (2011) study of ''Tsunami Vulnerability Assessment and Crisis Mapping of Actual Tsunami Damage in Miyagi, Japan'' by one-to-one application of the methodology to Miyagi Prefecture and using the 2011 Tohoku Earthquake and Tsunami. He conducted a tsunami vulnerability assessment of Miyagi prefecture based on the variables: elevation, slope, tsunami direction and coastal proximity. He also investigated how the Japan Crisis Map twitter were spatially distributed in Miyagi prefecture. To analyze the effectiveness of the vulnerability assessment and the crisis map, he analyzed the distribution of both with actual tsunami damage indicators; remotely-sensed tsunami inundation zones and official municipality casualty reports.

Mastronuzzi and Sansò (2006) also presented a case study of tsunami vulnerability in the Apulia Region, Italy. They aimed to define the vulnerability of the Apulian coast (southern Italy), therefore, the effects of tsunamis on different types of coast have been inferred from the available post-report events integrated by information gathered from the geological research on deposits and forms which have been related to tsunami action. This analysis allows the vulnerability of different type of coasts occurring in Apulia region to be assessed.

New Zealand (Bernard et al., 2007) undertook a probabilistic tsunami hazard assessment, developed relations between water velocity and structural damage, and made an estimate of the likely losses from significant tsunami events. Their studies are unprecedented in their scope, probabilistic framework for tsunami risk, societal impacts, and thorough social science framework for tsunami preparedness assessment, but are based on very little quantitative data or fragility relationships. They state that, to manage risks associated with tsunamis, risk assessments must be developed for a variety of tsunami scenarios, including defining credible worst case events that combine ground shaking, ground level changes, inundation, and scour so that the vulnerability of both the people and the built environment can be understood. Such models should also include vulnerability of vehicles subjected to tsunami surge.

In the study of "Tsunami Vulnerability and Risk Analysis Applied to the City of Alexandria, Egypt" by Jelínek et al. (2009) within the scope of TRANSFER (Tsunami Risk And Strategies For the European Region) Project, very high resolution satellite remote sensing data have been used to calculate the tsunami

hazard, the physical vulnerability and risk for a central and peri-urban district of the city of Alexandria. Based on historical records of past tsunamis, two inundation scenarios of 5 m and 9 m run-up height were assumed to perform the physical vulnerability and risk analysis. The vulnerability results presented in the study are based on a conference paper prepared by Eckert and Zeug(2009). According to their methodology, the building vulnerability is based on the four indicators: elevation, building type, number of floors and shoreline distance. These indicators were derived from stereo remote sensing data in combination with a field survey.

5.2 Tsunami Fragility

Koshimura et al. (2009b) proposed the term "Tsunami fragility" as a new measure for estimating tsunami damage. Tsunami fragility is defined as the structural damage probability or fatality ratio with particular regard to the hydrodynamic features of tsunami inundation flow, such as inundation depth, current velocity, and hydrodynamic force (Suppasri et al., 2011). Koshimura et al. (2009b) described three methods to develop tsunami fragility for structural damage; tsunami fragility determined from satellite remote sensing and numerical modeling, determined from satellite remote sensing and field surveys and determined from historical data. In the first case, Koshimura et al. (2007, 2009c) developed tsunami fragility curves from a numerical method. High-resolution satellite imagery in Banda Aceh, Indonesia was used for damage detection with visual interpretation. A numerical model of tsunami propagation and coastal inundation with high-resolution bathymetry/topography data was produced to determine the hydrodynamic features of tsunami inundation on land. The model results and interpretation of damaged buildings are then combined to define the relationship between the hydrodynamic features of tsunamis such as inundation depth, flow velocity, hydrodynamic force, and damage probabilities. Further research was carried out for the 1993 Hokkaido Nansei-oki tsunami (Okushiri tsunami) by Koshimura et al. (2009a). Secondly, based on investigation results and damage levels, Foytong (2007) and Ruangrassamee et al. (2006) used their survey database of about 120 buildings in tsunami-affected provinces in Thailand to construct fragility curves of reinforced-concrete buildings.. Damage levels are defined in terms of the overall damage of buildings. The four damage levels are those of no damage, damage in secondary members (roof and wall only) only, damage in primary members (beam, column and footing), and collapse. Their conclusions showed that the fragility curves are dependent on building capacity related to numbers of stories. Tsunami fragility is also expressed by building damage levels from numerous field surveys conducted by Matsutomi and Harada (2010). Finally, historical data on damaged buildings in Japan were used and tsunami fragility curves were developed by Koshimura et al. (2009b). Their database included post-tsunami surveys, documents and reports which include both tsunami height and inundation depths for the 1896 Meiji-Sanriku, 1933 Showa-Sanriku, and 1960 Chile tsunamis. Structural damage to houses was originally classified into four categories: washed away, completely destroyed, moderately damaged, and only flooded.

A case study of Seaside, Oregon for the application of fragility curves to estimate building damage and economic loss at a community scale was carried out by Wiebe and Cox, 2013. In their study, the damage estimates are based on fragility curves from the literature which relate flow depth with probability of damage for two different structural materials of buildings. They used the fragility curves developed by Suppasri et al. (2012) from the 2011 Tohoku event. As they stated, these curves have the advantage of providing four performance levels ranging from minor to complete damage for both wooden and concrete/steel buildings. However, a limitation of these fragility curves were that they are all based on the flow depth, and fragility curves for velocity and momentum flux from the 2011 event are still in development.

Another approach for the structural tsunami vulnerability issue comes from Peiris (2006). He presents vulnerability functions developed for residential and non-residential structures using the data available for the coastal areas of Sri Lanka and describes how the functions should be applied within a tsunami loss estimation calculation. Vulnerability functions have been developed for various types of buildings commonly found in coastal areas, e.g. unreinforced masonry, confined masonry, reinforced concrete with masonry infill, etc. The vulnerability functions were found to be dependent on the tsunami inundation distance, water height and estimated velocities of flow of water. In addition functions have been developed for the determination of casualties using their relationship with the building damage data. It is anticipated that the vulnerability functions developed here could be extended to other elements under risk e.g. infrastructure, ports and other facilities, and the methodology could be applied in other countries at risk from tsunami inundation, such as those surrounding the Mediterranean and other parts of Europe.

Performance-based engineering (PBE) allows for a structure to be designed for specified levels of performance under particular hazard scenarios. A possible methodology for assessing response of structures in coastal environments vulnerable to winds, storm surge, tsunamis, and earthquakes is presented in McCullough and Kareem's (2011) study. The three main steps of PBE include proper estimation of the hazard(s), evaluation of the vulnerability of the structure to these hazard(s), and accurate determination of the consequences of the hazard(s) at the system level (Tang et al. 2008). They start with modelling the hazards present and continue with determining the structural fragilities associated with the range of hazards and intensities. Fragility curves are the result of the combination of the vulnerability of the structure and the hazard loads and are typically assumed as a two-parameter lognormal distribution function.

The damage functions correspond to different building ages, structural types, and exposure categories. More detailed information about the methodology such as system fragility and empirical or analytical fragility curves is provided in Shinozuka et al. (2000) and Ellingwood (2005).

Furthermore, Reese et al. (2007) studied the July 2006 Java tsunami in South Java. The purpose of their work was to acquire data for calibration of models used to estimate tsunami inundations, casualty rates and damage levels. Therefore, together with the tsunami vulnerability of buildings, phenomena such as the vulnerability of people and mortality risks were also analysed by the team of scientists from New Zealand and Indonesia who undertook a reconnaissance mission to the South Java area affected by the tsunami. They state that, despite various natural warning signs, very few people were alerted to the impending tsunami. Hence, the death toll was significant, with average death and injury rates both being about 10% of the people exposed, for water depths of about 3 m tsunami. More recently there has been a tendency to relate casualties to levels of damage. The detailed Java data enabled the authors to analyse the data regarding a possible correlation between the death toll and the number of houses destroyed. They state that there appeared to be a clear correlation between the two parameters and gives it as a graph (Fig. 4.1) possibly providing a way of estimating casualties when direct counts are not available.

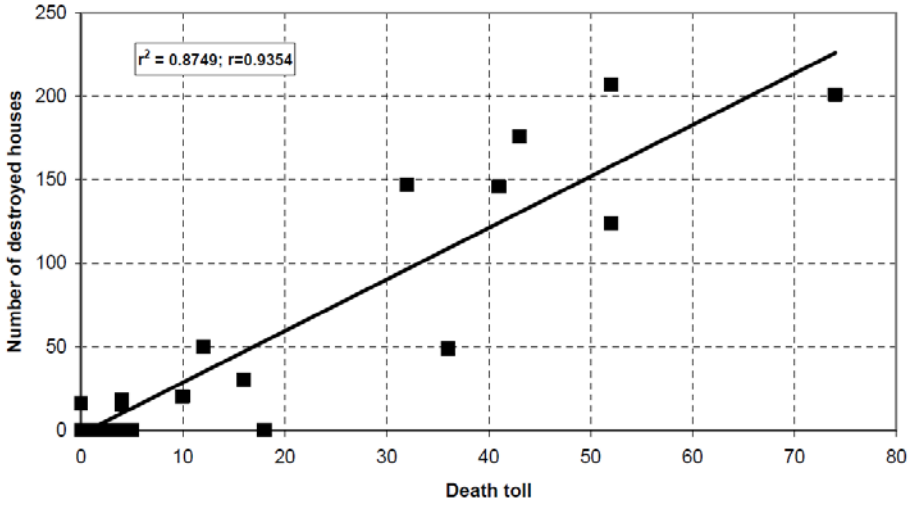

Fig. 5.1. Death rates as functions of building destruction. Source: (Reese et al., 2007)

Supprasi et al. (2013) used building and damage data of 2011 GEJE event and developed fragility functions. The data set they used cover information on number of stories per building, location (town), damage level and structural material such as reinforced concrete, wood and steel. The results show that reinforced concrete and steel buildings have a better resistant performance of over wood or masonry buildings. Also, buildings taller than two stories were confirmed to be much stronger than the buildings of one or two stories. Additionally, it is seen that at the same tsunami inundation depth, buildings along ria coast were much greater damaged than buildings from the plain coast. The difference in damage states can be explained by the faster flow velocities in the ria coast at the same inundation depth (Figure 5.2)

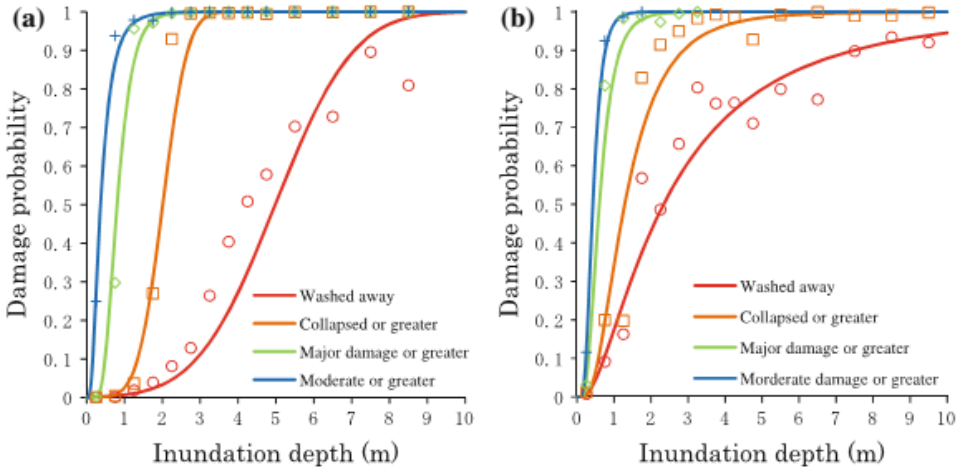

Fig. 5.2 Tsunami fragility curves using data from Ishinomaki city for a plain coast (a) and ria coast (b) Source: *(Suppasri et al., 2013)*

5.3 Social – Ecological Vulnerability

Social and ecological vulnerability to disasters are influenced by build-up or erosion of resilience both before and after disasters occur. Resilient social-ecological systems incorporate diverse mechanisms for living with, and learning from, change and unexpected shocks. Disaster management requires multilevel governance systems that can enhance the capacity to cope with uncertainty and surprise by mobilizing diverse sources of resilience. Coastal zones should be transformed into systems that are more resilient and adaptive to a rising incidence of large disturbances

Adger et al. (2005) review two case studies as examples. The first is the 2004 Asian tsunami, which shows that social-ecological resilience is an important determinant of both the impacts of the tsunami and of the reorganization by communities after the event. A key lesson is that resilient social-ecological systems reduced vulnerability to the impacts of the tsunami and encouraged a rapid, positive response. Social resilience, including institutions for collective action, robust governance systems, and a diversity of livelihood choices are important assets for buffering the effects of extreme natural hazards and promoting social reorganization. The 2004 Asian tsunami tragedy demonstrates that formal and informal institutions with the capacity to respond to rapid change in environmental and social conditions are a key to mitigating the social effects of extreme natural hazards. The hidden success story of the tsunami was the prevention of widespread secondary mortality of injured and traumatized victims from infection and disease, due in large part to the unprecedented scale of national and international responses (Adger et al., 2005).

Tsunami risk in U.S. coastal communities is a function of the extent of tsunami hazards, land use types, population, and economic patterns in threatened areas. To improve their Nation's ability to understand and manage risks associated with

tsunamis, they augment the traditional National Tsunami Hazard Mitigation Plan (NTHMP) research focus on hazard assessments with research dedicated to understanding societal vulnerability to these threats, defined as the exposure, sensitivity and resilience of communities. To address these impacts, the US Geological Survey initiated a project with several institutions. Results were summarized by evacuation zone and by Census Designated Place (CDP). Once the new evacuation maps are completed, the risk and vulnerability assessments can be updated to reflect the risk to additional facilities, structures, and infrastructure in the zone (State of Hawai‘i Multi-Hazard Mitigation Plan, 2010).

Going one step further takes us to the place of coastal ecosystems in vulnerability issue or in other words, the ecological resilience to coastal disasters. Hard and Knight (2009) presents a procedure for assessing the vulnerability of an open-coast dune system to tsunami hazard. Geographic Information System (GIS)-based analyses of Light Detection and Ranging (LIDAR) data are employed to classify a range of dune topographies in terms of four tsunami inundation scenarios, along the coast of Christchurch, New Zealand. Analysis reveals two key characteristics which together define the tsunami vulnerability of a narrow vegetated dune system: (i) the elevation or average height of the dune ridge and (ii) the continuity or standard deviation of height of its long shore profile. A tsunami inundation vulnerability index is developed to assist coastal managers in quickly assessing the relative vulnerability of sections of dune, while simultaneously identifying the nature and location of weaknesses. Relative to current field survey-based methods of determining tsunami inundation risk, the GIS-based procedures and vulnerability index developed in the study offer significant improvements in accuracy and efficiency at local to regional scales.

Kaplan et al. (2009) aimed to investigate the role of coastal vegetation in buffering communities against tsunamis and to capture the elements of vulnerability of affected communities in a tsunami-affected area in south-western Sri Lanka. The vulnerability assessment was based on a comprehensive vulnerability framework and on the Sustainable Livelihoods Framework in order to detect inherent vulnerabilities of different livelihood groups. Their study resulted in the identification of fishery and labour-led households as the most vulnerable groups. Unsurprisingly, analyses showed that damages to houses and assets decreased quickly with increasing distance from the sea. It could also be shown that the Maduganga inlet channelled the energy of the waves, so that severe damages were observed at relatively large distances from the sea. Some reports after the tsunami stated that mangroves and other coastal vegetation protected the people living behind them.

Römer et al. (2010 and 2012) investigated impacts of the 2004 tsunami on coastal ecosystem along the Andaman Sea coast of Thailand as well as the recovery in order to assess ecological tsunami vulnerability and resilience. They first analysed tsunami-induced damage of five different coastal forest ecosystems at the Phang-Nga with a remote sensing driven approach based on multi-date IKONOS imagery. The analysis (Römer et al., 2010) shows that mangroves were the worst damaged among the five forests, followed by casuarina forest and coconut plantation. Then they tried

to find out to what extent (in terms of percentage area and speed) the affected ecosystems were capable of recovering after the tsunami. Field measurements and multi-date IKONOS imagery were used to estimate the recovery and succession patterns of coastal vegetation types in the Phang-Nga province of Thailand, three years after the tsunami. Thus, this study contributes to a holistic understanding of the ecological vulnerability of the coastal area to tsunamis (Römer et al., 2012). According to the results, recovery processes vary based on the type of the ecosystem and they are strongly influenced by human activities. Among the forest ecosystems, recovery rates of casuarina forests were higher than for mangroves, but the recovery area was smaller.

5.4 Summary of the Vulnerability Approaches

Although, there is no general agreement between different disciplines on the definition of risk, tsunami risk is generally expressed as the product of hazard and vulnerability (e.g. Rynn and Davidson, 1999) where as some scientists also use the extended expression such as the product of hazard, vulnerability and economic value (e.g. Papadopoulos and Dermentzopoulus, 1998), or simply hazard and consequences or exposure (Clague et al. 2003). Vulnerability assessment as the second dimension of risk assessment plays a crucial role in tsunami disaster reduction strategies. The difference in the definition of risk has produced numerous methods to evaluate risks, ranging from highly technical, statistical, quantitative assessments to simple, qualitative assessments. The best assessments would combine these methods, treating each hazard separately, as well as incorporating considerations for multiple and cumulative hazards occurrences into the overall assessment framework and methodology. Summary of some of the vulnerability assessments are provided in Table 4.2.

Table 4.2. Summary of some vulnerability approaches. Some parts are adapted from: Jelínek, and Krausmann. "Approaches to tsunami risk assessment." (2008).

Source/level of analysis	Vulnerability, its indicators and elements at risk
Lee (1979)	*Structural vulnerability:* structural integrity and basement stability *Elements at risk* includes coastal structures, e.g. power plants, breakwaters, harbors, etc.
Pararas-Carayannis, (1988)	Consideration of public safety and protection of property (e.g. of high risk standards such as communication centers, chemical factories, nuclear power plants, and other important engineering structures; important facilities, as hospitals, fire stations or police services)
NTHMP (1997) (USA, local and regional level)	Inundation and evacuation maps as the fundamental basis of local tsunami hazard planning Population and infrastructure

Source/level of analysis	Vulnerability, its indicators and elements at risk
NSTC (2005) (USAl)	Coastal vulnerability including the population infrastructure, lifelines, economic activities, level of local preparedness
Sugimoto et al. (2003) (local scale, Usa town, Shikoku Island, Japan)	Map data, e.g. coastal lines, roads, buildings, evacuation places, population distribution etc. Inhabitant's evacuation activity
Rynn and Davidson (1999) (Australia, national level)	*Vulnerability inventory:* built environment (major ports, harbors, fishing industry, offshore oil and gas fields, industrial sites, residential communities, infrastructure, tourist centers, future significant developments, near-shore communities) and natural environments (significant coastal geography, tourist areas) *Map of vulnerable areas* in qualitative terms as low, medium and high vulnerability
Middelmann (2007) (Australia, national level)	*Vulnerability model* to characterize nature and magnitude of the damage from a wave of given velocity *Structural vulnerability* must be estimated based on damage from past events or using an engineering modeling approach (the loads on the structures) *Human vulnerability* estimated from the structural vulnerability, population density, the time of day of the event, height and velocity of tsunami *Exposure database* of the area of interest
Berryman (2006) (New Zealand, national level)	Upper and lower bound, i.e. *maximum* and *minimum* inundation using DEM (10 m cell size) and ground roughness (extracting land use data, 1:50,000) *Building asset model*, values, floor areas and plan areas; workplace and residential buildings; tsunami forces and building strength *Population model* for location of people *Death and injury model* to asses casualties as a portion of the population, tsunami casualties (death and injury) rates versus water depth, Assumption of no warning system, night-time scenario
Nadim and Glade (2006) (Thailand, national level)	Focusing on loss of human life only *Risk of human life* is dived into three groups: 1)

Source/level of analysis	Vulnerability, its indicators and elements at risk
	people who live in the exposed area permanently, 2) tourists, and 3) locals who do not live in the exposed areas but work there during tourist season. *Conditional probability:* week-day, time of the day, high/low tide, warning systems are considered
Cavalletti et al. (2006) (Thailand, local level) CRATER project	*Vulnerability parameters* included are population, built environment, socioeconomic aspects, environment, combined vulnerability and its impact elements (i.e. for buildings it is building material, number of floors, etc.) *Thematic vulnerability maps* such as socio-economic vulnerability map
Papadopoulus and Dermentzopoulus (1998) (Heraklion, Greece, local level)	*Elements at risk include:* population, properties, road network, important installations and life lines *Thematic maps of:* - Natural environment state - Tsunami hazard impact potential on soil foundation conditions - Land use/cover types - Tsunami wave surge impact force relative magnitude characteristics on land - Property damage potential - Road network, life lines, important installations - Distribution of socioeconomic and population
Papathoma and Dominey-Howes (2003) (Gulf of Corinth, Greece, local level)	Vulnerability of buildings, humans and the economy is ranked using 7 weighting factors
Tinti et al. (2008) (Sicily, regional level)	Vulnerability of people considers people in residential houses, industrial, commercial buildings, public structures (e.g. schools, universities and hospitals)
Dunbar and Weaver (2008)	Exposure and vulnerability assessment by identifying who and what is actually *exposed to tsunami inundation and run-up Structural design, material, condition of structure*, and distance from shoreline for physical structures; *Age, gender, education, mobility*, and physical health for people People and structures exposed to tsunami inundation

Source/level of analysis	Vulnerability, its indicators and elements at risk
Post et al. (2007)	Vulnerability and coastal risk towards tsunami threats for the socio-economic and physical dimensions *Who and What is vulnerable*: socio-economic spheres ("who" including social groups and institutions) linked with the physical-natural spheres ("what" in a sense of e.g. built environment, critical infrastructures, economic sectors).
Birkmann (2006)	BBC-Framework of vulnerability assessment (social, economic, environmental dimensions) *Exposed and susceptible elements* on one hand, and the *coping capacities of the affected entities* (for example social groups) on the other The population exposed (different social groups), basic infrastructure services and physical structures within coastal communities
Strunz et al., (2011)	*Vulnerability Assessment based on exposure estimation* (using in-situ assessment and remote sensing) and assessment of response capabilities and preparedness Geometrical and structural parameters of representative buildings & Warning dissemination, anticipated response, evacuation parameters for people Buildings and community
McCullough and Kareem (2011)	*Performance-Based Engineering, Vulnerability of the structure to hazard*s *Fragility curves:* Building ages, structural types, and exposure categories
Ismail et al. (2012)	*Vulnerability of the physical characteristics of the coastal area*(in Malaysia) Tsunami Impact Classification Maps, Tsunami Physical Vulnerability Index (PVI) maps, Structural (SVI) maps
Dall'Osso and Dominey-Howes (2009)	*GIS tool* to assess the *vulnerability of coastal infrastructure* to tsunami (spatial distribution of vulnerable structures)
NOAA CSC, USGS Wood et al., (2002)	A GIS-based vulnerability assessment methodology Using GIS and field surveys to identify the exposure of port and harbor infrastructure, facilities
Peiris (2006)	*Vulnerability functions for residential and non-residential structure*s Vulnerability functions dependent on: Tsunami

Source/level of analysis	Vulnerability, its indicators and elements at risk
	inundation distance, water height and estimated velocities of flow of water
Sinaga et al. (2010) (Local level)	*GIS mapping methodology for tsunami vulnerability assessment* (a case study of the Jembrana Regency in Bali, Indonesia) *Indicators:* Topographic elevation and slope, topographic relation to tsunami direction, coastal proximity, and coastal shape
Kameda (2011) (local level)	*GIS mapping methodology* (Miyagi, Japan) *Variables:* Elevation, slope, tsunami direction and coastal proximity
Mastronuzzi and Sansò (2006) (local level)	Tsunami vulnerability in the Apulia Region, Italy: Vulnerability of different type of coasts
Bernard et al., 2007 (New Zealand, local level)	*Probabilistic tsunami hazard assessment:* relations between water velocity and structural damage
Jelínek et al. (2009) (local level)	*Physical vulnerability and risk for the City of Alexandria, Egypt* using very high resolution satellite remote sensing data *Indicators:* Elevation, building type, number of floors and shoreline distance
Adger et al. (2005) (local level)	*Social-ecological resilience* (Case study: 2004 Asian Tsunami)
U.S. NTHMP (2010) (National Level)	*Tsunami risk in U.S. coastal communities* *Functions:* Extent of tsunami hazards, land use types, population, and economic patterns in threatened areas
Wood and Gregg (n.d.)	*Vulnerability of Human-Environmental Systems* Handles vulnerability in a framework of a combination of physical, social, economic, ecological, and political components
Hard and Knight (2009) (local level)	*Vulnerability of an open-coast dune system to tsunami hazard* (GIS-based analyses of Light Detection and Ranging (LIDAR) data) *Indicators* to vulnerability of a narrow vegetated dune system: (i) the elevation or average height of the dune ridge and (ii) the continuity or standard deviation of height of its longshore profile

Source/level of analysis	Vulnerability, its indicators and elements at risk
Kaplan et al. (2009)	*Investigation of the role of coastal vegetation against tsunamis* and to capture the elements of vulnerability of affected communities in a tsunami-affected area in southwestern Sri Lanka *Sustainable Livelihoods Framework* in order to detect inherent vulnerabilities of different livelihood groups
NGI (Norwegian Geotechnical Institute)	GIS-Based Structural Building Vulnerability and mortality risk *Vulnerability Criteria:* number of floors, barriers in place, material, use

Many of these vulnerability assessments start with determining the inundation area and depth calculated by the numerical models. Vulnerability of an area is usually considered as a combination of both physical and social characteristics including the structures such as buildings and infrastructure. Many of the vulnerability models are developed to understand the extent of structural damage (buildings specifically) as well as the number of people affected by the tsunami. There are models which include other aspects of vulnerability such as ecological vulnerability considering the ecosystem of the area as well as the possible impacts on economy and political components of the region however these types of models require higher integration of different parameters and they are not common in the literature. As more parameters defining vulnerability is included in the models, weighing methods have been applied. However, in general, the weights are either expert or available data dependent which increases the uncertainty of the overall results as well as affecting the applicability of the model to different regions negatively.

Most the vulnerability assessments require a tsunami event either as the most recent or the most devastating historical event or possible scenarios provided by the researchers to determine the inundation area. Additionally, probabilistic approach has started to gain attention to determine the input tsunami event to predict the possible risk of a region. On the contrary, some vulnerability assessment approaches use predetermined inundation heights considering the topography of the region.

Almost all of the vulnerability assessment models use GIS environment and the reliability of the results requires high resolution data as well as accurate representation of the tsunami event. This requires an assessment of the people, homes, commerce, industry, natural resources, etc., that are in the tsunami inundation zones for a given event. However, exposure does not equal vulnerability—the susceptibility to harm or damage during tsunami inundation. The vulnerability of a physical structure would be influenced by factors such as structural design, material, condition of structure, and distance from shoreline whereas the factors that would control the vulnerability of a person would include age, gender, education, mobility, and physical health. Thus, the amount of data required for a complete assessment of

vulnerability would also require GIS data of the mentioned parameters. This could be a major limitation in application of some the models as GIS based data is not available at every location and with the required resolutions.

Most of the predicted vulnerability or the damage is associated with inundation depth although recent research has shown that velocity and fluxes associated with the inundation could be more significant for accurate predictions. Tsunami fragility curves drawn to represent relationship between the damage level and inundation have been widely used in the literature however the classification of the damage levels are still subjective as they are based on the field assessments. Additionally, the classification of damage levels is not universal as different definitions are used by different research groups at different events.

Since many of the vulnerability assessments are part of the risk studies which are used as part of early warning systems or community based mitigation strategies, the results have to be reliable and easily utilized by the decision makers. For the 2011 tsunami, many of the assessments underestimated both the structural damage and the population at risk. Although this underestimation is believed to be due to an underestimation of the magnitude of the hazards involved, still as the uncertainties related to the methodology of vulnerability assessments including fragility concept decrease, the reliability and the performance of the non-structural mitigation strategies would increase significantly. Thus, working towards common approaches in determining the vulnerability and risk should be an objective of the scientific community.

6 Summary and Concluding Remarks

This deliverable has been prepared to summarize and identify the gaps of existing numerical modelling tools, failure mechanisms of coastal structures exposed to tsunamis as well as vulnerability assessment methods.

The number of numerical models developed is significant. Some of these models focus on the tsunami generation, propagation and inundation (eg. TUNAMI, NAMIDANCE, MOST). Some of them are developed for a wider range of applications such as nearshore wave processes, advection-dispersion or sediment transport that can be used for tsunami modelling (eg. BOSZ, MIKE21, etc). Different equations such as shallow water, Navier-Stokes and Bousinessq equations are solved with a variety of numerical schemes. Each of these solutions requires a set of assumptions that could affect the performance of the models. Structured, unstructured and nested meshes are the most common types of meshes/grids in the models. The type of grid used by the model can determine the accuracy of representing the bathymetry/topography, the accuracy of the inundation, as well as the computation duration. Nested meshes have become widely used in the recent years, as different resolutions could be used in the model that can decrease the computation time. Almost all of the numerical models have the capability of

modelling earthquake generated tsunamis. Some of the tools can model landslide generated tsunamis and only a few of them consider other tsunami generation mechanisms. The numerical tools have been applied to several different tsunami events around the world. Especially, after the 2004 and 2011 events, more attention has been paid to the accuracy of inundation modelling including the velocity and fluxes considering different roughness patterns, which turned out to be very important.

The assessment of the impact of tsunami on structures requires the calculation of tsunami forces, even though many building codes do not generally consider tsunami loading. However, a significant amount of damage has been observed during the 2011 Great East Japan Earthquake (GEJE) tsunami which put an emphasis on proper planning of buildings under tsunami flow. Forces associated with tsunami consist of: (1) hydrostatic force, (2) hydrodynamic (drag) force, (3) buoyant force, (4) surge force and (5) impact of debris. To model the tsunami forces, three parameters are essential: (1) inundation depth, (2) flow velocity, and (3) flow direction. The proposed formulas to calculate the forces mostly depend on accurate prediction of tsunami velocity and flux. Tsunami velocity at different locations under inundation is one of the topics that has to be further studied to increase the force calculations in the design of structures. The proposed formulas all have empirical coefficients thus there is a range of values for numerical prediction of tsunami velocity. One can either use conservative values – or work with range which actually gives 100% difference in terms of velocities. Additionally, the effects of run-up, backwash and direction of velocity are not addressed in current design codes.Thus it is important to have more experimental data on the forces generated by tsunamis acting on various types of structures. A failure modes matrix showing failure mechanisms of different land structures such as reinforced concrete and steel buildings, walls, columns, wooden structures according to tsunami impact pressure or the standing tsunami pressure is presented in the report. Debris impact is commonly observed in wooden structures and buildings whereas overturning, bending and punching shear failure and 1st story collapse are the other failure modes seen under impulsive tsunami loading. In case of standing tsunami pressure, scour and rebar fracture are the most common ones and overturning, rebar yielding and wash-away due to sustained force are the other present forms of failure. The analysis shows that the static and dynamic effects of debris on structures is significant in addition to tsunami pressure which requires further study to understand the exact effects on the overall damage. Also, the design approaches against erosion around concrete structures should be improved and extended since it occurs in most of the cases.

Considering tsunami loads on coastal structures such as breakwaters, the available design codes do not integrate tsunami loads explicitly. Thus the performance of these structures is assessed in the field as in the case of 2011 tsunami. The main function of coastal structures against tsunamis is to prevent overflow. Thus most of the time the design consideration is based on historical events or model results from possible tsunami scenarios. However, tsunami loads can cause damage on the structure (eg slope instability) and in return initiate overtopping during later stages due to long

duration of tsunami waves. Additionally, once overflow occurs, other types of failure modes can be seen such as scouring which further increases the damage. Design codes for coastal structures such as breakwaters are focused on wind waves and storm surges since the tsunami events does not occur frequently. Since experiments on the performance of coastal structures under tsunami loading and overflow have gained attention recently, most of the information on failure modes are based on the observations and field surveys of the latest tsunami events. Using this information, a failure mode matrix of coastal structures has been prepared. Water level differences across the structure and wave impact on the structure are the two main processes that initiate the failure. Many of the structures given in the table describe the types of structures located in Japan considering the vast amount of information collected after the 2011 GEJE tsunami. Functional failure of the structures (overflow) initiates several of the failure modes consecutively to generate the final damage observed. However, the exact sequence of the failure modes for many of the failures require more experiments and/or real time observations to accurately understand the overall damage caused by tsunami. A fault tree analysis could provide useful insight into the exact sequence and the impact of individual failure modes on the total damage. Thus this could be an important future work that needs to be considered. Additionally, not all the failure modes presented in the matrix have been observed for every type of the structure. This could either mean that that particular type of failure is not possible or the failure mode requires more research in order to reach a conclusive outcome. Most of the missing information is about performance of rubble mound breakwaters since they are not common in Japan. Additionally, failure modes due to wave impact have not been investigated much in the literature. Another important outcome of the failure matrix is that soil conditions and soil-structure interaction is very important in the case of overflow. Much of the observed failures were based on scouring on either side of the structures occurred during the tsunami event. Additionally, some of the failures were due to the tsunami drawdown (outflow) which was not considered in the design of these structures before 2011 observations.

Vulnerability assessment as the second dimension of risk assessment plays a crucial role in tsunami disaster reduction. Some of the vulnerability assessment methods have been provided as examples throughout the report. Many of these vulnerability assessments start with determining the inundation area and depth calculated by numerical models in order to understand the extent of structural damage (buildings specifically) as well as the number of people affected by the tsunami. There are models which also include other aspects of vulnerability such as ecological or environmental impacts, impacts on the economy, social or political aspects influencing the vulnerability of a region, which are aspects not depending on water depths alone. If more parameters defining vulnerability are included in the models, for example in terms of indicators, weighing methods have been applied to quantify vulnerability. However, in general, the weights are either gained by expert judgement or depending on available data, which increases the uncertainty of the overall results. Moreover, this affects the applicability of the models to different regions negatively. Most vulnerability assessments use historical tsunami events or possible scenarios to determine the inundation area. Additionally, probabilistic approaches have been used

to determine the input tsunami event to predict the possible risk of a region. Almost all of the vulnerability assessment models use GIS and the reliability of the results depends on the resolution of data as well as the accurate representation of the tsunami event. Most of the predicted vulnerability or the damage is associated with inundation depth although recent research has shown that velocity and fluxes associated with the inundation could be more significant for accurate predictions. Tsunami fragility curves drawn to represent the relationship between the damage level and the inundation have been widely used in the literature. Fragility curves gained from field surveys after real events are useful sources to understand and map tsunami damage. However, the classification of the damage levels is still subjective as it is based on the field assessments. Additionally, the classification of damage levels is not universal as different definitions are used by different research groups at different events. Many of the vulnerability assessments are part of the mitigation studies. However, for the 2011 tsunami many of the assessments underestimated both the structural damage and the population at risk. Although this underestimation is believed to be due to an underestimation of the magnitude of the hazards involved, the uncertainties related to the methodologies of vulnerability assessment including the fragility concept also influenced the reliability of the results. Working towards common approaches in determining the vulnerability and risk as well as key definitions used in the assessments should be an objective of the scientific community.

Considering the information collected and the results derived from this deliverable, the following studies are suggested for further progress:

- Enhance numerical models such as NAMI-DANCE focusing on the modelling of tsunami parameters in high resolution geometries (e.g. urban areas), see RAPSODI Deliverable 5 (METU 2015a) and Deliverable 6 (METU 2015b).
- Through experiments, fill the information gap on tsunami impact on rubble mound breakwaters (with and without crown wall) focusing on wave loading and the respective failure modes on different slopes and type of wave generation (solitary, bore), see RAPSODI Deliverable 7 (TU-BS 2015).
- Enhance the vulnerability assessment model developed by NGI by integrating building fragility curves and socio-economic, environmental, and physical information collected after the 2011 tsunami in the model in Deliverable 8 (NGI 2015). First steps are presented in RAPSODI Deliverable 8.

7 References

- [NTHMP] National Tsunami Hazard Mitigation Program (2012): Proceedings and Results of the 2011 NTHMP Model Benchmarking Workshop. Boulder: U.S. Department of Commerce/NOAA/NTHMP; (NOAA Special Report). 436 p.

- National Tsunami Hazard Mitigation Program (NTHMP) (2011): GeoClaw documentation. http://www.clawpack.org/geoclaw.
- Abadie S, Caltagirone JP, Watremez P. (1998): Splash-up generation in a plunging breaker. Comptes Rendus de l'Académie des Sciences -Series IIB - Mechanics-Physics-Astronomy, Volume 326, Issue 9, Pages 553-559
- Abadie S, Grilli S, Glockner S. (2006): A coupled numerical model for tsunami generated by subaerial and submarine mass failures, in Proc. 30th Intl. Conf. Coastal Engng., San Diego, California, USA. 1420-1431.
- Abadie S, Morichon D, Grilli S, Glockner S. (2010):A three fluid model to simulate waves generated by subaerial landslides. Coastal Engineering, 57, 9, 779-794.
- Abadie, S, Morichon, D, Grilli, S, Glockner, S. (2008): VOF/Navier-Stokes numerical modeling of surface waves generated by subaerial landslides, La Houille Blanche, 1, 21-26.
- Adger, W. Neil, et al. "Social-ecological resilience to coastal disasters." Science 309.5737 (2005): 1036-1039. Available at http://www.scd.hawaii.gov/documents/04_ExSumm_2010_SCDFinal_v2.pdf
- Ambraseys, N. and Synolakis, C. (2010): Tsunami catalogs for the Eastern Mediterranean revisited, J. Earthq. Eng., 14(3), 309–330. doi:10.1080/1363246090327759
- Arikawa, T. (2009): "Structural behavior under impulsive tsunami loading." J Disaster Res 4.6, 377-381.
- Arikawa, T. and Shimosako, K. (2013): "Failure mechanism of breakwaters due to tsunami; a consideration to the resiliency." 6th Civil Engineering Conference in the Asian Region, 20th-22nd August, 2013, Jakarta, Indonesia
- Arikawa, T. et. al. (2012): Failure mechanism of Kamaishi breakwaters due to the Great East JAPAN earthquake tsunami, International Conference on Coastal Engineering 2012
- Azvedo A, Oliveira A, Fortunato AB, Bertin X. (2009): Applicaiton of an Eulerian-Lagrangian oil spill modeling system to the Prestige accident: trajectory analysis. J. Coastal. Res., 56, 777-781.
- B. L. Turner II et al. (2003): Proc. Natl. Acad. Sci. U.S.A. 100, 8074.
- Baldock, T. E., et al. (2007): "Modelling tsunami inundation on coastlines with characteristic form." Proc. 16th Australasian Fluid Mechanics Conf. (AFMC).
- Bale DS, LeVeque RJ, Mitran S, Rossmanith JA. (2002): A wave propagation method for conservation laws and balance laws with spatially varying flux functions. SIAM J. Sci. Comput., 24:955–978.
- Behrens J, LeVeque RJ. (2011): Modeling and simulating tsunamis with an eye to hazard mitigation. SIAM News, 44(4), May.
- Behrens, Jörn (2008): "TsunAWI-Unstructured Mesh Finite Element Model for the Computation of Tsunami Scenarios with Inundation."
- Ben-Menahem, A., and Rosenman, M. (1972): "Amplitude patterns of tsunami waves from submarine earthquakes." J. Geophys. Res., 77(17), 3097–3128.

- Berger MJ, George DL, LeVeque RJ, Mandli KT (2011): The GeoClaw software for depth averaged flows with adaptive refinement. Adv. Water Res.
- Berger, Marsha J., et al. "Logically rectangular finite volume methods with adaptive refinement on the sphere." Philosophical Transactions of the Royal Society A: Mathematical, Physical and Engineering Sciences 367.1907 (2009): 4483-4496.
- Bernard, E.N., Dengler L.A., Yim, S.C. (2007): ‘’NATIONAL TSUNAMI RESEARCH PLAN: Report of a Workshop Sponsored by NSF/NOAA’’, Pacific Marine Environmental Laboratory.
- Birkmann, J. (Editor) (2006): Measuring Vulnerability to Hazards of Natural Origin –Towards Disaster- Resilient Societies. UNU press, Tokyo.
- Bogardi, J. and Birkmann, J. (2004): Vulnerability Assessment: The First Step towards Sustainable Risk Reduction. In: D. Malzahn and T. Plapp (Editor), Disasters and Society -From Hazard Assessment to Risk Reduction, Berlin, p. 82.
- Bryant, E. A. (2001): Tsunami: the Underrated Hazard, Cambridge University Press, London, UK, p. 320.
- Burla M, Baptista AM, Zhang Y, Frolov S. (2010): Seasonal and inter-annual variability of the Columbia River plume: a perspective enabled by multi-year simulation databases. Journal of Geophysical Research, 115, C00B16.
- C. Small, R. J. Nicholls, J. (2003): Coast. Res. 19, 584.
- Camfield, F. (1980): Tsunami Engineering, Coastal Engineering Research Center, US Army Corps of Engineers, Special Report (SR-6), p. 222.
- Camfield, F.E. (1991): Dynamic Response of Structures to Tsunami Attack. Tsunami Symposium, International Union of Geodesy and Geophysics.
- Camfield, Fred E. (1994): Tsunami effects on coastal structures. Journal of Coastal Research, 177-187.
- Cardona, O.D. (2001): Estimation Holistica del Riesgo Sismico. Utilizando Sistemas Dinamicos Complejos, Technical University of Catalonia, Barcelona.
- Carrier, G. F., Wu, T. T., and Yeh, H. (2003): “Tsunami runup and drawdown on a plane beach.” J. Fluid Mech., 475, 79–99.
- Castro M.J., Nieto F. (2012): A Class of Computationally Fast First Order Finite Volume Solvers: PVM Methods. SIAM J. Sci. Comput. 2173-2196, vol 34(4).
- Cavalletti, A., Polo, P., Gonella, M. and Cattarossi, A. (2006): CRATER Coastal Risk Analysis of Tsunamis and Environmental Remediation, 8 pp
- Chance, G (1966): Chronology of Physical Events as a Result of the Alaskan Earthquake, March 27, 1964, Valdez, Prince William Sound and Gulf of Alaska Localities, Cordova, Seward, Kodiak, Homer, and Kenai, Report to Committee on Alaska Earthquake, National Academy of Science, University of Alaska, 176pp.
- Cheung, K.F., Wei, Y., Yamazaki, Y., and Yim, S.C. (2011): Modeling of 500-year tsunamis for probabilistic design of coastal infrastructure in the Pacific Northwest. Coastal Engineering, in review.

- Chock, G., Carden, L., Robertson, I., Olsen, M., and Yu, G. (2013): Tohoku tsunami-induced building failure analysis with implications for U.S. tsunami and seismic design codes, Earthquake Spectra 29, S99–S126.
- Clague, J.J., Munro, A. and Murty, T. (2003): Tsunami hazard and risk in Canada, Natural Hazards 28: 433-461 pp
- COMCOT, Cornell University, n.d., website: http://ceeserver.cee.cornell.edu/pll-group/comcot.htm
- Cross, R.H. (1967): Tsunami Surge Forces, Journal of Waterways and Harbor Division, ASCE, 93(4), 201-231.
- D. Bellwood, T. Hughes, C. Folke, M. Nyström (2004): Nature 429, 827
- Dall'Osso, F. and Dominey-Howes, D. (2009): A method for assessing the vulnerability of buildings to catastrophic (tsunami) marine flooding. Report prepared for the Sydney Coastal Councils Group Inc. 138 pp.
- Dames and Moore (1980): Design and Construction Standards for Residential Construction in Tsunami-Prone Areas in Hawaii, (Prepared for the Federal Emergency Management Agency).
- Dao, M. H., and P. Tkalich (2013): "Recent Significant Earthquake and Tsunami Events in South East Asia'', International Tsunami Symposium.
- Dao, M. H., and P. Tkalich (2007): "Tsunami propagation modeling-a sensitivity study." Natural Hazards and Earth System Science 7.6, 741-754.
- Dominey-Howes, Dale, and Maria Papathoma (2007): Validating a tsunami vulnerability assessment model (the PTVA Model) using field data from the 2004 Indian Ocean tsunami. Natural Hazards 40.1, 113-136.
- Dunbar, Paula K., and Craig S. Weaver (2008): US States and Territories National Tsunami Hazard Assessment: Historical Record and Sources for Waves. US Department of Commerce, National Oceanic and Atmospheric Administration.
- Dutykh D., Mitsotakis D., (2009): On the Relevance of the Dam Break Problem in the Context of Nonlinear Shallow Water Equations, France.
- Dutykh D., Poncet R., Dias F. (2011): The VOLNA code for the numerical modeling of tsunami waves: Generation, propagation and inundation'', France.
- Earthquake Engineering Research Institute (2011): Learning from Earthquakes The Tohoku, Japan, Tsunami of March 11, 2011: Effects on Structures, EERI Special Earthquake Report, September 2011
- Eaton, J.P.; Richter, D.H., and Ault, W.U. (1961): The tsunami of May 23, 1960, on the Island of Hawaii. Bulletin of the Seismological Society of America, 51(2), 135-157.
- Eckert, S., and G. Zeug. (2009): Assessing Tsunami Vulnerability in Alexandria, Egypt by using optical VHR satellite data." 33rd ISPRS Conference, Stresa, Italy.
- Esteban, M., Danh Thao, N., Takagi, H. and Shibayama, T. (2009): Pressure Exerted by a Solitary Wave on the Rubble Mound Foundation of an Armoured Caisson Breakwater, 19th International Offshore and Polar Engineering Conference, Osaka.

- Esteban, M., Morikubo, I., Shibayama, T., Aranguiz Muñoz, R., Mikami, T., Danh Thao, N., Ohira, K. and Ohtani, A. (2012): Stability of Rubble Mound Breakwaters against Solitary Waves, Proc. Of 33nd Int. Conf. on Coastal Engineering, Santander, Spain.
- Esteban, Miguel, et al. (2013): Analysis of the Stability of Armour Units during the 2004 Indian Ocean and 2011 Tohoku Tsunami. Journal of Waterway, Port, Coastal, and Ocean Engineering.
- F. Dahdouh-Guebas et al. (2005): Curr. Biol. 15, R443 (2005).
- Federal Emergency Management Agency (2003): Coastal Construction Manual (3 vols.), 3rd Ed. (FEMA 55), Jessup, MD.
- Filipot J.F., Roeber V., Boutet M., Cédric O., Lathuiliere C., Louazel S., Schmitt T., Ardhuin F., Lusven A., Outré M., Suanez S., Hénaff A. (2013): Nearshore Wave Processes in the Iroise Sea: Field Measurements and Modelling, Coastal Dynamics.
- Foytong, P. (2007): Fragility of buildings damaged in the 26 December 2004 tsunami, Master thesis, Graduate School of Engineering, Chulalongkorn University, Bangkok, Thailand, (in Thai).
- Fraser, Stuart, et al. (2013): Tsunami damage to coastal defences and buildings in the March 11th 2011 M w 9.0 Great East Japan earthquake and tsunami. Bulletin of Earthquake Engineering 11.1, 205-239.
- Fritz, Hermann M., Fahad Mohammed, and Jeseon Yoo (2009): Lituya Bay landslide impact generated mega-tsunami 50th anniversary. Pure and Applied Geophysics 166.1-2, 153-175.
- Fukui, Y. (1963): Hydrodynamic study on tsunami. Coastal Engineering in Japan, 6, 67-82.
- Gayer, G., et al. (2010): Tsunami inundation modelling based on detailed roughness maps of densely populated areas. Natural Hazards and Earth System Sciences 10.8, 1679-1687.
- George D. (2010): Adaptive finite volume methods with well-balanced Riemann solvers for modeling floods in rugged terrain: Application to the Malpasset dam-break flood (France, 1959). Int. J. Numer. Meth. Fluids.
- George DL, LeVeque RJ. (2006): Finite volume methods and adaptive refinement for global tsunami propagation and local inundation. Science of Tsunami Hazards, 24:319–328.
- George DL. (2006): Finite Volume Methods and Adaptive Refinement for Tsunami Propagation and Inundation. PhD thesis, University of Washington.
- George DL. (2008): Augmented Riemann solvers for the shallow water equations over variable topography with steady states and inundation. J. Comput. Phys., 227(6):3089–3113, March.
- González-Vida, J. M., et al. (2012): "Simulation of landslide-generated tsunamis with the HySEA platform: Application to the the Lituya Bay 1958 tsunami." EGU General Assembly Conference Abstracts. Vol. 14.
- González-Vida, J. M., et al. (2013): HySEA-Landslide Gpu-Based Model: Validation Experiments and Application to the 1958 Lituya Bay Megatsunami'', International Tsunami Symposium.

- Gopinath, G., et al. (2014): Impact of the 2004 Indian Ocean tsunami along the Tamil Nadu coastline: field survey review and numerical simulations." Natural Hazards: 1-27.
- Hanzawa M, Matsumoto A and Tanaka H (2012): Stability of Wave-Dissipating Concrete Blocks of Detached Breakwaters Against Tsunami. Proc. of the 33rd Int. Conference on Coastal Engineering (ICCE).
- Harig, S., Chaeroni, Pranowo, W. S. and Behrens, J. (2008): Tsunami simulations on several scales: Comparison of approaches with unstructured meshes and nested grids, Ocean Dynamics. 58, 429–440. doi:10.1007/s10236-008-0162-5.
- Hart, Deirdre E., and Gemma A. Knight (2009): Geographic information system assessment of tsunami vulnerability on a dune coast. Journal of Coastal Research, 131-141.
- HHC (2000): Department of Planning and Permitting of Honolulu Hawai, Chapter 16, City and County of Honolulu Building Code, Article 11.
- Hibberd, S., and Peregrine, D. H. (1979): “Surf and runup on a beach: A uniform bore.” J. Fluid Mech., 95, 323–345.
- Ho, D. V., and Meyer, R. E. (1962): “Climb of a bore on a beach. Part 1: Uniform beach slope.” J. Fluid Mech., 14, 305–318.
- Horrillo J, Kowalik Z, Shigihara Y. (2006): Wave dispersion study in the Indian Ocean tsunami of December 26, 2004. Marine Geodesy **29**(1):149–166.
- Horrillo J. (2006): Numerical Method for Tsunami Calculation Using Full Navier-Stokes Equations and Volume of Fluid Method. Thesis dissertation presented to the University of Alaska Fairbanks.
- Hoshino, D. (2012): Coastal forest in Iwate coast by Tohoku earthquake and tsunami and related damage to villages, Journal of the Japanese Forest Society, 5 pp., in press (in Japanese).
- Iizuka, H. and Matsutomi, H. (2000): Proc. Conf. Coastal Engrg., JSCE, 47. (in Japanese).
- Imamura F., Yalçıner A.C., Özyurt G.(2006): Tsunami Modelling Manual.
- Imamura, F. (1995): Tsunami numerical simulation with the staggered leap-frog scheme, manuscript for TUNAMI code. School of Civil Engineering, Asian Inst. Tech., 45 p.
- Ishimoto, M. and Hagiwara, T. (1934): The phenomenon of sea water overflowing the land. Bulletin of the Earthquake Research Institute. Tokyo, Japan: Tokyo Imperial University, Supplementary 1, 17-2.
- Ismail, H., et al. (2012): A 3-tier tsunami vulnerability assessment technique for the north-west coast of Peninsular Malaysia." Natural hazards 63.2, 549-573.
- Iwasaki, T. and Horikawa, K. (1960): Tsunami caused by Chile earthquake in May, 1960 and outline of disasters in northeastern coasts of Japan. Coastal Engineering in Japan, 3, 33-48.
- Jakeman, John Davis, et al. (2010): Towards spatially distributed quantitative assessment of tsunami inundation models. Ocean Dynamics 60.5, 1115-1138.

- Japan Coast Guard (2011): Raw footage released by the Japan coast guard of the tsunami and fires in Kesennuma. Retrieved 31 August 2011, from https://picasaweb.google.com/lh/photo/cNrrglyXPo5W6-6l4ysuvl6-HV4XK8khGfVE4K2xJdY?feat=embedwebsite
- Jayaratne, R., et al. (2013): Investigation of coastal structure failure due to the 2011 Great Eastern Japan Earthquake Tsunami. Coasts, Marine Structures and Breakwaters 2013 (2013).
- Jelínek R., Eckert S., Zeug G., Krausmann E., (2009): Tsunami Vulnerability and Risk Analysis Applied to the City of Alexandria, Egypt. JRC Scientific and Technical Reports.
- Jelínek, Róbert, and Elisabeth Krausmann (2008): Approaches to tsunami risk assessment.
- Kameda R. (2011): Tsunami Vulnerability Assessment and Crisis Mapping of Actual Tsunami Damage in Miyagi, Japan, UEP 232. Available at http://as.tufts.edu/environmentalstudies/documents/GISpostersKameda.pdf
- Kaiser, G., et al. (2011): The influence of land cover roughness on the results of high resolution tsunami inundation modeling. Natural Hazards & Earth System Sciences 11.9.
- Kaplan, M., F. G. Renaud, and G. Lüchters (2009): Vulnerability assessment and protective effects of coastal vegetation during the 2004 Tsunami in Sri Lanka. Natural Hazards & Earth System Sciences 9.4 (2009).
- Kato, F., Suwa, Y., Watanabe, K. and Hatogai, S. (2012): Mechanism of Coastal Dike Failure Induced by the Great East Japan Earthquake Tsunami. Proc. of 33nd Int. Conf. on Coastal Engineering Santander, Spain.
- Kazama M (2011): The 2011 off the Pacific Coast of Tohoku earthquake—after two months. In: 14th Asian regional conference on soil mechanics and geotechnical engineering. Hong Kong. Retrieved from http://www.jiban.or.jp/file/file/kazama520e2.pdf
- Keulegan, G.H. (1950): Wave motion. Engineering Hydraulics. New York: Wiley, pp. 711-768.
- Kirby J.T. (1998): FUNWAVE 1.0 Fully Nonlinear Boussinesq Wave Mode. Documentation and User's Manual, Research Report NO. CACR-98-06, Center for Applied Coastal Research.
- Kirby, J. T. (1997): "Nonlinear, dispersive long waves in water of variable depth", Chapter 3 in Gravity Waves in Water of Variable Depth, J. N. Hunt (ed). Advances in Fluid Mechanics, 55-126. Computational Mechanics Publications.
- Kirkoz, M.S. (1983): 10th IUGG International Tsunami Symposium, Sendai-shi/Miyagi-ken, Japan, Terra Scientific Publishing, Tokyo, Japan.
- Kortenhaus, Andreas, et al. (2002): Failure mode and fault tree analysis for sea and estuary dikes." Coastal Engineering Conference. Vol. 2. ASCE American Society of Civil Engineers.
- Koshimura S, Nishimura Y, Nakamura Y, Namegaya Y, Fryer GJ, Akapo A, Kong LS, Vargo D. (2009): Field survey of the 2009 tsunami in American

Samoa. EOS Transactions of the American Geophysical Union, 90(52), Fall Meeting Supplemental Abstract U23F-07.

- Koshimura, S. and Yanagisawa, H. (2007): Developing fragility curves for tsunami damage estimation using the numerical model and satellite imagery, in: Proceedings of the 5th International Workshop on Remote Sensing for Disaster Response, George Washington University, Washington, United States.
- Koshimura, S., Matsuoka, M., and Kayaba, S. (2009a): Tsunami hazard and structural damage inferred from the numerical model, aerial photos and SAR imageries, in: Proceedings of the 7th International Workshop on Remote Sensing for Post Disaster Response, University of Texas, Texas, United States.
- Koshimura, S., Namegaya, Y., and Yanagisawa, H. (2009b): Tsunami Fragility – A new measure to assess tsunami damage, Journal of Disaster Research, 4, 479–488.
- Koshimura, S., Oie, T., Yanagisawa, H., and Imamura, F. (2009c): Developing fragility curves for tsunami damage estimation using numerical model and post-tsunami data from Banda Aceh, Indonesia, Coast. Eng. J., 51, 243–273.
- Kowalik Z, Knight W, Logan T, Whitmore P. (2005): Numerical modeling of the global tsunami: Indonesian tsunami of 26 December 2004. Science of Tsunami Hazards; **23**(1):40–56.
- Kowalik Z, Murty TS. (1993): Numerical Modeling of Ocean Dynamics. World Scientific, Singapore, 481 pp.
- Kowalik Z, Murty TS. (1993): Numerical simulation of two-dimensional tsunami runup. Marine Geodesy 16(2): 87–100.
- Langtangen, H.P., Pedersen, G. (1998): Computational models for weakly dispersive and nonlinear water waves. Comput. Methods Appl. Mech. Eng. 160, 337–358.
- Lay, T., Ammon, C.J., Kanamori, H., Yamazaki, Y., and Cheung, K.F. (2011): The 25 October 2010 Mentawai tsunami earthquake (Mw 7.8) and the tsunami hazard presented by shallow megathrust ruptures. Geophysical Research Letters, in press.
- LeVeque RJ, Berger MJ, et al. No date (n.d.) Clawpack. http://www.clawpack.org. Accessed n.d.
- LeVeque RJ, George DL, Berger MJ. (2011): Tsunami modeling with adaptively refined finite volume methods. Acta Numerica, pages 211–289.
- LeVeque RJ, George DL. (2004): High-resolution finite volume methods for the shallow water equations with bathymetry and dry states. In PL-F. Liu, H. Yeh, and C. Synolakis, editors, Proceedings of Long-Wave Workshop, Catalina, volume 10, pages 43–73. World Scientific. http://www.amath.washington.edu/~rjl/pubs/ catalina04/.
- Liu, P. L.-F., Synolakis, C., and Yeh, H. (1991): "Report on the International Workshop on Long-Wave Runup." J. Fluid Mech., 229, 675–688.

- Liu, PHILIP L-F. (1994): Model equations for wave propagations from deep to shallow water. Advances in coastal and ocean engineering 1: 125-158.
- Liu, Philip L-F., et al. (1995): Numerical simulations of the 1960 Chilean tsunami propagation and inundation at Hilo, Hawaii. Tsunami: Progress in prediction, disaster prevention and warning. Springer Netherlands, 99-115.
- Løvholt, F., G. Pedersen, and G. Gisler (2008): Oceanic propagation of a potential tsunami from the La Palma Island. Journal of Geophysical Research: Oceans (1978–2012) 113.C9.
- Løvholt, F., G. Pedersen, and S. Glimsdal (2010): "Coupling of Dispersive Tsunami Propagation and Shallow Water Coastal Response." Open Oceanography Journal.
- Løvholt, F., Setiadi, N.J., Birkmann, J., Harbitz, C.B., Bach, C., Fernando, N., Kaiser, G., Nadim, F. (2014): Tsunami Risk Reduction – Are We Better Prepared Today than in 2004? International Journal of Disaster Risk Reduction 10, 127-142.
- Lubin P, Vincent S, Abadie S, Caltagirone JP. (2006): Three-dimensional Large Eddy Simulation of air entrainment under plunging breaking waves, Coastal Engineering, Volume 53, issue 8, .631-655.
- Macias J., Castro J.M., Gonzalez J.M., Ortega S., Asuncion M. (2013): ‘’HySEA Tsunami Gpu-Based Model. Application to Ftrt Simulations’’, International Tsunami Symposium.
- Magoon, O.T. (1962): The tsunami of May 1960 as it affected northern California. Hydraulics Division Conference (American Society of Civil Engineers), unpublished.
- Mase, H. (1995): "Frequency down drift of swash oscillation compared to incident waves." J. Hydr. Res., 33 (3), 397-411.
- Mastronuzzi, G. I. U. S. E. P. P. E., and S. Sansò. (2006): Coastal geomorphology and tsunami vulnerability. The case study of Apulia region (Italy). Geografia Fisica e Dinamica Quaternaria 29.2, 83-91.
- Matsumoto, T. and Suzuki, Y. (1983): Design and construction of Ohfunato Tsunami Protection Breakwater. In: Iida, K. and Iwasaki, T. (eds.), Tsunamis: Their Science and Engineering. Tokyo, Japan: Terra Scientific Publishing Co., pp. 397-407.
- Matsutomi, H. and Harada, K. (2010): Tsunami-trace distribution around building and its practical use, in: Proceedings of the 3rd International tsunami field symposium, Sendai, Japan, 10–11 April 2010, session 3–2.
- Matuo, H (1934): Estimation of energy of tsunami and protection of coasts. Bulletin of the Earthquake Research Institute. (Tokyo, Japan), pp. 55-64.
- McCullough, M. C., and Ahsan Kareem (2011): A framework for performance-based engineering in multi-hazard coastal environments. Structures Congress 2011. ASCE.
- METU (2015a): Computed tsunami parameter values in shallow waters and around structures. Deliverable D5 of the RAPSODI Project. Norwegian Geotechnical Report 20120768-05-R. http://www.ngi.no/en/Project-pages/RAPSODI/Reports-and-Publications/

- METU (2015b): Numerical Modelling of Tsunamis in Harbours and Bays. Deliverable D6 of the RAPSODI Project. Norwegian Geotechnical Report 20120768-06-R http://www.ngi.no/en/Project-pages/RAPSODI/Reports-and-Publications/
- Middelmann, M.H. (2007): Natural hazards in Australia: identifying risk analysis requirements, Canberra, Geoscience Australia, 173 pp
- MIKE 21 and MIKE 3 Flow Model FM Hydrodynamic Module (2013): www.mikebydhi.com
- Mizutani, Suguru, and Fumihiko Imamura (2001): Dynamic wave force of tsunamis acting on a structure." ITS 2001 Proceedings.
- Mori N, Takahashi T, Yasuda T, Yanagisawa H (2011): Survey of 2011 Tohoku earthquake tsunami inundation and run-up. Geophys Res Lett 38:L00G14. doi:10.1029/2011GL049210
- Mori, Nobuhito, et al. (2013): Overview of the 2011 Tohoku earthquake tsunami damage and its relation to coastal protection along the Sanriku Coast." Earthquake Spectra 29.s1, S127-S143.
- Murty, T.S. (1997): Bulletin of the Fisheries Research Board of Canada- no. 198, Department of Fisheries and the Environment, Fisheries and Marine Service, Scientific Information and Publishing Branch, Ottawa, Canada.
- NAGASAWA, Tsuyoshi, and Hitoshi TANAKA: Study of Structural Damages with massive Geomorphic Change due to Tsunami.
- NGI (2008): The Åknes/Tafjord project — semi-annual report: tsunami impact in the outer part of Storfjorden, testing of numerical models for rock slide and tsunami, coupling to laboratory experiments. Norwegian Geotechnical Institute Report 20051018-2.
- NGI (2009): Local tsunami risk assessment approach. The Bridgetown Demonstration project. Norwegian Geotechnical Institute Report 20081430-2.
- NGI (2011): Analysis of the 2011 Tohoku tsunami. Norwegian Geotechnical Institute Report 20081430-00-11-R.
- NGI (2015): A GIS tsunami vulnerability and risk assessment model. Deliverable D8 of the RAPSODI Project. Norwegian Geotechnical Report 20120768-08-R. http://www.ngi.no/en/Project-pages/RAPSODI/Reports-and-Publications/
- Nielsen O, Roberts S, Gray D, McPherson A and Hitchman A. (2005): Hydrodynamic Modelling of Coastal Inundation. MODSIM 2005 International Congress on Modelling and Simulation, Modelling and Simulation Society of Australia & New Zealand, 518-523.
- Nielsen O. (2004): Water flow software, open to all. In: AusGEO news, No. 75, September 2004, 8-9.
- Nielsen, Ole et al. (2006): Modelling answers tsunami questions. AusGeo News 83: 1-5.
- Nistor, I., Palermo, D., Nouri, Y., Murty, T. and Saatcioglu, M. (2008): Tsunami Induced Forces on Structures, Chapter 11 of Handbook of Coastal and Ocean Engineering.

- NOAA Center for Tsunami Research, National Oceanic and Atmospheric Administration, Pacific Marine Environmental Laboratory, n.d., web site: http://nctr.pmel.noaa.gov/index.html
- Noguchi, K., S. Sato, and S. Tanaka (1997): Large-scale experiments on tsunami overtopping and bed scour around coastal revetment, Proceedings of Coastal Engineering, JSCE, 44, 296-300 (in Japanese).
- Okada, T., Sugano, T., Ishikawa, T., Ohgi, T., Takai, S., and Hamabe, C. (2005): "Structural design methods of buildings for tsunami resistance." (SMBTR), the Building Centre of Japan.
- Okal EA, Fritz HM, Synolakis CE, Borrero JC, Weiss R, Lynett PJ, Titov VV, Foteinis S, Jaffe BE, Liu PL-F, Chan IC (2010): Field Survey of the Samoa Tsunami on 29 September 2009. Seismological Society of America, 81(4), 577-591.
- Okal, E. A., and Synolakis, C. E. (2004): “Source discriminants for nearfield tsunamis.” Geophys. J. Int., 1583, 899–912.
- Oumeraci, H., H. Schüttrumpf, and M. Bleck (1999): "Untersuchungen zur Ermittlung der mittleren Wellenüberlaufrate ohne Freibord bei Stromdeichen." Berichte Leichtweiß-Institut für Wasserbau, Technische Universität Braunschweig 842.
- P. Blaikie, T. Cannon, I. Davis, B. Wisner (1994): At Risk: Natural Hazards, People’s Vulnerability, and Disasters (Routledge, London).
- P. L.-F. Liu et al. (1995): Science 308, 1595.
- P. O’Keefe, K. Westgate, B. Wisner (1976): Nature 260, 566.
- Papadopoulos, G.A. and Dermentzopoulos, Th. (1998): A Tsunami Risk Management Pilot Study in Heraklion, Crete, Natural Hazards 18: 91–118
- Papathoma, M. (2003): Assessing tsunami vulnerability using GIS with special reference to Greece. Unpublished PhD thesis, Coventry University (UK), 290 pp.
- Papathoma, M. and Dominey-Howes, D. (2003): Tsunami vulnerability assessment and its implications for coastal hazard analysis and disaster management planning, Gulf of Corinth, Greece, Natural Hazards and Earth System Sciences 3: 733–747 pp
- Papathoma, M., Dominey-Howes, D., Zong, Y. and Smith, D. (2003): Assessing tsunami vulnerability, an example from Herakleio, Crete, Natural Hazards and Earth System Sciences 3: 377–389 pp.
- Pedersen, Geir, and Finn Løvholt (2008): "Documentation of a global Boussinesq solver." Preprint series. Mechanics and Applied Mathematics http://hdl. handle.net/10852/10470.
- Peiris, Navin (2006): Vulnerability functions for tsunami loss estimation." First European Conference on Earthquake Engineering and Seismology, Geneva, Switzerland.
- Pinto L, Fortunato AB, Zhang Y, Oliveira A, Sancho FE.P (2011): Development and validation of a three dimensional morphodynamic modelling system, Ocean Modelling (submitted).

- Post, J., et al. (2007): Risk and vulnerability assessment to tsunami and coastal hazards in Indonesia: conceptual framework and indicator development." A paper for the international symposium on disaster in Indonesia, Padang, Indonesia.
- Post, J., Mück, M., Steinmetz, T., Riedlinger, T., Strunz, G., Mehl, H., Dech, S., Birkmann, J., Gebert, N., Anwar, H., and Harjono, H. (2008): Tsunami Risk Assessment for Local Communities in Indonesia to Provide Information for Early Warning and Disaster Management. In: Proc. International Conference on Tsunami Warning (ICTW). Bali, Indonesia.
- Post, J., Wegscheider, S., M¨uck, M., Zosseder, K., Kiefl, R., Steinmetz, T., and Strunz, G. (2009): Assessment of human immediate response capability related to tsunami threats in Indonesia at a sub-national scale, Nat. Hazards Earth Syst. Sci., 9, 1075–1086, doi:10.5194/nhess-9-1075-2009.
- Rakowsky, Natalja, et al.(2013): Operational tsunami modelling with TsunAWI–recent developments and applications. Nat. Hazards Earth Syst. Sci. 13, 1629-1642.
- Reese, S., et al. (2007): Tsunami vulnerability of buildings and people in South Java--field observations after the July 2006 Java tsunami. Natural Hazards & Earth System Sciences 7.5.
- Roberts, S., et al. (2009): ANUGA User Manual." Geoscience Australia.
- Rodrigues M, Oliveira A, Costa M, Fortunato AB, Zhang Y. (2009b): Sensitivity analysis of an ecological model applied to the Ria de Aveiro. Journal of Coastal Research, SI56, 448-452.
- Rodrigues M, Oliveira A, Queiroga H, Fortunato AB, Zhang Y. (2009a): Three-Dimensional Modeling of the Lower Trophic Levels in the Ria de Aveiro (Portugal), Ecological Modelling, 220(9-10), 1274-1290.
- Roeber V, Cheung KF, Kobayashi MH. (2010): Shock-capturing Boussinesq-type model for nearshore wave processes, Coastal Engineering, 57 (4), 407–423
- Roeber V. (2010): Boussinesq-type model for nearshore wave processes in fringing reef environment. PhD Dissertation, University of Hawaii, Honolulu.
- Roeber, V., Yamazaki, Y., and Cheung, K.F. (2010): Resonance and impact of the 2009 Samoa Tsunami around Tutuila, American Samoa. Geophysical Research Letters, 37(21), L21604, doi: 10.1029/2010GL044419.
- Roeber, Volker, Kwok Fai Cheung, and Marcelo H. Kobayashi (2010): Shock-capturing Boussinesq-type model for nearshore wave processes." Coastal Engineering 57.4, 407-423.
- Roemer, H., et al. (2010): Using remote sensing to assess tsunami-induced impacts on coastal forest ecosystems at the Andaman Sea coast of Thailand." Natural Hazards & Earth System Sciences 10.4.
- Römer, Hannes, et al. (2012): Monitoring post-tsunami vegetation recovery in Phang-Nga province, Thailand, based on IKONOS imagery and field investigations–a contribution to the analysis of tsunami vulnerability of coastal ecosystems." International Journal of Remote Sensing 33.10, 3090-3121.

- Roland A, Zhang Y, Wang HV, Maderich V, Brovchenko I. (2011): A fully coupled wave-current model on unstructured grids, Compt. & Geosciences (submitted).
- Ruangrassamee, A., Yanagisawa, H., Foytong, P., Lukkunaprasit, P., Koshimura, S., and Imamura, F. (2006): Investigation of Tsunami-Induced Damage and Fragility of Buildings in Thailand after the December 2004 Indian Ocean Tsunami, Earthq. Spectra, 22, 377–401.
- Rynn, J. and Davidson, J. (1999): Contemporary assessment of tsunami risk and implication for early warnings for Australia and its island territories, Science of Tsunamis Hazards: 17/2, 107-125 pp.
- Saatçioğlu, Murat (2009): Performance of structures during the 2004 Indian Ocean tsunami and tsunami induced forces for structural design." Earthquakes and Tsunamis. Springer Netherlands, 153-178.
- Sagara, Junko; Saito, Keiko (2013): Risk Assessment and Hazard Mapping. World Bank, Washington, DC. World Bank. https://openknowledge.worldbank.com/handle/10986/16146 License: CC BY 3.0 Unported.
- Sakakiyama, T. (2012): Stability of Armour Units of Rubble Mound Breakwater against Tsunamis, Proc. of 32nd Int. Conf. on Coastal Engineering, Santander, Spain.
- Shen, M. C., and Meyer, R. E. (1963): Climb of a bore on a beach. Part 3. Run-up. J. Fluid Mech., 16, 113–125.
- Shepard, F.P., MacDonald, G.A., and Cox, D.C. (1950): The tsunami of April 1, 1946. Bulletin of the Scripps Institution of Oceanography, 5(6), 391-528.
- Shi F, Kirby JT, Tehranirad B, Harris JC, Grilli ST. (2011): FUNWAVE-TVD Version 1.0. Fully nonlinear Boussinesq wave model with TVD solver. Documentation and user's manual. Research Report No. CACR-11-04, Center for Applied Coastal Research, University of Delaware.
- Shibayama, T., Esteban, M., Nistor, I., Takagi, H., Danh Thao, N., Matsumaru, R., Mikami, T., , Aranguiz, R., Jayaratne, R. and Ohira, K. (2013): Classification of Tsunami and Evacuation Areas, Journal of Natural Hazards (accepted)
- Shuto N., Goto C., Imamura F. (1990): Numerical Simulation as a means of Warning for Near Field Tsunamis, Coastal Engineering in Japan 33, No:2 173-193, 1990.
- Shuto, Nobuo (2009): Damage to coastal structures by tsunami-induced currents in the past. Journal of Disaster Research 4.6, 462-468.
- Sinaga, Tumpal PT, et al. (2011): GIS mapping of tsunami vulnerability: Case study of the Jembrana regency in Bali, Indonesia." KSCE Journal of Civil Engineering 15.3, 537-543.
- Song Y, Haidvogel DB. (1994): A semi-implicit ocean circulation model using a generalized topography-following coordinate system. J. Comp. Phys., 115(1), 228-244.
- Spaeth, M.G. and Berkman, S.C. (1972): The tsunamis as recorded at tide stations and the Seismic Sea Wave Warning System. The Great Alaska

Earthquake of 1964, Oceanography and Coastal Engineering. Washington, D.C.: National Academy of Sciences, pp. 38-110.

- State of Hawai‘i Multi-Hazard Mitigation Plan (2010).
- Strunz, G., et al. (2011): Tsunami risk assessment in Indonesia." Natural Hazards and Earth System Science 11.1, 67-82.
- Sumaryono, S., Strunz, G., Ludwig, R., Post, J., and Zosseder, K. (2008): Measuring urban vulnerability to tsunami hazards using integrative remote sensing and GIS approaches, International Conference on TsunamiWarning (ICTW), Bali, Indonesia, 9 pp.
- Sumer, B. Mutlu, et al. (2007): Earthquake-induced liquefaction around marine structures. Journal of waterway, port, coastal, and ocean engineering 133.1, 55-82.
- Suppasri, A., et al. (2011): Developing tsunami fragility curves based on the satellite remote sensing and the numerical modeling of the 2004 Indian Ocean tsunami in Thailand." Natural Hazards & Earth System Sciences 11.1.
- Suppasri, A., Mas, E., Koshimura, S., Imai, K., Harada, K., & Imamura, F. (2012): Developing tsunami fragility curves from the surveyed data of the 2011 Great East Japan tsunami in Sendai and Ishinomaki plains. Coast Eng.
- Suppasri et al. (2013): Building damage characteristics based on surveyed data and fragility curves of the 2011 Great East Japan tsunami. Nat Hazards 66:319–341.
- Synolakis, C. E. (2003): Tsunamis and seiches. Earthquake engineering handbook, W. F. Chow and C. Scawthorn, eds., CRC, Boca Raton, Fla., 9-1–9-90.
- Synolakis, C. E., and Skjelbreia, J. E. (1993): Evolution of maximum amplitude of solitary waves on plane beaches. J. Waterway, Port, Coastal, Ocean Eng., 119(3), 323–342.
- T. Hughes et al. (2005): Trends Ecol. Evol. 20, 380.
- Tadepalli, S., and Synolakis, C. E. (1996): Model for the leading waves of tsunamis.” Phys. Rev. Lett., 7710, 2141–2144.
- Takahashi, S., et al. (2007): Simulation of Damage of a Wide Coastal Area due to the Huge Tsunami. Annual Report of the Earth Simulator Center April 2008.
- Takahashi S, Kuriyama Y, Tomita T, Kawai Y, Arikawa T, Tatsumi D, Negi T (2011b): Urgent survey for 2011 Great East Japan earthquake and tsunami disaster in ports and coasts (English summary) (p 9). Retrieved from http://www.pari.go.jp/en/files/3653/460607839.pdf
- Tanimoto, K. (1983): On the hydraulic aspects of tsunami break waters in Japan. In: Iida, K. and Iwasaki, T. (eds.), Tsunamis: Their Science and Engineering. Tokyo, Japan: Terra Scientific Publishing Co., pp. 423-435.
- Taubenböck H., et al. (2009): "Last-Mile" preparation for a potential disaster-Interdisciplinary approach towards tsunami early warning and an evacuation information system for the coastal city of Padang, Indonesia. Natural Hazards & Earth System Sciences 9.4.

- The 2011 Tohoku Earthquake Tsunami Joint Survey Group (2011): The 2011 off the Pacific coast of Tohoku earthquake tsunami information—field survey results. Coastal Engineering Committee of the Japan Society of Civil Engineers. Retrieved 18 November 2011 from http://www.coastal.jp/tsunami2011/index.php?Fieldsurveyresults
- Titov, V. V., et al. (2011): A new tool for inundation modeling: Community Modeling Interface for Tsunamis (ComMIT). Pure and Applied Geophysics 168.11, 2121-2131.
- Tomita, T., Kazuhiko H., and Taro K. (2006): Application of Storm Surge and Tsunami Simulator in Oceans and Coastal Areas (STOC) to Tsunami Analysis. Technical Memorandum of Public Works Research Institute 4022, 90.
- TRANSFER WORK PACKAGE-5 (2009): http://www.transferproject.eu/
- TU-BS (2015): Results of the laboratory analysis and wave flume tests. Deliverable D7 of the RAPSODI Project. Norwegian Geotechnical Report 20120768-07-R http://www.ngi.no/en/Project-pages/RAPSODI/Reports-and-Publications/
- Tudor, W. J. (1964): Tsunami Damage at Kodiak, Alaska, and Crescent City, California, from Alaska Earthquake of 27 March 1964. U.S. Naval Civil Engineering Laboratory Technical Note No. N-622, Port Hueneme, California, 128p.
- Turner, Billie L., et al. (2003): A framework for vulnerability analysis in sustainability science. Proceedings of the national academy of sciences 100.14, 8074-8079.
- U.S. Army Engineer District, Honolulu (1960): The Tsunami of 23 May 1960 in Hawaii. Final Post Flood Report, 38pp.
- United Nations International Strategy for Disaster Reduction (UN/ISDR) (2004): Living with Risk. A Global Review of Disaster Reduction Initiatives. UN Publications, Geneva.
- Van Drie, R., P. Milevski, and M. Simon (2010): ANUGA: Identifying Real Hazard by Direct Hydrology in 2D Hydraulic Model and the role of roughness. NOVATECH 2010.
- Vaselali A., Azarmsa S.A. (2009): Analysis of Breakwater Construction Effects on Sedimentation Pattern, Journal of Applied Sciences 9, 19.
- W. N. Adger, P. M. Kelly, N. H. Ninh, Eds. (2001): Living with Environmental Change: Social Vulnerability, Adaptation and Resilience in Vietnam (Routledge, London).
- Wang X., Liu P.L. (2006): An analysis of 2004 Sumatra earthquake fault plane mechanisms and Indian Ocean tsunami. Journal of Hydraulic Research 44.2, 147-154.
- Wang X., Liu P.L. (2005): A numerical investigation of Boumerdes-Zemmouri (Algeria) earthquake and tsunami. Computer Modeling in Engineering and Sciences 10.2, 171.
- Wang X. (2009): User Manual For COMCOT Version 1.7. Institute of Geological & Nuclear Science, New Zealand.

http://ceeserver.cee.cornell.edu/pll-group/doc/COMCOT_User_Manual_v1_7.pdf

- Wang, R., Martin, F. L., and Roth, F. (2003): Computation of deformation induced by earthquakes in a multi-layered elastic crust—FORTRAN programs EDGRN/EDCMP, Computers & Geosciences Vol. 29, 195–207.
- Watts, P., et al. (1999): Landslide tsunami case studies using a Boussinesq model and a fully nonlinear tsunami generation model. Natural Hazards and Earth System Science 3.5, 391-402.
- White, W.R.H. (1966): The Alaska earthquake - Its effect in Canada. Canadian Geographic Journal, 72(6), 210-219.
- Wiebe, Dane M., and Daniel T. Cox (2014): Application of fragility curves to estimate building damage and economic loss at a community scale: a case study of Seaside, Oregon. Natural Hazards 04, 1-19.
- Wiegel, R.L. (1970): Tsunamis. Earthquake Engineering. Engle wood Cliffs, New Jersey: Prentice-Hall, pp. 253-306.
- Wigen, S.O. and White, W.R.H. (1964): Tsunami of March 27, 1964, West Coast of Canada. Department of Mines and Technnical Surveys Technical Report, Victoria, British Columbia, Canada, 12pp.
- Wilson, B.W. and Torum, A. (1968): The Tsunami of the Alaska Earthquake, 1964: Engineering Evaluation. TM-25, U.S. Army Engineer Waterways Experiment Station, Coastal Engineering Research Center, Vicksburg, Mississippi, 444pp.
- Wood N., Gregg C. (n.d.): Societal Vulnerability to Tsunamis, USGS.
- Wood, Nathan, James Good, and Robert Goodwin (2002): Reducing vulnerability of ports and harbors to earthquake and tsunami hazards. Proceedings, solutions to coastal disasters, American Society of Civil Engineers, Reston, Virginia, 949-963.
- Yagyu, T. (2011): Sailing ahead (PIANC ENewsletter), 8. Retrieved from http://www.pianc.org/downloads/sailingahead/SailingAheadApril2011/JapanEarthquake.pdf
- Yalciner, A. C., Alpar, B., Altinok, Y., Ozbay, I., and Imamura, F. (2002): Tsunamis in the Sea of Marmara: Historical documents for the past, models for future. Marine Geology, 190(1–2), 445–463.
- Yalciner, A. C., et al. (2001): Field surveys and modeling 1999 Izmit Tsunami. Int. Tsunami Symp. ITS 2001, Seattle, Paper 4-6, 557–563.
- Yalciner, A. C., Pelinovsky, E., Zaytsev, A., Kurkin, A., Ozer, C., And Karakus, H. (2006): NAMI DANCE Manual, METU, Civil Engineering Department, Ocean Engineering Research Center, Ankara, Turkey http://namidance.ce.metu.edu.tr
- Yalciner, A. C., Pelinovsky, E., Zaytsev, A., Kurkin, A., Ozer, C., And Karakus, H., (2007a): Modeling and visualization of tsunamis: Mediterranean examples, from, Tsunami and Nonlinear Waves (Ed: Anjan Kundu), Springer, 2007, 2731-2839.
- Yalciner, A. C., Perincek, D., Ersoy, S., Prasetya, G., Rahman, H., and McAdoo, B. (2005): Report on January 21–31, 2005 North Sumatra survey

on December, 26, 2004 Indian Ocean Tsunami. ITST of UNESCO IOC, http://ioc.unesco.org/iosurveys/Indonesia/yalciner/yalciner.htm (Nov. 11, 2006).

- Yalciner, A. C., Synolakis, C. E: , Gonzales, M., Kanoglu, U., (2007b): Joint Workshop on Improvements of Tsunami Models, Inundation Map and Test Sites of EU TRANSFER Project, June 11-14, Fethiye, Turkey
- Yalciner, A., Pelinovsky, E., Talipova, T., Kurkin, A., Kozelkov, A., and Zaitsev, A. (2004): Tsunamis in the Black Sea. J. Geophys. Res., 109(C12), C12023.1–C12023.13.
- Yalciner, A.C., Alpar, B., Altinok, Y., Ozbay, I., Imamura, F. (2002a): Tsunamis in the Sea of Marmara: Historical Documents for the Past, Models for Future, Marine Geology, 190, pp. 445-463
- Yalciner, A.C., Imamura, F., Synolakis, E.C., (2002b): Simulation of Tsunami Related to Caldera Collapse and a Case Study of Thera Volcano in Aegean Sea. Abstract Published and paper presented in EGS XXVII General Assembly, Nice, France, April 2002 Session NH8.
- Yalciner, A.C., Kuran, U., Akyarli, A. And Imamura, F. (1995): An Investigation on the Generation and Propagation of Tsunamis in the Aegean Sea by Mathematical Modeling. Chapter in: Tsunami: Progress in Prediction, Disaster Prevention and Warning, book series of Advances in Natural and Technological Hazards Research by Kluwer Academic Publishers (1995), Ed. Yashuito Tsuchiya and Nobuo Shuto, pp 55-71
- Yalciner, A.C., Pelinovsky, E.N., Talipova, T.G., Kurkin, A.A., Kozelkov, A.C., Zaitsev, A.I. (2002b): Tsunamis in the Black Sea: comparison of the historical, instrumental and numerical data. J. Geophys.Research, 2004, vol. 109, No. C12, C12023 10.1029/2003JC002113
- Yalciner, A. C., Aytore, B.,Guler, H. G., Kanoglu, U., Duzgun, S., Zaytsev, A., Arikawa, T., Tomita, T., Ozer Sozdinler, C., Necmioglu, O., Ozel, N. M. (2014): High Resolution Tsunami Modeling and Assessment of Harbor Resilience: Case Study in Istanbul. European Geosciences Union (EGU) General Assembly, April 27 - May 02, 2014, Vienna, Austria
- Yamazaki Y, Cheung KF, Kowalik Z. (2011): Depth-integrated, non-hydrostatic model with grid nesting for tsunami generation, propagation, and run-up. International Journal for Numerical Methods in Fluids 67(12), 2081-2107.
- Yamazaki Y, Kowalik Z, Cheung KF. (2009): Depth-integrated, non-hydrostatic model for wave breaking and runup. International Journal for Numerical Methods in Fluids, 61(5), 473-497.
- Yamazaki, Y., and Cheung, K.F. (2011): Shelf resonance and impact of near-field tsunami generated by the 2010 Chile Earthquake. Geophysical Research Letters, in review.
- Yamazaki, Y., Cheung,K.F., and Kowalik, Z. (2010): Depthintegrated, non-hydrostatic model with grid nesting for tsunami generation, propagation and run-up. International Journal for Numerical Methods in Fluids, DOI: 10.1002/ftd.2485.

- Yeh, H., Liu, P., and Synolakis, C. (1997): “Long-wave runup models.” Proc., Int. Workshop, Friday Harbor, USA, 1995, World Scientific, Singapore.
- Yeh, Harry, Shinji Sato, and Yoshimitsu Tajima (2012): The 11 March 2011 East Japan earthquake and tsunami: Tsunami effects on coastal infrastructure and buildings. Pure and Applied Geophysics (2012), 1-13.
- Yeh, Harry (2006): Maximum fluid forces in the tsunami runup zone. Journal of waterway, port, coastal, and ocean engineering 132.6, 496-500.
- Zahibo, N., Pelinovsky, E., Kurkin, A., And Kozelkov A. (2003b): Estimation of far-field tsunami potential for the Caribbean Coast based on numerical simulation. Science Tsunami Hazards. 2003, vol. 21, N. 4, p: 202 -222.
- Zahibo, N., Pelinovsky, E., Yalciner, A.C., Kurkin, A., Kozelkov A., Zaitsev, A. (2003a): The 1867 Virgin Island Tsunami: Observations and Modeling, Oceanologica Acta, Vol. 26, N. 5-6, Pp: 609-621.
- Zhang Y, Baptista AM (2008a): SELFE: A semi-implicit Eulerian-Lagrangian finite-element model for cross-scale ocean circulation. Ocean Modelling, 21(3-4), 71-96
- Zhang Y, Baptista AM. (2008b): An Efficient and Robust Tsunami Model on Unstructured Grids. Part I: Inundation Benchmarks. Pure and Applied Geophysics 165, 2229–2248.
- Zhang Y, Witter RW, Priest GP. (2011): Nonlinear Tsunami-Tide Interaction in 1964 Prince William Sound Tsunami, Ocean Modelling (submitted).

Review and reference page

Document information		
Document title Deliverable D1- Existing tools, data, and literature on tsunami impact, loads on structures, failure modes and vulnerability assessment		***Document No.*** 20120768-01-R
Type of document Report	***Distribution*** Unlimited	***Date*** 17 March 2014 **Rev. No & date** 1 / February 2015
Client CONCERT-Japan Joint Call Secretariat		
Keywords tsunami impact, loads on structures, failure modes, vulnerability assessment		

Geographical information	
Country, County	***Offshore area***
Municipality	***Field name***
Location	***Location***
Map	***Field, Block No.***
UTM-coordinates	

Document control

Quality assurance according to NS-EN ISO9001

Rev.	Reason for revision	Self review by:		Colleague review by:		Independent review by:		Inter-disciplinary review by:	
0	Original document								
1	Revision according to comments								

Document approved for release	**Date** 1 February 2015	**Project Manager** Carl B. Harbitz

CONCERT JAPAN

Connecting and Coordinating
European Research and Technology Development with Japan

concertjapan.eu